Application to Food Standards Australia New Zealand for the Inclusion of Maize MON 95379 in *Standard 1.5.2 - Food Derived from Gene Technology*

Submitted by:

Bayer CropScience Proprietary Limited

[redacted]

March, 2021

TABLE OF CONTENTS

LIST OF FIGURES

LIST OF TABLES

UNPUBLISHED REPORTS BEING SUBMITTED

Appendix 1. [redacted]2020. Amended from MSL0030839: Molecular Characterization of Insect Protected Maize MON 95379. **TRR0000070**. Monsanto Company. (CBI)

Appendix 2. [redacted] 2020. Updated Bioinformatics Evaluation of the T-DNA in MON 95379 Utilizing the AD_2020, TOX_2020, and PRT_2020 Databases. **TRR0000120**. Monsanto Company.

Appendix 3. [redacted] 2020. Updated Bioinformatics Evaluation of Putative Flank-Junction Peptides in MON 95379 Utilizing the AD_2020, TOX_2020, and PRT_2020 Databases. **TRR0000119**. Monsanto Company.

Appendix 4. [redacted]2019. Segregation Analysis of the T-DNA Insert in Insect Protected Maize MON 95379 Across Three Generations. **MSL0030175**. Monsanto Company.

Appendix 5. [redacted]2019. Demonstration of the Presence of Cry1Da_7 and Cry1B.868 Proteins in Maize Seed Samples Across Multiple Generations of MON 95379. **MSL0030807**. Monsanto Company.

Appendix 6. [redacted] 2020. Amended Report for MSL0030779: Characterization of the Cry1B.868 Protein Purified from the Maize Grain of MON 95379 and Comparison of the Physicochemical and Functional Properties of the Plant-Produced and *Bacillus thuringiensis* (*Bt*)-Produced Cry1B.868 Proteins. **TRR0000416**. Monsanto Company.

Appendix 7. [redacted] 2020. Characterization of the Cry1Da_7 Protein Purified from the Maize Grain of MON 95379 and Comparison of the Physicochemical and Functional Properties of the Plant-Produced and *Bacillus thuringiensis* (*Bt*)-Produced Cry1Da_7 Proteins. **MSL0030547**. Monsanto Company.

Appendix 8. [redacted] 2020. Assessment of Cry1B.868 and Cry1Da_7 Protein Levels in Leaf, Roof, Pollen, Forage and Grain Tissues Collected from MON 95379 Produced in United States Field Trials During 2018. **TRR0000556**. Bayer CropScience LP.

Appendix 9. [redacted] 2020. Updated Bioinformatics Evaluation of Cry1Da_7 and Cry1B.868 in MON 95379 Utilizing the AD_2020, TOX_2020, and PRT_2020 Databases. **TRR0000118**. Monsanto Company.

Appendix 10. [redacted]. 2020. Amended Report for MSL0030730: Assessment of the *in vitro* Digestibility of Cry1B.868 Protein by Pepsin and Pancreatin. **TRR0000667**. Bayer CropScience LP.

Appendix 11. [redacted] 2019. Assessment of the *in vitro* Digestibility of Cry1Da_7 Protein by Pepsin and Pancreatin. **MSL0030568**. Monsanto Company.

Appendix 12. [redacted] 2020. The Effect of Heat Treatment on the Functional Activity of *Bacillus thuringiensis*-produced Cry1B.868 Protein. **MSL0031013**. Monsanto Company.

Appendix 13. [redacted] 2020. Amended Report for MSL0031014: The Effect of Heat Treatment on the Functional Activity of *Bacillus thuringiensis*-produced Cry1Da_7 Protein. **TRR0000145**. Monsanto Company.

Appendix 14. [redacted] 2019. Amended Report for MSL0029995: Compositional Analyses of Maize Grain and Forage Harvested from MON 95379 Grown in the United States During the 2018 Season. **MSL0030947**. Monsanto Company.

CHECKLIST

General Requirements (3.1.1)	Reference
A Form of application	
☑ *Application in English*	*Available*
☑ *Executive Summary (separated from main application electronically)*	*Separate document prepared*
☑ *Relevant sections of Part 3 clearly identified*	*Completed*
☑ *Pages sequentially numbered*	*Completed*
☑ *Electronic copy (searcahable)*	*Prepared*
☑ *All references provided*	*Prepared*
B Applicant details	*Page 1*
C Purpose of the application	*Page 1*
D Justification for the application	
☑ *Regulatory impact information*	*Page 2*
☑ *Impact of international trade*	*Page 3*
E Information to support the application	
☑ *Data requirement*	*14*
F Assessment procedure	
☑ *General*	*Page 3*
☐ *Major*	
☐ *Minor*	
☐ *Hight level heath claim variation*	
G Confidential Commercial Information	
☑ *CCI material separated from other application material*	*Completed*
☐ *Formal request including reasons*	
☐ *Non-confidential summary provided*	
H Other confidential information	
☑ *Confidential material separated from other application material*	*Completed*
☐ *Formal request including reasons*	
I Exclusive Capturable Commercial Benefit	

☑ *Justification provided*	*Page 3*
J International and Other National Standards	
☑ *International standards*	*Page 3*
☑ *Other national standards*	*Page 4*
K Statutory Declaration	*Page 145*
L Checklist/s provided with Application	
☑ *3.1.1 Checklist*	*Page xii*
☑ *All page number references from application included*	*Completed*
☑ Any other relevant checklists for Sections 3.2 – 3.7	*Checklist 3.5.1*

Foods Produced using Gene Technology (3.5.1)	
☑ A.1 Nature and identity of the GM food	*Page 5*
☑ A.2 History of use of host and donor organisms	*Page 6*
☑ A.3 Nature of genetic modification	*Page 10*
☑ B.1 Characterisation and safety assessment of new substances	*Page 53*
☑ B.2 New proteins	*Page 98*
☑ B.3 Other (non-protein) new sustances	*Page 126*
☑ B.4 Novel herbicide metabolites in GM herbicide-tolerant plants	*Page 126*
☑ B.5 Compositional assessment	*Page 126*
☑ C Information related to the nutritional impact of the food produced using gene technology	*Page 144*
☑ D Other information	*Page 144*

ABBREVIATIONS AND DEFINITIONS[1]

AA	Amino Acid
aadA	Aminoglycoside-modifying enzyme, 3"(9) –*O*–nucleotidyltransferase from the transposon Tn*7*
Act	Actin
ADF	Acid Detergent Fiber
APHIS	Animal and Plant Health Inspection Service
aroA	5-enolpyruvylshikimate-3-phosphate synthetase gene from *Agrobacterium* sp. Strain CP4
bp	Basepair
Bt	*Bacillus thuringiensis*
bw	Body Weight
CEW	Corn Earworm
COA	Certificate of Analysis
COMPARE	COMprehensive Protein Allergen REsource
CP4 EPSPS	*Agrobacterium tumefaciens* strain CP4, 5-enolpyruvlshikimate-3-phosphate synthase protein
Cry	Crystalline Proteins
Cry1	Subspecies of Cry Proteins
Cry1B.868	Cry1B.868 is a chimeric protein comprised of domains I and II from Cry1Be (*Bt*), domain III from Cry1Ca (*Bt* subsp.*aizawai*) and C-terminal protoxin domain from Cry1Ab (*Bt* subsp. *kurstaki*)
Cry1Da_7	Modified Cry1Da protein derived from *Bt* subsp. *aizawai*
CTP	Chloroplast Transit Peptide
d	Day(s)
DNA	Deoxyribonucleic Acid
dw	Dry Weight
E-score	Expectation score
E. coli	*Escherichia coli*
EFSA	European Food Safety Authority
ELISA	Enzyme-linked Immunosorbent Assay
EPA	Environmental Protection Agency
ETS	Excellence Through Stewardship
FA	Fatty Acid
FAW	Fall Armyworm
FDA	Food and Drug Administration (U.S.)
FMV	Figwort Mosaic Virus
fw	Fresh Weight
ICP	Insect Control Proteins
ILSI	International Life Science Institute
kb	Kilobase
kDa	Kilodalton
LC	Liquid Chromatography
LOD	Limit of Detection

[1] Alred, G.J., C.T. Brusaw, and W.E. Oliu. 2003. Handbook of Technical Writing, 7th edn., pp. 2-7. Bedford/St. Martin's, Boston, MA.

LOQ	Limit of Quantitation
LTP	Lipid Transfer Protein
mRNA	Messenger RNA
MS	Mass Spectrometry
MW	Molecular Weight
NDF	Neutral Detergent Fiber
NGS	Next Generation Sequencing
OECD	Organization for Economic Co-operation and Development
OR	Origin of Replication
ORF	Open Reading Frame
OSL	Over Season Leaf
OSR	Over Season Root
PCR	Polymerase Chain Reaction
SCB	Sugarcane borer
SDS-PAGE	Sodium Dodecyl Sulfate–Polyacrylamide Gel Electrophoresis
S.E.	Standard Error
ShkG	5-enolpyruvylshikimate-3-phosphate synthase from *Arabidopsis thaliana*
T-DNA	Transfer Deoxyribonucleic Acid
TDF	Total Dietary Fiber
TIP	Tonoplast Intrinsic Protein
Tub	Tubulin
Ubq	Ubiquitin gene
U.S.	United States
USDA	United States Department of Agriculture
UTR	Untranslated Region
WHO	World Health Organization
v/v	Volume per Volume
w/v	Weight per Volume

PART 1 GENERAL INFORMATION

1.1 Applicant Details

(a) Applicant's name/s	[redacted]
(b) Company/organisation name	Bayer CropScience Pty Ltd
(c) Address (street and postal)	[redacted]
(d) Telephone number	[redacted]
(e) Email address	[redacted]
(f) Nature of applicant's business	Technology Provider to the Agricultural and Food Industries
(g) Details of other individuals, companies or organisations associated with the application	

1.2 Purpose of the Application

This application is submitted to Food Standards Australia New Zealand by Bayer CropScience Proprietary Limited on behalf of Bayer Group.

The purpose of this submission is to make an application to vary **Standard 1.5.2** – *Food Produced Using Gene Technology* of the *Australia New Zealand Food Standards Code* to seek the addition of maize line MON 95379 and products containing maize line MON 95379 (hereafter referred to as MON 95379) to the Table to Clause 2 (see below).

Food derived from gene technology	Special requirements
Food derived from maize line MON 95379	None

1.3 Justification for the Application

1.3(a) The need for the proposed change

Insect-protected maize MON 95379 was developed to produce two insecticidal proteins, Cry1B.868 and Cry1Da_7, which protect against feeding damage caused by targeted lepidopteran insect pests. Cry1B.868 is a chimeric protein comprised of domains I and II from Cry1Be (*Bacillus thuringiensis*, *Bt*), domain III from Cry1Ca (*Bt* subsp. *aizawai*) and C-terminal protoxin domain from Cry1Ab (*Bt* subsp. *kurstaki*). Cry1Da_7 is a modified Cry1Da protein derived from *Bt* subsp. *aizawai*.

1.3(b) The advantages of the proposed change over the status quo, taking into account any disadvantages

MON 95379 was developed to provide growers in South America an additional tool for controlling target lepidopteran maize pests, including fall armyworm resistant to current *Bt* technologies. MON 95379 will be combined through traditional breeding with other deregulated traits to provide protection against both above-ground and below-ground maize pests, as well as herbicide tolerance. These next generation combined-trait maize products will offer broader grower choice, improved production efficiency, increased pest control durability, and enhanced grower profit potential.

MON 95379 will not be commercialized in the U.S., but is intended to only be cultivated in small-scale breeding, testing, and seed increase nurseries to develop seed for future products in South America. These intended cultivation uses will be subject to the terms and conditions of an EPA breeding registration, which we have proposed to be limited to no more than 100 acres per growing season across Nebraska, Hawaii, and Iowa.

1.4 Regulatory Impact Information

Costs and benefits

If the draft variation to permit the sale and use of food derived from MON 95379 is approved, possible affected parties may include consumers, industry sectors and government. The consumers who may be affected are those that consume food containing ingredients derived from maize. Industry sectors affected may be food importers and exporters, distributors, processors and manufacturers. Lastly, government enforcement agencies may be affected.

A cost/benefit analysis quantified in monetary terms is difficult to determine. In fact, most of the impacts that need to be considered cannot be assigned a dollar value. Criteria would need to be deliberately limited to those involving broad areas such as trade, consumer information and compliance. If the draft variation is approved:

Consumers:

- There would be benefits in the broader availability of maize products.
- There is unlikely to be any significant increase in the prices of foods if manufacturers are able to use comingled maize products.
- Consumers wishing to do so will be able to avoid GM maize products as a result of labeling requirements and marketing activities.

Government:

- Benefit that if maize MON 95379 was detected in food products, approval would ensure compliance of those products with the Code. This would ensure no potential for trade disruption on regulatory grounds.
- Approval of maize MON 95379 would ensure no potential conflict with WTO responsibilities.
- In the case of approved GM foods, monitoring is required to ensure compliance with the labeling requirements, and in the case of GM foods that have not been approved, monitoring is required to ensure they are not illegally entering the food supply. The costs of monitoring are thus expected to be comparable, whether a GM food is approved or not.

Industry:

- Sellers of procesed foods containing maize derivatives would benefit as foods derived from maize MON 95379 would be compliant with the Code, allowing broader market access and increased choice in raw materials. Retailers may be able to offer a broader range of maize products or imported foods manufactured using maize derivatives.
- Possible cost to food industry as some food ingredients derived from maize MON 95379 would be required to be labelled

1.5 Impact of International Trade

If the draft variation to permit the sale and use of food derived from MON 95379 was rejected it would result in the requirement for segregation of any maize derived products containing MON 95379 from those containing approved maize, which would be likely to increase the costs of imported maize derived foods.

It is important to note that if the draft variation is approved, maize MON 95379 will not have a mandatory introduction. The consumer will always have the right to choose not to use/consume this product.

1.6 Assessment Procedure

Bayer CropScience is submitting this application in anticipation that it will fall within the General Procedure category.

1.7 Exclusive Capturable Commercial Benefit

This application is likely to result in an amendment to the Code that provides exclusive benefits and therefore Bayer CropScience intends to pay the full cost of processing the application.

1.8 International and Other National Standards

1.8(a) International standards

Bayer CropScience makes all efforts to ensure that safety assessments are aligned, as closely as possible, with relevant international standards such as the Codex Alimentarius Commission's *Principles for the Risk Analysis of Foods Derived from Modern Biotechnology*

and supporting *Guideline for the Conduct of Food Safety Assessment of Foods Derived from Recombinant-DNA Plants* (Codex Alimentarius, 2009).

In addition, the composition analysis is conducted in accordance with OECD guidelines and includes the measurement of OECD-defined maize nutrients and anti-nutrients based on conventional commercial maize varieties (OECD, 2002a).

1.8(b) Other national standards or regulations

Bayer CropScience has submitted a food and feed safety and nutritional assessment summary for MON 95379 to the United States Food and Drug Administration (FDA) and has also requested a Determination of Nonregulated Status for MON 95379, including all progenies derived from crosses between MON 95379 and other maize, from the Animal and Plant Health Inspection Service (APHIS) of the U.S. Department of Agriculture (USDA).

Consistent with our commitments to the Excellence Through Stewardship® (ETS) Program[2], regulatory submissions have been or will be made to countries that import significant maize or food and feed products derived from U.S. maize and have functional regulatory review processes in place.

[2] Excellence Through Stewardship is a registered trademark of Excellence Through Stewardship, Washington, DC. (http://www.excellencethroughstewardship.org)

PART 2 SPECIFIC DATA REQUIREMENTS FOR SAFETY ASSESSMENT

A. TECHNICAL INFORMATION ON THE GM FOOD

A.1 Nature and Identity of the Genetically Modified Food

A.1(a) A description of the new GM organism from which the new GM food is derived

Lepidopteran-protected maize MON 95379 was developed to provide growers in South America with new options for protection against the feeding damage of targeted lepidopteran pests, including fall armyworm (FAW; *Spodoptera frugiperda*), sugarcane borer (SCB; *Diatraea saccharalis*) and corn earworm (CEW; *Helicoverpa zea*). The larval feeding behavior of these species typically limits the efficacy of synthetic insecticides by creating additional difficulties for the sprayed active ingredients to reach the insects (Burtet *et al.*, 2017; Grimi *et al.*, 2018; Reay-Jones, 2019). MON 95379 produces two insecticidal proteins, Cry1B.868 and Cry1Da_7, which protect against feeding damage caused by these lepidopteran pests. Cry1B.868 is a chimeric protein comprised of domains I and II from Cry1Be (*Bacillus thuringiensis, Bt*), domain III from Cry1Ca (*Bt* subsp. *aizawai*) and the C-terminal protoxin domain from Cry1Ab (*Bt* subsp. *kurstaki*). Cry1Da_7 is a modified Cry1Da protein derived from *Bt* subsp. *aizawai*.

A.1(b) Name, line number and OECD Unique Identifier of each of the new lines or strains of GM organism from which the food is derived

In accordance with OECD's "Guidance for the Designation of a Unique Identifier for Transgenic Plants" MON 95379 has been assigned the unique identifier MON-95379-3.

A.1(c) The name the food will be marketed under (if known)

Maize containing the transformation event MON 95379 will be produced in North America. There are currently no plans to produce this product in Australia and New Zealand. A commercial trade name for the product has not been determined at the time of this submission and will be available prior to commercial launch of the product in North America.

A.2 History of Use of the Host and Donor Organisms

A.2(a) For the donor organism(s) from which the genetic elements are derived:

A.2(a)(i) Any known pathogenicity, toxicity or allergenicity relevance to the food

The Cry1B.868 and Cry1Da_7 proteins are derived from genetic elements that code for crystalline proteins (Cry) that are expressed as parasporal inclusions (or δ-endotoxins) in the ubiquitous gram-positive bacterium *Bacillus thuriengensis* (*Bt*) (Gill *et al.*, 1992; Schnepf *et al.*, 1998; Vachon *et al.*, 2012). *Bt* isolates have a long, documented history of safe use in agriculture and safe human consumption. Since the first *Bt* isolate was registered as a pesticide in 1961, over 180 microbial *Bt* products have been registered in the United States (U.S.), with more than 120 microbial products registered in the European Union (EU) (Hammond, 2004). *Bt* microbial biopesticides have been safely and directly applied to consumed agricultural commodities including berry crops, cabbage, grapes, tomatoes, celery, lettuce, and spinach (U.S. EPA, 1998). For certain crops, a significant percentage of the total U.S. grown crop has been treated with *Bt* crystal/spore preparations (*e.g.,* blackberries (50%), celery (46%), and cabbage (39%)) (U.S. EPA, 1998). In Europe, residual levels of *Bt* microbials of up to 100,000 CFUs (colony forming units) were observed on fresh vegetables following application of *Bt* microbial pesticides (Frederiksen *et al.*, 2006). Thus, the use of *Bt* microbials for pest control in agriculture, including in organic farming, provides a 50-year history of safe consumption of food crops sprayed with *Bt* microbial pesticides. Due to the high efficacy and safety, global demand for *Bt* biopesticides as a preferred substitution for chemical pesticides is expected to increase 5.3% from 2018 to 2022 (Chen, 2018) and is projected to continue increasing (Seiber *et al.*, 2014; Damalas and Koutroubas, 2018).

Several different *Bt* subspecies, including *Bt* subsp. *kurstaki* and *Bt* subsp. *aizawai*, have been subjected to toxicity testing and showed no evidence for adverse effects on human health (Baum *et al.*, 1999; Betz *et al.*, 2000; Federici and Siegel, 2008; McClintock *et al.*, 1995; Mendelsohn *et al.*, 2003; Hammond, 2004; U.S. EPA, 2001; Siegel, 2001; U.S. EPA, 1986). These subspecies are extensively used in formulations for commercial biopesticides and express a diverse array of Cry1 proteins (e.g., Cry1Aa, Cry1Ab, Cry1Ac, Cry1C, Cry1D and Cry1B proteins) (Betz *et al.*, 2000). Additionally, direct toxicity assessments of *Bt* microbial biopesticide formulations containing these strains, such as Dipel®[3], Cutlass® OF[4], Crymax®[5], Xentari®[6] WG, Turex® 50 WG[7] and Thuricide®[8], have shown no evidence for adverse effects on human or mammalian health (Fisher and Rosner, 1959; McClintock *et al.*, 1995; Hadley *et al.*, 1987; Betz *et al.*, 2000; U.S. EPA, 1986; U.S. EPA, 1996; VKM, 2016).

The *cry1B.868* coding sequence in MON 95379 is under the regulation of the promoter, 5' untranslated region (UTR) and intron for a ubiquitin gene (*Ubq*) from *Zea mays* subsp. *Mexicana* (Mexican teosinte) that directs transcription in plant cells (Cornejo *et al.*, 1993). The *cry1B.868* coding sequence also utilizes the 3′ UTR sequence of the *Lipid Transfer Protein-like* gene (*LTP*) from *Oryza sativa* (rice) that directs polyadenylation of mRNA (Hunt, 1994).

[3] Dipel is a registered trademark of Abbott, Inc.
[4] Cutlass is a registered trademark of Certis USA
[5] Crymax is a registered trademark of Ecoypergen, Inc.
[6] Xentari is a registered trademark of Valent USA
[7] Turex is a registered trademark of Certis USA
[8] Thuricide is a registered trademark of Certis USA

The codon optimized *cry1Da_7* coding sequence in MON 95379 is under the regulation of the promoter and 5' UTR from *Setaria italica* (foxtail millet) *tonoplast membrane integral protein* (*Tip*) gene (Hernandez-Garcia and Finer, 2014). In addition to the promoter and 5' UTR, the *cry1Da_7* coding sequence is regulated by the enhancer from the 35S RNA of *Figwort mosaic virus* (FMV) (Richins *et al.*, 1987) that enhances transcription in most plant cells (Rogers, 2000) and the intron and flanking UTR sequence from the *Actin 15* (*Act 15*) gene from *Oryza sativa* (rice) that is involved in regulating gene expression (Rose, 2008). The *cry1Da_7* coding sequence also utilizes 3' UTR sequence from the *GOS2* gene encoding a translation initiation factor from *Oryza sativa* (rice) that directs polyadenylation of mRNA (Hunt, 1994).

The *cp4 epsps* selectable marker cassette is also part of the originally inserted T-DNA in MON 95379. The selectable marker cassette is under the regulation of the promoter, 5' UTR, intron and 3′ UTR sequences of the *OsTubA* gene family from *Oryza sativa* (rice) encoding α-tubulin (Jeon *et al.*, 2000) that directs transcription and polyadenylation of mRNA in plant cells. The *cp4 epsps* expression cassette was excised from progeny plants using the Cre/*lox* recombination system for marker removal as described in Section A.3(c)(i), (Hare and Chua, 2002; Zhang *et al.*, 2003).

A.2(a)(ii) History of use of the organism in food supply or history of human exposure to the organism through other than intended food use (e.g. as a normal contaiminant)

The long history of safe use in agriculture and the comprehensive toxicity testing of *Bt* subspecies and *Bt*-derived biopesticides provides strong support for the conclusions that the Cry1B.868 and Cry1Da_7 donor organism (*Bt*) presents no health hazard to mammals when present in food or feed or in the environment.

A.2(b) For the host organism into which the genes were transferred:

A.2(b)(i) Its history of safe use for food

Maize has been a staple of the human diet for centuries, and its processed fractions are consumed in a multitude of food and animal feed products. For the 2016/2017 market year, values for U.S. domestic maize usage were 37% for feed and residual uses; 37% for alcohol for fuel; 10% for food, seed, and industrial uses other than alcohol for fuel; and 16% for exports (Capehart *et al.*, 2019). Global demand for maize has increased due to greater meat consumption in emerging economic countries including China, and biofuels production (Edgerton, 2009).

Maize is used extensively as a livestock feed for reasons that include its palatability, digestibility, and metabolizable energy (Loy and Lundy, 2019) and its relatively low cost (OECD, 2002a). Maize grain may be fed whole (Watson, 1988), but in many cases it is ground and mixed with other ingredients to provide a balanced ration (Leath and Hill, 1987). As reviewed by Loy and Lundy (2019), animal feed products from the wet milling process include maize gluten feed and maize gluten meal. Animal feed products from the dry milling process include hominy feed (Loy and Lundy, 2019). Ethanol production from dry milled maize provides distillers grains, another source of animal feed (Loy and Lundy, 2019). Maize can also be fed as a whole plant silage.

From 2016/17 to 2019/20, global maize production averaged approximately 1,111 million metric tons (MMT) per marketing year (USDA-FAS, 2020). During this same period, the top maize producers were the United States, China, Brazil, and the European Union (EU),

together accounting for approximately 71% of average annual global maize production (USDA-FAS, 2020). Also during this period, global maize production per marketing year ranged from 1,078 MMT to 1,127 MMT (USDA-FAS, 2020).

In the 2019/20 trade year, the top maize exporters were the United States, Brazil, Argentina, and Ukraine. Together, these countries accounted for approximately 86% of global exports (USDA-FAS, 2020). In the same trade year, the top maize importers were the European Union, Mexico, Japan, and South Korea, together accounting for 37% of global imports (USDA-FAS, 2020).

A.2(b)(ii) The part of the organism typically used as food

Maize kernels are typically used as food. The main components of maize kernels are endosperm (83%), germ (11%), and pericarp (bran) (5%) (Watson, 1988). Milling separates the grain into these components, with subsequent products dependent on the milling type (Watson, 1988).

A.2(b)(iii) The types of products likely to include the food or food ingredient

Food uses of maize include processed products from field maize and direct consumption of sweet maize and popcorn. Food products derived from the wet milling process include starch and sweetener products (e.g. high fructose maize syrup) (May, 1987). Food products derived from the dry milling process include maize grits, maize meal, and maize flour (Watson, 1988). Maize oil may be derived from either milling process (Watson, 1988).

A.2(b)(iv) Whether special processing is required to render food safe to eat

Products from wet milling: As reviewed by (Rausch *et al.*, 2019), the products of the wet milling include starch and sweeteners used in foodstuffs. Native or modified maize starch is used in a wide range of foods, including bakery products, puddings and custards, snack foods, salad dressings, meat products, prepared soups, and many others (Rausch *et al.*, 2019). Starch is also converted into a variety of sweetener products including high fructose maize syrup (Watson, 1988). The various sweeteners are also used in a wide range of foods, including bakery products, breakfast foods, desserts, prepared soups, canned fruits and juices and many others (Rausch *et al.*, 2019). In addition to starch and sweeteners, oil is obtained from the germ fraction that is separated during the wet milling process (Rausch *et al.*, 2019).

Products from dry milling: The products of the dry milling process include maize grits, maize meal, and maize flours, each of which is derived from the endosperm (Watson, 1988). The food uses of these products have been reviewed by (Rooney and Serna-Saldivar, 2003). Maize grits have the largest particles and have less than 1% oil content (Rooney and Serna-Saldivar, 2003). Grits are used in making breakfast cereals and snacks (Rooney and Serna-Saldivar, 2003), and are eaten in the U.S. as side dish (Watson, 1988). Maize meal has smaller particles than maize grits (Rooney and Serna-Saldivar, 2003). It is used in baked products like maize bread and muffins, and may be enriched with vitamins and minerals like thiamine, riboflavin, niacin, and iron (Rooney and Serna-Saldivar, 2003). Maize flour is made up of fine endosperm particles and has many uses as a food ingredient (e.g. in ready to eat snacks or pancake mixes) or binder (e.g. in processed meats) (Rooney and Serna-Saldivar, 2003). In addition to endosperm products, oil is obtained from the germ faction that is separated during the dry milling process (Watson, 1988).

Products from fermentation: Products from the wet and dry milling processes (e.g. corn syrups, grits) can also be used in producing distilled beverages through fermentation (Rooney and Serna-Saldivar, 2003; Watson, 1988).

A.3 The Nature of the Genetic Modification

Characterisation of the genetic modification in MON 95379 was conducted using a combination of sequencing, PCR, and bioinformatics. The results of this characterisation demonstrate that MON 95379 contains a single copy of the intended T-DNA containing the *cry1B.868* and *cry1Da_7* expression cassettes that is stably integrated at a single locus and is inherited according to Mendelian principles over multiple generations. These conclusions are based on the following:

- Molecular characterisation of MON 95379 by NGS demonstrated that MON 95379 contained a single intended DNA insert. These whole-genome analyses provided a comprehensive assessment of MON 95379 to determine the presence and identity of sequences derived from PV-ZMIR522223 and demonstrated that MON 95379 contains a single T-DNA insert, with no detectable backbone or *cp4 epsps* selectable marker from sequences from PV-ZMIR522223 or any sequences from PV-ZMOO513642.
- Directed sequencing (locus-specific PCR, DNA sequencing and analyses) performed on MON 95379 was used to determine the complete sequence of the single DNA insert from PV-ZMIR522223, the adjacent flanking DNA, and the 5' and 3' insert-to-flank junctions. This analysis confirmed that the sequence and organisation of the DNA is identical to the corresponding region in the PV-ZMIR522223 T-DNA. Directed sequencing also confirmed that the *cp4 epsps* selectable marker cassette which was excised, along with one *lox*P site, by Cre recombinase, is not present in the MON 95379 sequence. Furthermore, the genomic organisation at the insertion site in MON 95379 was assessed by comparing the sequences flanking the T-DNA insert in MON 95379 to the sequence of the insertion site in conventional maize. This analysis determined that 160 bases were deleted at the insertion site in MON 95379 upon DNA integration.
- Generational stability analysis by NGS demonstrated that the single PV-ZMIR522223 T-DNA insert in MON 95379 has been maintained through five breeding generations, thereby confirming the stability of the T-DNA in MON 95379.
- Segregation data confirm that the inserted T-DNA segregated according to Mendelian inheritance patterns, which corroborates the insert stability demonstrated by NGS and independently establishes the nature of the T-DNA at a single chromosomal locus.

Taken together, the characterisation of the genetic modification in MON 95379 demonstrates that a single copy of the intended T-DNA was stably integrated at a single locus of the maize genome and that no PV-ZMIR522223 plasmid backbone, *cp4 epsps* selectable marker, or PV-ZMOO513642 sequences are present in MON 95379.

A.3(a) A description of the method used to transform the host organism

MON 95379 was developed through *Agrobacterium tumefaciens* mediated transformation of immature maize embryos based on the method described by Sidorov and Duncan (2009) utilizing PV-ZMIR522223. Immature embryos were excised from a post-pollinated maize ear of LH244. After co-culturing the excised immature embryos with *Agrobacterium* carrying the plasmid vector, the immature embryos were placed on selection medium containing glyphosate and carbenicillin disodium salt in order to inhibit the growth of untransformed plant cells and excess *Agrobacterium*, respectively. Once transformed callus developed, the callus was placed on media conducive to shoot and root development. The

rooted plants (R0) with normal phenotypic characteristics were selected and transferred to soil for growth and further assessment.

The R0 plants were self-pollinated to produce R1 seed. Subsequently, the R1 population was screened for the presence of T-DNA and absence of vector backbone sequences by construct-level PCR assay and Southern blot analysis. Only plants that were homozygous positive for T-DNA and negative for vector backbone were selected for further development and their progenies were subjected to further molecular and phenotypic assessments. As is typical of a commercial event production and selection process, hundreds of different transformation events (regenerants) were generated in the laboratory using PV-ZMIR522223. Selected R2 events were crossed with a line expressing the Cre recombinase protein and screened for the absence of *cp4 epsps* and the *cre* genes. After careful selection and evaluation of these events in the laboratory, greenhouse and field, MON 95379 was selected as the lead event based on superior trait efficacy, agronomic, phenotypic, and molecular characteristics according to the general process described in Prado *et al.* (2014). Studies on MON 95379 were initiated to further characterize the genetic insertion and the expressed product, and to establish the food, feed, and environmental safety relative to conventional maize. The major steps involved in the development of MON 95379 are depicted in Figure 1. The result of this process was the production of MON 95379 maize with the *cry1B.868* and *cry1Da_7* expression cassettes.

For details, please refer to Appendix 1 ([redacted], 2020 (TRR0000070)).

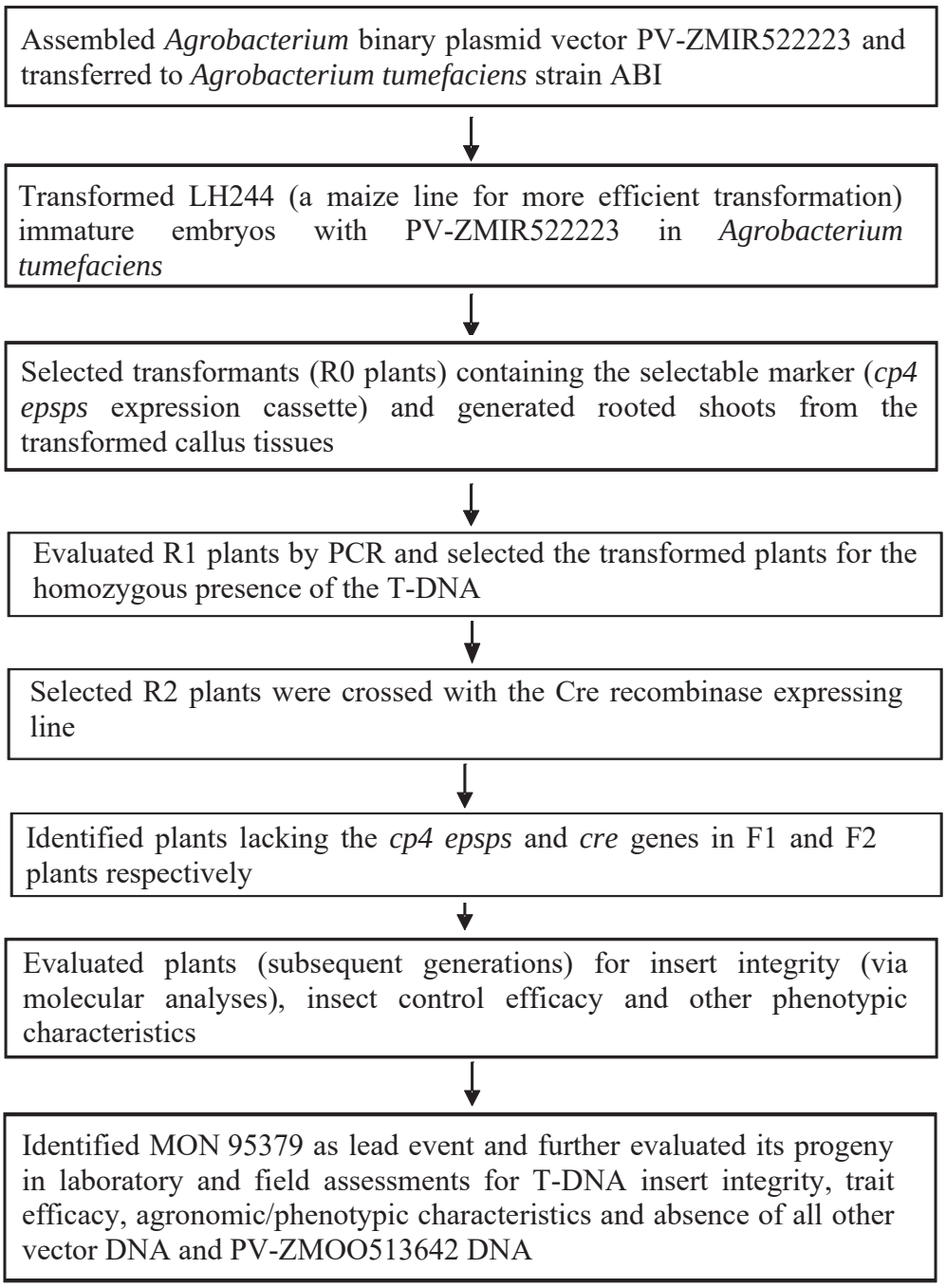

Figure 1. Schematic of the Development of MON 95379

A.3(b) A description of the construct and the transformation vectors used, including:

A.3(b)(i) The size, source and function of all the genetic components including marker genes, regulatory and other elements

PV-ZMIR522223

Plasmid Vector PV-ZMIR522223 was used for the transformation of conventional maize to produce MON 95379 and its plasmid map is shown in Figure 4. A description of the genetic elements and their prefixes (e.g., B, P, TS, CS, T, I, E, and OR) in PV-ZMIR522223 is provided in Table 1. PV-ZMIR522223 is approximately 21.6 kb and contains one T-DNA (transfer DNA), that is delineated by Right and Left Border regions. The T-DNA contains the *cp4 epsps* expression cassette, *cry1B.868* expression cassette, and the *cry1Da_7* expression cassette. During transformation, the T-DNA was inserted into the maize genome. Following transformation, traditional breeding, Cre/*lox* recombination, segregation, molecular screening and selection were used to isolate those plants that contained the *cry1B.868* and *cry1Da_7* expression cassettes and did not contain the backbone sequences from the transformation vector, the *cp4 epsps* selectable marker or any sequence from the *cre* gene-containing vector PV-ZMOO513642.

The *cry1B.868* coding sequence in MON 95379 is under the regulation of the promoter, 5' untranslated region (UTR) and intron for a ubiquitin gene (*Ubq*) from *Zea mays* subsp. *Mexicana* (Mexican teosinte) that directs transcription in plant cells (Cornejo *et al.*, 1993). The *cry1B.868* coding sequence also utilizes the 3′ UTR sequence of the *Lipid Transfer Protein-like* gene (*LTP*) from *Oryza sativa* (rice) that directs polyadenylation of mRNA (Hunt, 1994).

The codon optimized *cry1Da_7* coding sequence in MON 95379 is under the regulation of the promoter and 5' UTR from *Setaria italica* (foxtail millet) *tonoplast membrane integral protein* (*Tip*) gene (Hernandez-Garcia and Finer, 2014). In addition to the promoter and 5' UTR, the *cry1Da_7* coding sequence is regulated by the enhancer from the 35S RNA of *Figwort mosaic virus* (FMV) (Richins *et al.*, 1987) that enhances transcription in most plant cells (Rogers, 2000) and the intron and flanking UTR sequence from the *Actin 15* (*Act 15*) gene from *Oryza sativa* (rice) that is involved in regulating gene expression (Rose, 2008). The *cry1Da_7* coding sequence also utilizes 3' UTR sequence from the *GOS2* gene encoding a translation initiation factor from *Oryza sativa* (rice) that directs polyadenylation of mRNA (Hunt, 1994).

The *cp4 epsps* selectable marker cassette is also part of the originally inserted T-DNA in MON 95379. The selectable marker cassette is under the regulation of the promoter, 5' UTR, intron and 3′ UTR sequences of the *OsTubA* gene family from *Oryza sativa* (rice) encoding α-tubulin (Jeon *et al.*, 2000) that directs transcription and polyadenylation of mRNA in plant cells. The *cp4 epsps* expression cassette was excised from progeny plants using the Cre/*lox* recombination system for marker removal as described in Section A.3(c)(i), (Hare and Chua, 2002; Zhang *et al.*, 2003).

The backbone region of PV-ZMIR522223, located outside of the T-DNA, contains two origins of replication for maintenance of the plasmid vector in bacteria (*oripBR322* and *ori V*) and a bacterial selectable marker gene (*aadA*).

Marker Removal Through Cre/*lox* Recombination System

The use of the Cre/*lox* recombination system for marker removal has been previously described (Russell *et al.*, 1992; Zhang *et al.*, 2003; Hare and Chua, 2002). The Cre/*lox* recombination system is derived from the bacteriophage P1 and consists of the Cre recombinase and a stretch of DNA flanked by two copies of the *lox*P sites. The *lox*P site is 34bp in length and consists of two 13-bp inverted repeats and an asymmetrical 8-bp spacer. The 13-bp inverted repeats are the Cre recombinase binding sequence, and the 8-bp spacer is essential for the recombination reaction. Cre recombinase binds to the inverted repeat sequence in the *lox*P site, catalyzing a crossover in the 8-bp spacer regions of the two *lox*P sites. The results of this crossover are two-fold: one is the excision of the DNA fragment flanked by the two half *lox*P sites (in MON 95379 this is the *cp4 epsps* selectable marker cassette) forming a circular extra-genomic DNA fragment, the other is the recombination of linear DNA between the remaining two half *lox*P sites within the maize genome (Gilbertson, 2003).

As reviewed (Gilbertson, 2003), one of the advantages of the Cre/*lox* system is the specificity of the enzyme for the wild-type *lox*P 34-bp recognition sequence. The frequency of Cre recombinase-mediated DNA recombination can be significantly reduced with even a single nucleotide change in specific regions of the *lox*P sequence (Hartung and Kisters-Woike, 1998; Hoess *et al.*, 1986; Lee and Saito, 1998). Therefore, neither the specific DNA insert nor the usage of the Cre/*lox* system was expected to negatively influence the stability of the T-DNA in MON 95379 across breeding generations, which has been confirmed, and is described in Section A.3(e). This technology was previously reviewed for LY038 maize by the FSANZ in a Food and Feed Safety Assessment (Food Standards 2002, Amendment No. 18).

A maize line expressing Cre recombinase (developed with the transformation plasmid vector PV-ZMOO513642) was crossed with lines transformed with PV-ZMIR522223. In the resulting hybrid plants, the *cp4 epsps* selectable marker cassette that was flanked by the *lox*P sites was excised. The excised *cp4 epsps* selectable marker cassette (circular extra-genomic DNA) was subsequently not maintained during cell division. The *cre* gene and associated genetic elements were subsequently segregated away from the *cry1B.868* and *cry1Da_7* expression cassettes by conventional breeding to produce the MON 95379 product lacking the *cp4 epsps* gene cassette. The absence of both the *cp4 epsps* gene and *cre* gene were confirmed in the F4 generation (Figure 8). Since the *cp4 epsps* gene and sequence derived from PV-ZMOO513642 were eliminated through conventional breeding, the resulting progeny only contain the genes of interest (*cry1B.868* and c*ry1Da_7*) and not the gene used for selection.

Table 1. Summary of Genetic Elements in PV- ZMIR522223

Genetic Element	Location in Plasmid Vector	Function (Reference)
T-DNA		
B[1]-Left Border Region	1-442	DNA region from *Agrobacterium tumefaciens* containing the left border sequence used for transfer of the T–DNA (Barker *et al.*, 1983).
Intervening Sequence	443-477	Sequence used in DNA cloning
***lox*P**	478-511	Sequence from Bacteriophage P1 for the *lox*P recombination site recognized by the Cre protein (Russell *et al.*, 1992).
Intervening Sequence	512-517	Sequence used in DNA cloning
T[4]-*TubA*	518-1099	3' UTR sequence of the *OsTubA* gene from *Oryza sativa* (rice) encoding α–tubulin (Jeon *et al.*, 2000) that directs polyadenylation of mRNA.
Intervening Sequence	1100-1106	Sequence used in DNA cloning
CS[3]-*cp4 epsps*	1107-2474	Coding sequence of the *aroA* gene from *Agrobacterium* sp. strain CP4 encoding the CP4 EPSPS protein that provides herbicide tolerance (Barry *et al.*, 2001; Padgette *et al.*, 1996).
TS[5]-*CTP2*	2475-2702	Targeting sequence of the *ShkG* gene from *Arabidopsis thaliana* encoding the EPSPS transit peptide region that directs transport of the protein to the chloroplast (Klee *et al.*, 1987; Herrmann, 1995).
Intervening Sequence	2703-2706	Sequence used in DNA cloning
P[2]-*TubA*	2707-4887	Promoter, 5' UTR and intron sequences of the *OsTubA* gene family from *Oryza sativa* (rice) encoding α-tubulin (Jeon *et al.*, 2000) that directs transcription in plant cells.
Intervening Sequence	4888-4893	Sequence used in DNA cloning
***lox*P**	4894-4927	Sequence from Bacteriophage P1 for the *lox*P recombination site recognized by the Cre protein (Russell *et al.*, 1992).

Table 1. Summary of Genetic Elements in PV- ZMIR522223 (Continued)

Genetic Element	Location in Plasmid Vector	Function (Reference)
Intervening Sequence	4928-5038	Sequence used in DNA cloning
T[4]-*Ltp*	5039-5338	3' UTR sequence of a *Lipid Transfer Protein-like* gene (*LTP*) from *Oryza sativa* (rice) that directs polyadenylation of mRNA (Hunt, 1994).
Intervening Sequence	5339-5347	Sequence used in DNA cloning
CS[3]-*Cry1B.868*	5348-8947	Coding sequences of three domains and a protoxin sourced from *Bacillus thuringiensis* (*Bt*) parental proteins arranged as a single chimeric pesticidal protein (Cry1B.868) that confers protection against lepidopteran insects via insect midgut disruption (Wang *et al.*, 2019).
Intervening Sequence	8948-8973	Sequence used in DNA cloning
P[2]-*Zm.Ubq*	8974-10981	Promoter, 5' UTR and first intron sequences of the ubiquitin (*Ubq*) gene from *Zea mays* subsp. *Mexicana* (Mexican teosinte) that directs transcription in plant cells (Cornejo *et al.*, 1993).
Intervening Sequence	10982-11008	Sequence used in DNA cloning
E[9]-*FMV*	11009-11545	Enhancer from the 35S RNA of *Figwort mosaic virus* (FMV) (Richins *et al.*, 1987) that enhances transcription in most plant cells (Rogers, 2000).
Intervening Sequence	11546-11556	Sequence used in DNA cloning
P[2]-*Tip*	11557-12537	Promoter and 5' UTR sequences from *Setaria italica* (foxtail millet) *tonoplast membrane integral protein* (*Tip*) gene (Hernandez-Garcia and Finer, 2014).
Intervening Sequence	12538-12545	Sequence used in DNA cloning
I[7]-*Act15*	12546-13838	Intron and flanking UTR sequence from the *Actin 15* (*Act 15*) gene from *Oryza sativa* (rice) that is involved in regulating gene expression (Rose, 2008).
Intervening Sequence	13839-13856	Sequence used in DNA cloning

Table 1. Summary of Genetic Elements in PV- ZMIR522223 (Continued)

Genetic Element	Location in Plasmid Vector	Function (Reference)
CS[3]-*Cry1Da_7*	13857-17357	Codon optimized coding sequence of *cry1Da_7* from *Bacillus thuringiensis* (*Bt*) encoding a modified Cry1Da_7 protein that confers protection against lepidopteran insects via insect midgut disruption (Wang *et al.*, 2019).
Intervening Sequence	17358-17373	Sequence used in DNA cloning
T[4]-*GOS2*	17374-17841	3' UTR sequence from the *GOS2* gene encoding a translation initiation factor from *Oryza sativa* (rice) that directs polyadenylation of mRNA (Hunt, 1994).
Intervening Sequence	17842-18045	Sequence used in DNA cloning
B[1]-Right Border Region	18046-18376	DNA region from *Agrobacterium tumefaciens* containing the right border sequence used for transfer of the T–DNA (Depicker *et al.*, 1982; Zambryski *et al.*, 1982).
Vector Backbone		
Intervening Sequence	18377-18520	Sequence used in DNA cloning
aadA	18521-19409	Bacterial promoter, coding sequence, and 3' UTR for an aminoglycoside-modifying enzyme, 3"(9)–*O*–nucleotidyltransferase from the transposon Tn*7* (Fling *et al.*, 1985) that confers spectinomycin and streptomycin resistance
Intervening Sequence	19410-19943	Sequence used in DNA cloning
OR[8]-*ori-pBR322*	19944-20532	Origin of replication from plasmid pBR322 for maintenance of plasmid in *E. coli* (Sutcliffe, 1979).
Intervening Sequence	20533-21154	Sequence used in DNA cloning
OR[8]-*ori V*	21155-21551	Origin of replication from the broad host range plasmid RK2 for maintenance of plasmid in *Agrobacterium* (Stalker *et al.*, 1981).
Intervening Sequence	21552-21637	Sequence used in DNA cloning

[1] B, Border
[2] P, Promoter
[3] CS, Coding Sequence
[4] T, Transcription Termination Sequence
[5] TS, Targeting Sequence
[6] L, Leader
[7] I, Intron
[8] OR, Origin of Replication
[9] E, Enhancer

The *cry1B.868* Coding Sequence and Cry1B.868 Protein

The *cry1B.868* expression cassette in MON 95379 encodes a 127 kDa Cry1B.868 protein consisting of a single polypeptide of 1199 amino acids (Figure 2). As is typical for plant-expressed proteins, the lead methionine of the Cry1B.868 protein is not present. The *cry1B.868* coding sequence is the coding sequence of domains I and II from Cry1Be, domain III from Cry1Ca, and the C-terminal domain from Cry1Ab from various subspecies of soil bacterium *B. thuringiensis*. The presence of Cry1B.868 protein in maize provides protection against lepidopteran pests.

```
   1 MTSNRKNENE IINALSIPAV SNHSAQMNLS TDARIEDSLC IAEGNNIDPF
  51 VSASTVQTGI NIAGRILGVL GVPFAGQIAS FYSFLVGELW PRGRDPWEIF
 101 LEHVEQLIRQ QVTENTRDTA LARLQGLGNS FRAYQQSLED WLENRDDART
 151 RSVLYTQYIA LELDFLNAMP LFAIRNQEVP LLMVYAQAAN LHLLLLRDAS
 201 LFGSEFGLTS QEIQRYYERQ VEKTREYSDY CARWYNTGLN NLRGTNAESW
 251 LRYNQFRRDL TLGVLDLVAL FPSYDTRVYP MNTSAQLTRE IYTDPIGRTN
 301 APSGFASTNW FNNNAPSFSA IEAAVIRPPH LLDFPEQLTI FSVLSRWSNT
 351 QYMNYWVGHR LESRTIRGSL STSTHGNTNT SINPVTLQFT SRDVYRTESF
 401 AGINILLTTP VNGVPWARFN WRNPLNSLRG SLLYTIGYTG VGTQLFDSET
 451 ELPPETTERP NYESYSHRLS NIRLISGNTL RAPVYSWTHR SADRTNTISS
 501 DSINQIPLVK GFRVWGGTSV ITGPGFTGGD ILRRNTFGDF VSLQVNINSP
 551 ITQRYRLRFR YASSRDARVI VLTGAASTGV GGQVSVNMPL QKTMEIGENL
 601 TSRTFRYTDF SNPFSFRANP DIIGISEQPL FGAGSISSGE LYIDKIEIIL
 651 ADATFEAESD LERAQKAVNE LFTSSNQIGL KTDVTDYHID QVSNLVECLS
 701 DEFCLDEKKE LSEKVKHAKR LSDERNLLQD PNFRGINRQL DRGWRGSTDI
 751 TIQGGDDVFK ENYVTLLGTF DECYPTYLYQ KIDESKLKAY TRYQLRGYIE
 801 DSQDLEIYLI RYNAKHETVN VPGTGSLWPL SAPSPIGKCA HHSHHFSLDI
 851 DVGCTDLNED LGVWVIFKIK TQDGHARLGN LEFLEEKPLV GEALARVKRA
 901 EKKWRDKREK LEWETNIVYK EAKESVDALF VNSQYDRLQA DTNIAMIHAA
 951 DKRVHSIREA YLPELSVIPG VNAAIFEELE GRIFTAFSLY DARNVIKNGD
1001 FNNGLSCWNV KGHVDVEEQN NHRSVLVVPE WEAEVSQEVR VCPGRGYILR
1051 VTAYKEGYGE GCVTIHEIEN NTDELKFSNC VEEEVYPNNT VTCNDYTATQ
1101 EEYEGTYTSR NRGYDGAYES NSSVPADYAS AYEEKAYTDG RRDNPCESNR
1151 GYGDYTPLPA GYVTKELEYF PETDKVWIEI GETEGTFIVD SVELLLMEE
```

Figure 2. Deduced Amino Acid Sequence of the Cry1B.868 Protein

The amino acid sequence of the MON 95379 Cry1B.868 protein was deduced from the full-length coding nucleotide sequence present in PV-ZMIR522223 (See Table 1 for more details). The lead methionine (boxed with solid line) of the Cry1B.868 protein produced in MON 95379 is cleaved *in vivo*.

The *cry1Da_7* Coding Sequence and Cry1Da_7 Protein

The *cry1Da_7* expression cassette in MON 95379 encodes a 132 kDa Cry1Da_7 protein consisting of a single polypeptide of 1166 amino acids (Figure 3). The lead methionine of the Cry1Da_7 protein is cleaved *in vivo*. The *cry1Da_7* coding sequence is a modified version of the *cry1Da* gene in soil bacterium *Bacillus thuringiensis* that encodes the Cry1Da protein. The Cry1Da_7 protein expressed in MON 95379 is highly homologous (approximately 99.7% sequence similarity) to the amino acid sequence of wild-type Cry1Da from *B. thuringiensis*, with one amino acid addition (alanine in position 2) and three amino acid substitutions (S282V, Y316S, I368P). The presence of Cry1Da_7 protein in maize provides protection against lepidopteran pests.

```
   1 MAEINNQNQC VPYNCLSNPK EIILGEERLE TGNTVADISL GLINFLYSNF
  51 VPGGGFIVGL LELIWGFIGP SQWDIFLAQI EQLISQRIEE FARNQAISRL
 101 EGLSNLYKVY VRAFSDWEKD PTNPALREEM RIQFNDMNSA LITAIPLFRV
 151 QNYEVALLSV YVQAANLHLS ILRDVSVFGE RWGYDTATIN NRYSDLTSLI
 201 HVYTNHCVDT YNQGLRRLEG RFLSDWIVYN RFRRQLTISV LDIVAFFPNY
 251 DIRTYPIQTA TQLTREVYLD LPFINENLSP AAVYPTFSAA ESAIIRSPHL
 301 VDFLNSFTIY TDSLARSAYW GGHLVNSFRT GTTTNLIRSP LYGREGNTER
 351 PVTITASPSV PIFRTLSYPT GLDNSNPVAG IEGVEFQNTI SRSIYRKSGP
 401 IDSFSELPPQ DASVSPAIGY SHRLCHATFL ERISGPRIAG TVFSWTHRSA
 451 SPTNEVSPSR ITQIPWVKAH TLASGASVIK GPGFTGGDIL TRNSMGELGT
 501 LRVTFTGRLP QSYYIRFRYA SVANRSGTFR YSQPPSYGIS FPKTMDAGEP
 551 LTSRSFAHTT LFTPITFSRA QEEFDLYIQS GVYIDRIEFI PVTATFEAEY
 601 DLERAQKVVN ALFTSTNQLG LKTDVTDYHI DQVSNLVACL SDEFCLDEKR
 651 ELSEKVKHAK RLSDERNLLQ DPNFRGINRQ PDRGWRGSTD ITIQGGDDVF
 701 KENYVTLPGT FDECYPTYLY QKIDESKLKA YTRYQLRGYI EDSQDLEIYL
 751 IRYNAKHEIV NVPGTGSLWP LSVENQIGPC GEPNRCAPHL EWNPDLHCSC
 801 RDGEKCAHHS HHFSLDIDVG CTDLNEDLGV WVIFKIKTQD GHARLGNLEF
 851 LEEKPLLGEA LARVKRAEKK WRDKRETLQL ETTIVYKEAK ESVDALFVNS
 901 QYDRLQADTN IAMIHAADKR VHRIREAYLP ELSVIPGVNA AIFEELEERI
 951 FTAFSLYDAR NIIKNGDFNN GLLCWNVKGH VEVEEQNNHR SVLVIPEWEA
1001 EVSQEVRVCP GRGYILRVTA YKEGYGEGCV TIHEIENNTD ELKFNNCVEE
1051 EVYPNNTVTC INYTATQEEY EGTYTSRNRG YDEAYGNNPS VPADYASVYE
1101 EKSYTDRRRE NPCESNRGYG DYTPLPAGYV TKELEYFPET DKVWIEIGET
1151 EGTFIVDSVE LLLMEE
```

Figure 3. Deduced Amino Acid Sequence of the Cry1Da_7 Protein

The amino acid sequence of the MON 95379 Cry1Da_7 protein was deduced from the full-length coding nucleotide sequence present in PV-ZMIR522223 (See Table 1 for more details). The lead methionine (boxed with solid line) of the Cry1Da_7 protein produced in MON 95379 is cleaved *in vivo*.

Regulatory Sequences

The *cry1B.868* coding sequence in MON 95379 is under the regulation of the promoter, 5' untranslated region (UTR) and intron for a ubiquitin gene (*Ubq*) from *Zea mays* subsp. *Mexicana* (*Mexican teosinte*) that direct transcription in plant cells (Cornejo *et al.*, 1993). The *cry1B.868* coding sequence also utilizes the 3′ UTR sequence of the *Lipid Transfer Protein-like* gene (*LTP*) from *Oryza sativa* (rice) that directs polyadenylation of mRNA (Hunt, 1994).

The codon optimized *cry1Da_7* coding sequence in MON 95379 is under the regulation of the enhancer from the 35S RNA of *Figwort mosaic virus* (FMV) (Richins *et al.*, 1987) that enhances transcription in most plant cells (Rogers, 2000). In addition to the enhancer the *cry1Da_7* coding sequence is regulated by the promoter and 5' UTR from *Setaria italica* (foxtail millet) *tonoplast membrane integral protein* (*Tip)* gene (Hernandez-Garcia and Finer, 2014) and the intron and flanking UTR sequence from the *Actin 15* (*Act 15*) gene from *Oryza sativa* (rice) that is involved in regulating gene expression (Rose, 2008). The *cry1Da_7* coding sequence also utilizes 3' UTR sequence from the *GOS2* gene encoding a translation initiation factor from *Oryza sativa* (rice) that directs polyadenylation of mRNA (Hunt, 1994).

The *cp4 epsps* selectable marker cassette is also part of the originally inserted T-DNA in MON 95379. The selectable marker cassette is under the regulation of the promoter, 5' UTR, intron and 3′ UTR sequences of the *OsTubA* gene family from *Oryza sativa* (rice) encoding α-tubulin (Jeon *et al.*, 2000) that directs transcription and polyadenylation of mRNA in plant cells. The *cp4 epsps* gene was eliminated from subsequent progeny using the Cre/*lox* recombination system for marker removal (Hare and Chua, 2002; Zhang *et al.*, 2003). The *cp4 epsps* cassette was flanked by *lox*P sites that allowed the cassette to be excised by Cre recombinase when plants were crossed with maize plants expressing the *cre* gene (the "Cre line" was developed with the transformation plasmid vector PV-ZMOO513642). The *cre* gene was subsequently segregated out by conventional breeding to produce the MON 95379 product from which the *cp4 epsps* gene was eliminated. The absence of both the *cp4 epsps* gene, the *cre* gene and their associated genetic elements were confirmed in the F4 generation (Figure 8). Since the *cp4 epsps* gene and sequence derived from PV-ZMOO513642 were eliminated through conventional breeding, the resulting progeny only contain the genes of interest (*cry1B.868* and *cry1Da_7*) and not the gene used for selection.

T-DNA Border Regions

PV-ZMIR522223 contains Left and Right Border regions (Figure 4 and Table 1) that were derived from *A. tumefaciens* plasmids. The border regions each contain a nick site that is the site of DNA exchange during transformation (Barker *et al.*, 1983; Depicker *et al.*, 1982; Zambryski *et al.*, 1982). The border regions separate the T-DNA from the plasmid backbone region and are involved in the efficient transfer of T-DNA into the maize genome.

Genetic Elements Outside of the T-DNA Border Regions

Genetic elements that exist outside of the T-DNA border regions are those that are essential for the maintenance or selection of PV-ZMIR522223 in bacteria and are referred to as plasmid backbone. The origin of replication, *ori V*, is required for the maintenance of the plasmid in *Agrobacterium* and is derived from the broad host range plasmid RK2 (Stalker *et al.*, 1981). The origin of replication, *ori-pBR322*, is required for the maintenance of the plasmid in *E. coli* and is derived from the plasmid vector pBR322 (Sutcliffe, 1979). The selectable marker *aadA* is the coding sequence for an aminoglycoside-modifying enzyme, 3"(9)–*O*–nucleotidyltransferase from the transposon Tn*7* (Fling *et al.*, 1985) that confers spectinomycin and streptomycin resistance in *E. coli* and *Agrobacterium* during molecular cloning. Because these elements are outside the border regions, they are not expected to be

transferred into the maize genome. The absence of the backbone and other unintended plasmid sequence in MON 95379 was confirmed by sequencing and bioinformatic analyses (Section A.3(c)(ii)).

For details, please refer to Appendix 1 ([redacted]., 2020 (TRR0000070)).

A.3(b)(ii) A detailed map of the location and orientation of all genetic elements contained within the construct and vector, including the location of relevant restriction sites

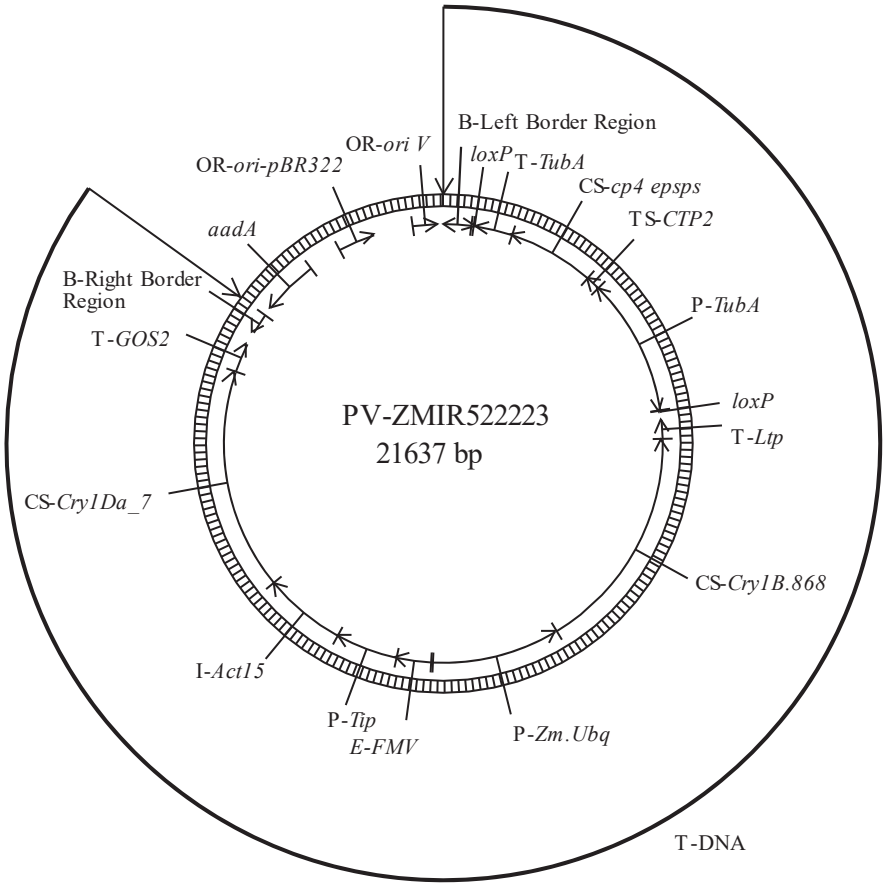

Figure 4. Circular Map of PV-ZMIR522223

A circular map of PV-ZMIR522223 used to develop MON 95379 is shown. PV-ZMIR522223 contains one T–DNA. Genetic elements are shown on the exterior of the map.

A.3(c) A full molecular characterisation of the genetic modification in the new organism, including:

A.3(c)(i) Identification of all transferred genetic material and whether it has undergone any rearrangements

This section describes the methods and results of a comprehensive molecular characterisation of the genetic modification present in MON 95379. It provides information on the DNA insertion(s) into the plant genome of MON 95379, and additional information regarding the arrangement and stability of the introduced genetic material. The information provided in this section addresses the relevant factors in Codex Plant Guidelines, Section 4, paragraphs 30, 31, 32, and 33 (Codex Alimentarius, 2009).

A schematic representation of the Next Generation Sequencing (NGS) methodology and the basis of the characterisation using NGS and PCR sequencing are illustrated in Figure 5 below.

For details, please refer to Appendix 1 ([redacted], 2020 (TRR0000070)).

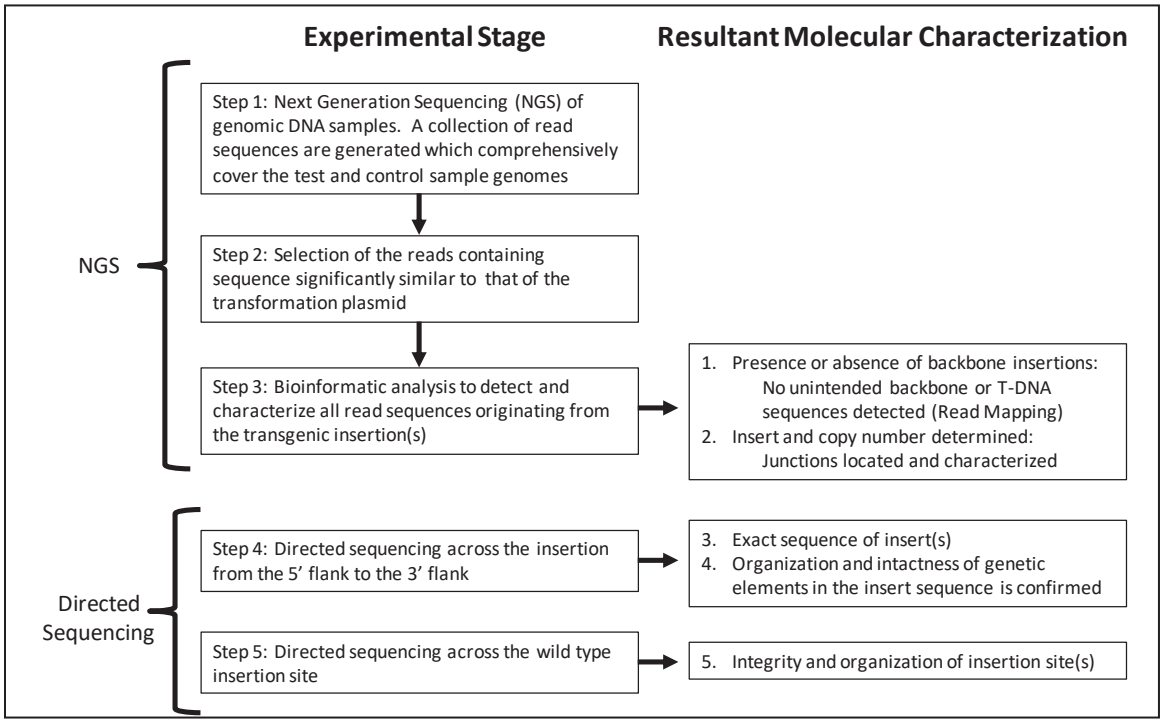

Figure 5. Molecular Characterisation using Sequencing and Bioinformatics

Genomic DNA from the test and the conventional control was sequenced using technology that produces a set of short, randomly distributed sequence reads that comprehensively cover test and control genomes (Step 1). Utilizing these genomic sequence reads, bioinformatics searches are conducted to identify all sequence reads that are significantly similar to the transformation plasmid (Step 2). These captured reads are then mapped and analyzed to determine the presence/absence of transformation plasmid backbone sequences, identify insert junctions, and to determine the insert and copy number (Step 3). Overlapping PCR products are also produced which span any insert and their wild type locus (Step 4 and Step 5, respectively); these overlapping PCR products are sequenced to allow for detailed characterisation of the inserted DNA and insertion site.

The NGS method was used to characterize the genomic DNA from MON 95379 and the conventional control by generating short (~150 bp) randomly distributed sequence fragments (sequencing reads) generated in sufficient number to ensure comprehensive coverage of the sample genomes. It has been previously demonstrated that whole genome sequencing at 75× depth of coverage is adequate to provide comprehensive coverage and ensure detection of inserted DNA (Kovalic *et al.*, 2012). A comprehensive analysis of NGS as a characterisation method demonstrated that coverage depth as low as 11× is sufficient to detect both intended transgenes as well as unintended inserted vector-derived fragments as small as 25 base pairs in length (Cade *et al.*, 2018). Therefore, 75× coverage is a robust level of sequencing for the complete characterisation of both homozygous and hemizygous transgenes, and, well in excess of the levels which have been demonstrated as sufficient for identifying unintended inserted fragments. To confirm sufficient sequence coverage of the genome, the 150 bp sequence reads were analyzed to determine the coverage of a known single-copy endogenous maize gene. This establishes the depth of coverage (the median number of times each base of the genome is independently sequenced). Furthermore, the sensitivity of the method was assessed by sequencing the transformation plasmid and then sampling the data to represent a single genome equivalent dataset and a $1/10^{th}$ genome equivalent dataset. This confirms the method's ability to detect any sequences derived from the transformation plasmid. Bioinformatics analysis was then used to select sequencing reads that contained sequences similar to the transformation plasmid, and these were analyzed in depth to determine the number of DNA inserts. NGS was run on five breeding generations of MON 95379 and the appropriate conventional controls. Results of NGS are shown in Sections A.3(c)(ii) to A.3(c)(iii).

Directed sequencing (locus-specific PCR and DNA sequencing analyses, Figure 5, Step 4) complements the NGS method. Sequencing of the insert and flanking genomic DNA determined the complete sequence of the insert and flanks by evaluating if the sequence of the insert was identical to the corresponding sequence from the T-DNA in PV-ZMIR522223, and if each genetic element in the insert was intact. It also characterizes the flank sequence beyond the insert corresponding to the genomic DNA of the transformed maize. Results are described in Sections A.3(c)(i) and A.3(c)(ii).

A.3(c)(ii) A determination of number of insertion sites, and the number of copies at each insertion site

The number of DNA inserts in MON 95379 was determined by mapping of sequencing reads relative to the transformation plasmid and identifying junctions and unpaired read mappings adjacent to the junctions. Examples of five types of NGS reads are shown in Figure 6. The junctions of the DNA insert and the flanking DNA are unique for each insertion (Kovalic *et al.*, 2012). Therefore, insertion sites can be recognized by analyzing for sequence reads containing such junctions.

For details, please refer to Appendix 1 ([redacted] 2020 (TRR0000070)).

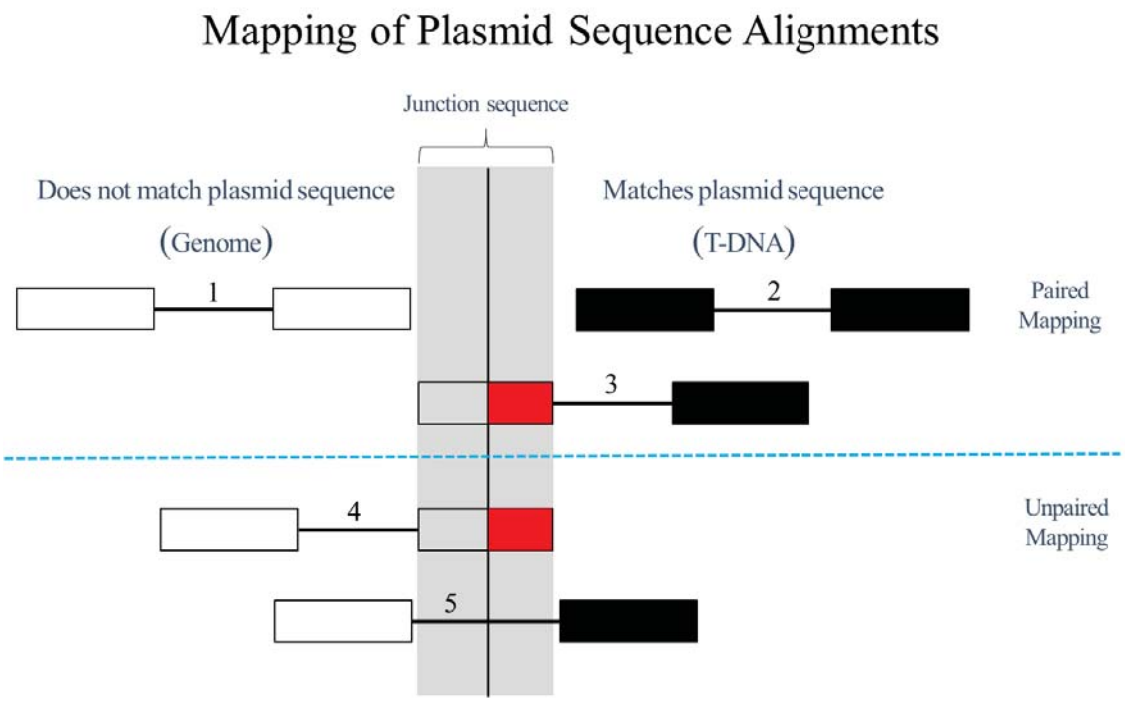

Figure 6. Five Types of NGS Reads

NGS yields data in the form of read pairs where sequence from each end of a size selected DNA fragment is returned. Depicted above are five types of sequencing reads/read pairs generated by NGS sequencing which can be found spanning or outside of junction points. Sequence boxes are color-filled if it matches with plasmid sequence, and empty if it matches with genomic sequence. Grey highlighting indicates sequence reads spanning the junction. Junctions are detected by examining the NGS data for reads having portions of plasmid sequences that span less than the full read, as well as reads mapping adjacent to the junction points where their mate pair does not map to the plasmid sequence. The five types of sequencing reads/read pairs being (1) Paired and unpaired reads mapping to genomic sequence outside of the insert, greater than 99.999% of collected reads fall into this category and are not evaluated in this analysis, (2) Paired reads mapping entirely to the transformation plasmid sequence, such reads reveal the presence of transformation sequence in planta, (3) Paired reads where one read maps entirely within the inserted DNA and the other read maps partially to the insert (indicating a junction point), (4) Single read mapping partially to the transformation plasmid DNA sequence (indicating a junction point) where its mate maps entirely to the genomic flanking sequence and (5) Single read mapping entirely to the transformation plasmid DNA sequence where its mate maps entirely to genomic flanking sequence, such reads are part of the junction signature.

The number of inserted DNA sequences from PV-ZMIR522223 in MON 95379 was assessed by generating a comprehensive collection of reads via NGS of MON 95379 genomic DNA using the F4 generation (Figure 8). A plasmid map of PV- ZMIR522223 is shown in Figure 4. Table 2 provides descriptions of the genetic elements present in MON 95379. A schematic representation of the insert and flanking sequences in MON 95379 is shown in Figure 7.

Next Generation Sequencing for MON 95379 and Conventional Control Genomic DNA

Genomic DNA from five distinct breeding generations of MON 95379 (Figure 8) and conventional controls were isolated from seed and prepared for sequencing. These genomic DNA libraries were used to generate short (~150 bp) randomly distributed sequencing reads of the maize genome (Figure 5, Step 1).

To demonstrate sufficient sequence coverage the ~150 bp sequence reads were analyzed by mapping all reads to a known single copy endogenous gene (*Zea mays* pyruvate decarboxylase (*pdc3*), GenBank Accession: AF370006.2) in each of the five distinct breeding generations. The analysis of sequence coverage plots showed that the depth of coverage (i.e., the median number of times any base of the genome is expected to be independently sequenced) was 82× or greater for the five generations of MON 95379 (F4, F5, F4F1, F5F1, and F6F1) and the conventional controls. It has been previously demonstrated that whole genome sequencing at 75× depth of coverage provides comprehensive coverage and ensures detection of inserted DNA (Kovalic *et al.*, 2012; Cade *et al.*, 2018).

To demonstrate the method's ability to detect any sequences derived from the PV-ZMIR522223 transformation plasmid or the Cre recombinase-containing transformation plasmid vector PV-ZMOO513642, a sample of PV-ZMIR522223 and PV-ZMOO513642, were sequenced by NGS following the same processes outlined for all samples in Appendix 1. The resulting PV-ZMIR522223 and PV-ZMOO513642 reads were randomly selected to achieve a depth of one and 1/10th genome equivalent (relative to the median coverage of the LH244 conventional control). In all cases, 100% coverage of the known PV-ZMIR522223 or PV-ZMOO513642 sequences were observed. This result demonstrates that all nucleotides of PV-ZMIR522223 and PV-ZMOO513642 are detectable by the sequencing and bioinformatic assessments performed and that a detection level of at least 1/10th genome equivalent was achieved for the plasmid DNA sequence assessment.

Table 2. Summary of Genetic Elements in MON 95379

Genetic Element[1]	Location in Sequence[2]	Function (Reference)
5' Flanking DNA	1-1000	DNA sequence flanking the 5' end of the insert
B[3]-Left Border Region r1	1001-1186	DNA region from *Agrobacterium tumefaciens* containing the left border sequence used for transfer of the T–DNA (Barker *et al.*, 1983).
Intervening Sequence	1187-1221	Sequence used in DNA cloning
***lox*P**	1222-1255	Sequence from Bacteriophage P1 for the *lox*P recombination site recognized by the Cre recombinase (Russell *et al.*, 1992).
Intervening Sequence	1256-1366	Sequence used in DNA cloning
T[4]-*Ltp*	1367-1666	3' UTR sequence of a *Lipid Transfer Protein-like* gene (*LTP*) from *Oryza sativa* (rice) that directs polyadenylation of mRNA (Hunt, 1994).
Intervening Sequence	1667-1675	Sequence used in DNA cloning
CS[5]-*Cry1B.868*	1676-5275	Coding sequences of three domains and a protoxin sourced from *Bacillus thuringiensis* (*Bt*) parental proteins arranged as a single chimeric pesticidal protein (Cry1B.868) that confers protection against lepidopteran insect pests via insect midgut disruption (Wang *et al.*, 2019).
Intervening Sequence	5276-5301	Sequence used in DNA cloning
P[6]-*Zm.Ubq*	5302-7309	Promoter, 5' UTR and first intron sequences of the ubiquitin (*Ubq*) gene from *Zea mays* subsp. *Mexicana* (Mexican teosinte) that directs transcription in plant cells (Cornejo *et al.*, 1993).
Intervening Sequence	7310-7336	Sequence used in DNA cloning
E[7]-*FMV*	7337-7873	Enhancer from the 35S RNA of *Figwort mosaic virus* (FMV) (Richins *et al.*, 1987) that enhances transcription in most plant cells (Rogers, 2000).
Intervening Sequence	7874-7884	Sequence used in DNA cloning

Table 2. Summary of Genetic Elements in MON 95379 (Continued)

Genetic Element[1]	Location in Sequence[2]	Function (Reference)
P-*Tip*	7885-8865	Promoter and 5' UTR sequences from *Setaria italica* (foxtail millet) *tonoplast membrane integral protein* (*Tip*) gene (Hernandez-Garcia and Finer, 2014).
Intervening Sequence	8866-8873	Sequence used in DNA cloning
I[8]-*Act15*	8874-10166	Intron and flanking UTR sequence from the *Actin 15* (*Act 15*) gene from *Oryza sativa* (rice) that is involved in regulating gene expression (Rose, 2008).
Intervening Sequence	10167-10184	Sequence used in DNA cloning
CS-*Cry1Da_7*	10185-13685	Codon optimized coding sequence of *cry1Da_7* from *Bacillus thuringiensis* (*Bt*) encoding a modified Cry1Da_7 protein that confers protection against lepidopteran insect pests via insect midgut disruption (Wang *et al.*, 2019).
Intervening Sequence	13686-13701	Sequence used in DNA cloning
T-*GOS2*	13702-14169	3' UTR sequence from the *GOS2* gene encoding a translation initiation factor from *Oryza sativa* (rice) that directs polyadenylation of mRNA (Hunt, 1994).
Intervening Sequence	14170-14322	Sequence used in DNA cloning
3' Flanking DNA	14323-15322	DNA sequence flanking the 3' end of the insert

[1] Although flanking sequences and intervening sequences are not functional genetic elements, they comprise a portion of the sequence.
[2] Numbering refers to the sequence of the insert in MON 95379 and adjacent DNA
[3] B, Border
[4] T, Transcription Termination Sequence
[5] CS, Coding Sequence
[6] P, Promoter
[7] E, Enhancer
[8] I, Intron
[r1] Superscript in Left indicate that the sequence in MON 95379 was truncated compared to the sequences in PV-ZMIR522223

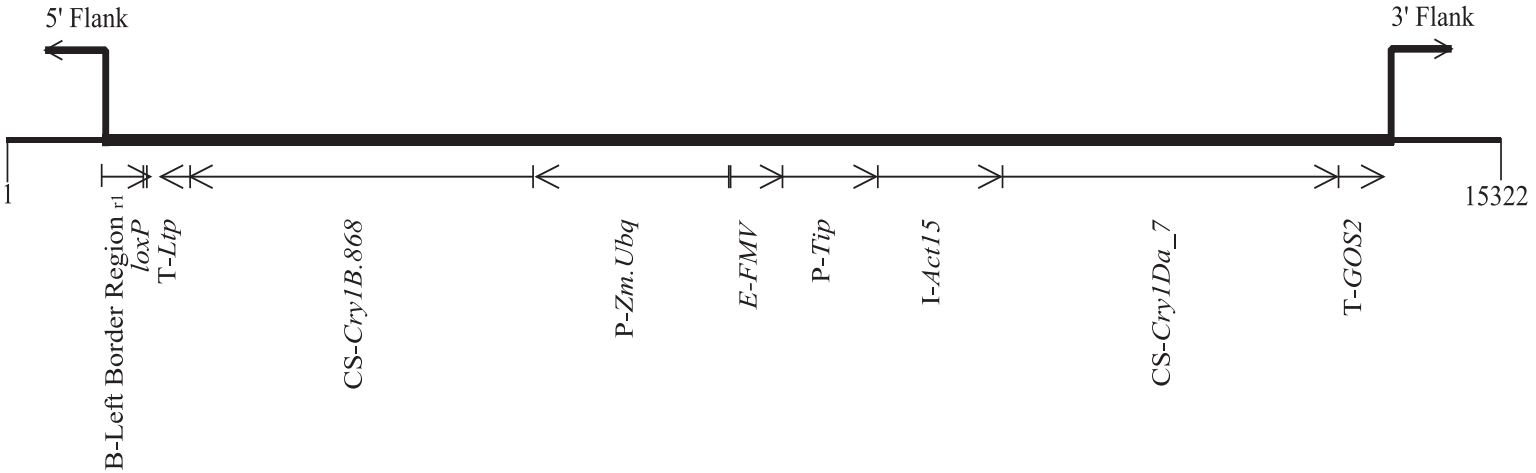

Figure 7. Schematic Representation of the Insert and Flanking Sequences in MON 95379

DNA derived from T-DNA of PV-ZMIR522223 integrated in MON 95379. Right-angled arrows indicate the ends of the integrated T-DNA and the beginning of the flanking sequence. Identified on the map are genetic elements within the insert. This schematic diagram may not be drawn to scale.

[r1] Superscript in Left Border Regions indicate that the sequence in MON 95379 was truncated compared to the sequences in PV-ZMIR522223.

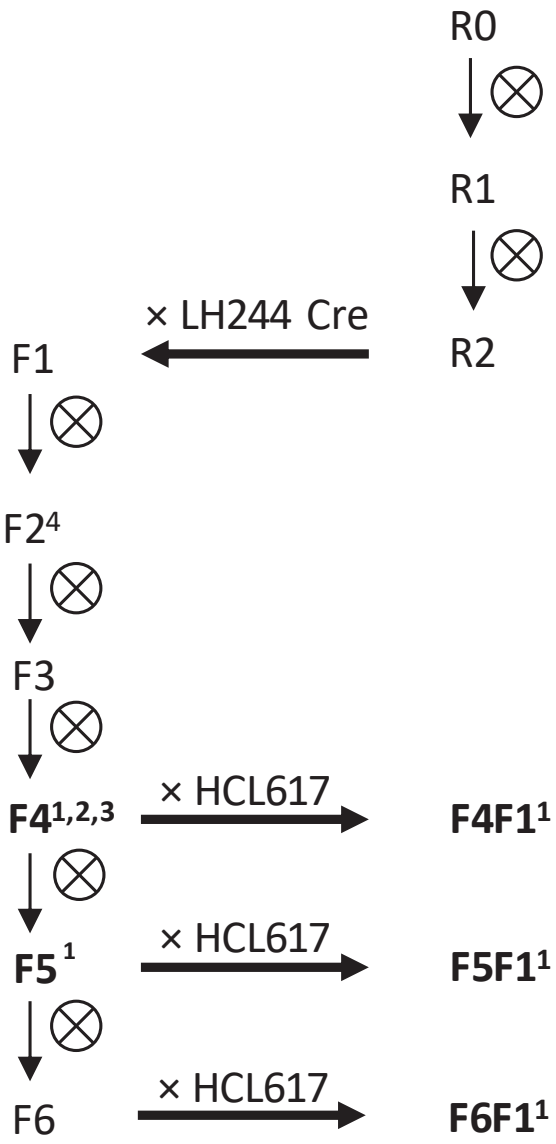

Figure 8. Breeding History of MON 95379

The generations used for molecular characterisation and insert stability analyses are indicated in bold text. R0 corresponds to the transformed plant, ⊗ designates self-pollination.

[1]Generations used to confirm insert stability
[2] Generation used for molecular characterisation
[3] Generation used for commercial development of MON 95379
[4] The F2 generation was screened for plants lacking the *cre* gene. Only those plants lacking the *cre* gene were self-pollinated to create a F3 population of plants lacking the *cre* gene.

Selection of Sequence Reads Containing Sequence of the PV-ZMIR522223 and PV-ZMOO513642

The transformation plasmid, PV-ZMIR522223, was transformed into the parental variety LH244 to produce MON 95379. Consequently, any DNA inserted into MON 95379 will consist of sequences that are similar to the PV-ZMIR522223 DNA sequence. Therefore, to fully characterize the DNA from PV-ZMIR522223 inserted in MON 95379, it is sufficient to completely analyze only the sequence reads that have similarity to PV-ZMIR522223 (Figure 5, Step 2). Similarly, to confirm the absence of the Cre-containing transformation plasmid vector, PV-ZMOO513642, in MON 95379 it is sufficient to completely analyze only the sequence reads that have similarity to PV-ZMOO513642.

Using established criteria (described in Appendix 1), any sequence reads similar to PV-ZMIR522223 and PV-ZMOO513642 were selected from MON 95379 sequence datasets (PV-ZMOO513642 selection was only conducted on the F4 generation) and were then used as input data for bioinformatic junction sequence analysis. PV-ZMIR522223 and PV-ZMOO513642 sequences were also compared against the conventional control sequence datasets.

Determination of T-DNA Copy Number and Presence or Absence of Plasmid Vector Backbone

Mapping sequence reads relative to the transformation plasmid allows for the identification of junction signatures, the presence or absence of plasmid backbone sequence and the number of T-DNA insertions. For a single copy T-DNA insert sequence at a single genomic locus and the complete absence of plasmid vector backbone, a single junction signature pair and few if any reads aligning with the transformation plasmid backbone sequences are expected.

When reads from the LH244 dataset were aligned with the transformation plasmid sequence, a number of reads mapped to the T-DNA promoter element *Zm.Ubq* sequence (Figure 9). The alignment of these sequence reads is the result of an endogenous maize sequence that is homologous to the T-DNA encoded promoter element *Zm.Ubq* sequence. No other regions of homology were identified between the PV-ZMIR522223 transformation plasmid reference sequence and the conventional control.

When reads from the MON 95379 (F4) dataset were aligned with the transformation plasmid sequence, large numbers of reads mapped to the intended T-DNA sequence, one paired read was identified which aligned to the transformation plasmid backbone, a number of unpaired reads aligned to the T-DNA promoter element *Zm.Ubq*, and no reads mapped to the selectable marker cassette (Figure 10). The presence of unpaired reads aliging to this *Zm.Ubq* are indicative of sequences from an endogenous maize element mapping to the transformation vector. This is most readily observed by comparing and contrasting the unpaired reads aligning to the *Zm.Ubq* region to those observed in the LH244 conventional control dataset (Panel 1, Figure 9 and Figure 10). A comparison of mapped reads from F4 and the conventional control reveals that mapped reads are present at sample equivalent levels and show virtually identical mapping signatures. This, in conjunction with an absence of junction sites, indicates that all additional reads and subsequent relative increases of depth across this region are entirely derived from the endogenous maize *Zm.Ubq* homolog, and therefore not indicative of any additional T-DNA insertion (partial or whole). The mapping of large numbers of reads from the MON 95379 (F4) dataset to the intended T-DNA sequence is expected and fully consistent with the presence of the inserted DNA.

A single pair of reads was found to align with OR-*ori-pBR322* sequences (Figure 10). The sporadic low-level detection of plasmid sequences such as OR-*ori-pBR322* has previously

been described (Zastrow-Hayes *et al.*, 2015), and reported (see Supplemental Figure S1 in Yang *et al.* (2013)), and is due to the presence of environmental bacteria in tissue samples used in the preparation of genomic DNA used for library construction. The presence of this sequence from environmental bacteria does not indicate the presence of backbone sequence in the MON 95379 (F4) generation. This analysis indicates that MON 95379 (F4) does not contain inserted sequence from the transformation plasmid backbone.

No reads mapped to the selectable marker cassette (T-*TubA*, TS-*CTP2,* CS- *cp4 epsps*, and P-*TubA*). This result is expected as MON 95379 was crossed with a Cre recombinase expressing line that enable the removal of the *cp4 epsps* gene cassette positioned between two excision targeting *lox* sites (Hare and Chua, 2002; Zhang *et al.*, 2003). After excision, a single *lox* site remained, as expected. The absence of the selectable marker cassette results in a gap in reads as illustrated in Figure 10.

To determine the insert number in MON 95379 (F4), selected reads mapping to T-DNA as described above were analyzed to identify junctions. This bioinformatic analysis is used to find and classify partially matched reads characteristic of the ends of insertions. The number of unique junctions determined by this analysis are shown in Table 3.

Table 3. Unique Junction Sequence Results

Sample	Junctions Detected
MON 95379 (F4)	2
LH244	0

Detailed mapping information of the junction sequences is shown in Figure 10. The location and orientation of the junction sequences relative to T-DNA insert determined for MON 95379 are illustrated in Figure 10, panels 1 and 2. As shown in the figure, there are two junctions identified in MON 95379. Both junctions contain the T-DNA border sequence joined to flanking genomic sequence, indicating that they represent the sequences at the junctions of the intended T-DNA insert and the maize genome. As described earlier, no junctions were detected in any of the conventional maize control samples.

Considered together, the absence of plasmid backbone and the presence of two junctions (joining T-DNA borders and flanking sequences) indicate a single intended T-DNA at a single locus in the genome of MON 95379. Both of these junctions originate from the same locus of the MON 95379 genome and are linked by contiguous, previously determined and expected DNA sequence (with the exception of the selectable marker cassette which was excised as described earlier). This is demonstrated by complete coverage of the sequenced reads spanning the interval between the junctions and the directed sequencing of overlapping PCR products described in Section A.3.

Based on the comprehensive NGS and junction identification it is concluded that MON 95379 contains one copy of the T-DNA inserted into a single locus. This conclusion is confirmed by the sequencing and analysis of overlapping PCR products from this locus as described in Section A.3 below.

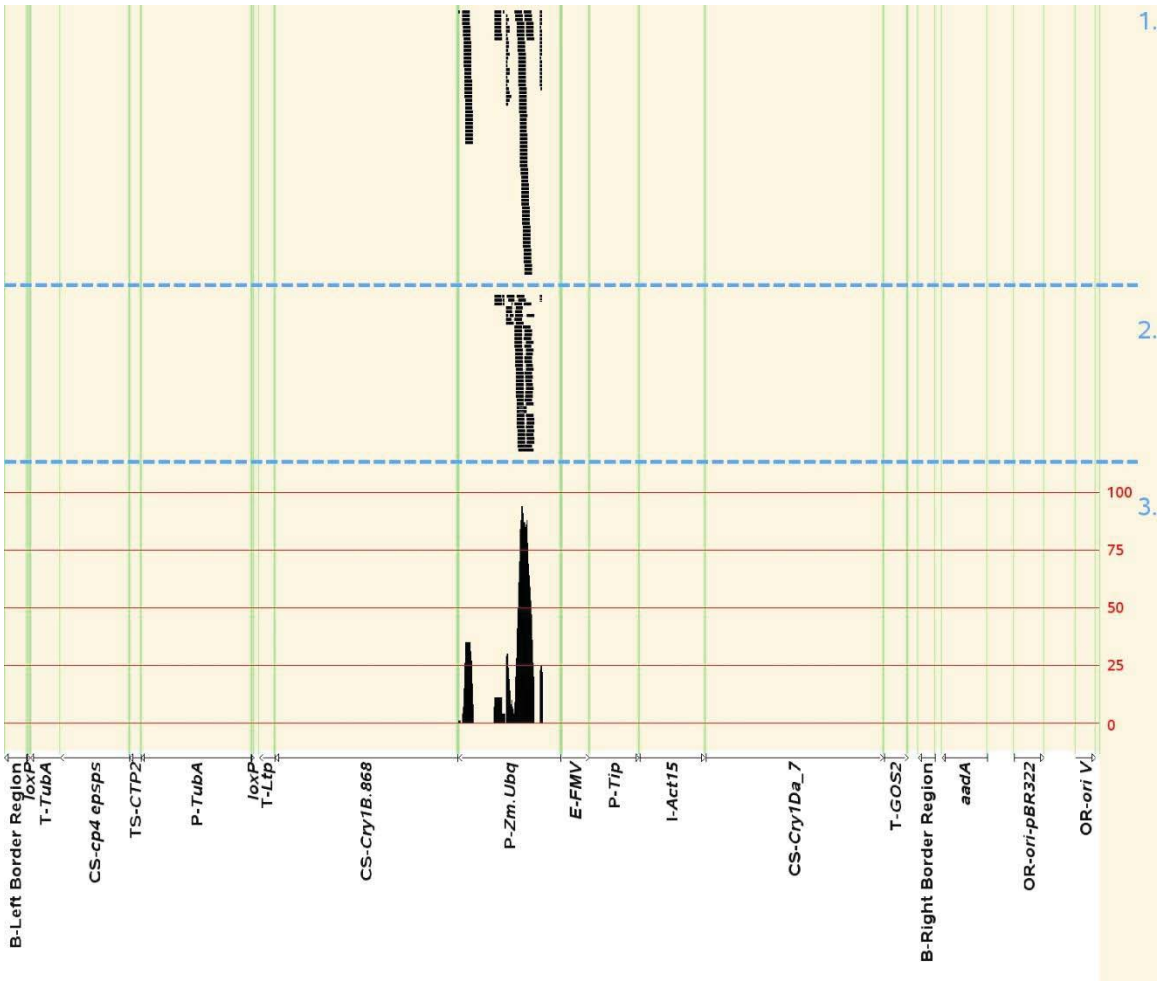

Figure 9. Read Mapping of Conventional Maize LH244 Versus PV-ZMIR522223

Panel 1 shows the location of unpaired mapped reads, Panel 2 shows paired mapped reads, and Panel 3 shows a representation of combined raw read depth for unpaired and paired reads across the reference sequence.
Vertical lines show genetic element boundaries.

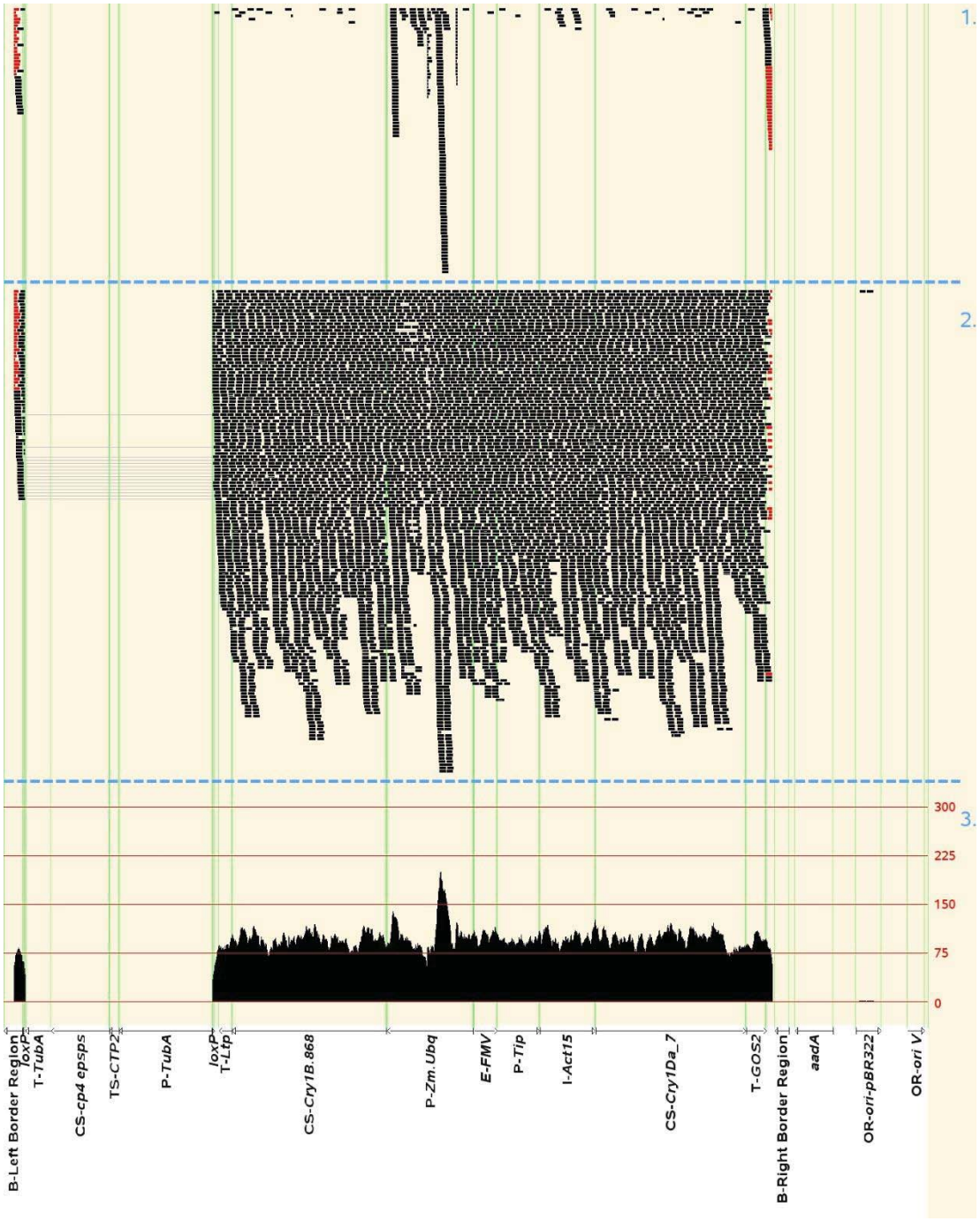

Figure 10. Read Mapping of MON 95379 (F4) Versus PV-ZMIR522223

Panel 1 shows the location of unpaired mapped reads. Panel 2 shows paired mapped reads and Panel 3 shows a representation of combined raw read depth for unpaired and paired reads across the reference sequence. Vertical lines show genetic element boundaries. The region of flank junction sequences that align with the transformation plasmid are shown in red.

Determination of Absence of Plasmid Vector PV-ZMOO513642

At the R2 generation (Figure 8), MON 95379 was crossed with a Cre recombinase expressing line. The Cre/*lox* technology enables the removal of the selectable marker cassette (T-*TubA*, TS-*CTP2,* CS-*cp4 epsps*, and P-*TubA*) which was inserted during the transformation as part of the T-DNA insertion that also included the *cry1B.868* and *cry1Da_7* trait cassettes. The resulting F1 progeny were self-pollinated and plants from the F2 generation were screened for the absence of the *cre* gene and associated genetic elements (and other sequences from plasmid PV-ZMOO513642), allowing for selection of lines lacking the Cre recombinase cassette that were used as the progenitor of subsequent generations and the final product.

To confirm the absence of the Cre recombinase cassette and any part of the *cre* gene containing transformation vector, MON 95379 was assessed by utilizing the comprehensive collection of generation F4 NGS reads and subsequently mapping them to the *cre* gene containing transformation plasmid (PV-ZMOO513642) sequence Figure 11. In the absence of any PV-ZMOO513642 insertions there should be zero junction signature pairs and limited reads aligning with the PV-ZMOO513642 sequences.

When reads from the MON 95379 (F4) dataset were aligned with the PV-ZMOO513642 sequence, a number of reads aligned to the left border region (B-Left Border Region). Only a small number of reads mapping to the promoter element *Ract1* mapped to T-DNA, and only one paired read was identified which aligned to the PV-ZMOO513642 backbone (Figure 11).

The mapping of a number of reads from the MON 95379 (F4) dataset to the left border region (B-Left Border Region) is expected since PV-ZMOO513642 and PV-ZMIR522223 share the same left border region sequence and PV-ZMIR522223's left border region is present in MON 95379 (Figure 10). The small number of reads mapping to the promoter element *Ract1* are also present in the LH244 control background. This is fully consistent with the presence of a homologous sequence being present in the LH244 control background (Figure 12) and does not indicate the presence of PV-ZMOO513642 T-DNA in MON 95379. Additionally, a single pair of reads was found to align with OR-*ori-pBR322* sequences (Figure 11). The sporadic low level detection of plasmid sequences such as OR-*ori-pBR322* has previously been described (Zastrow-Hayes *et al.*, 2015), and reported (see Supplemental Figure S1 in Yang *et al.* (2013)), and is due to the presence of environmental bacteria in tissue samples used in the preparation of genomic DNA used for library construction. As such, the incidence of this sequence from environmental bacteria does not indicate the presence of backbone sequence in the MON 95379 (F4) generation. Considered together, the limited reads aligning with the PV-ZMOO513642 sequences and the absence junctions (joining T-DNA borders and flanking sequences; Table 4) indicate that MON 95379 (F4), and subsequent generations, do not contain inserted sequence from the *cre* gene containing transformation plasmid, PV-ZMOO513642.

Table 4. Unique Junction Sequence Results

Sample	Junctions Detected
MON 95379 (F4)	0
LH244	0

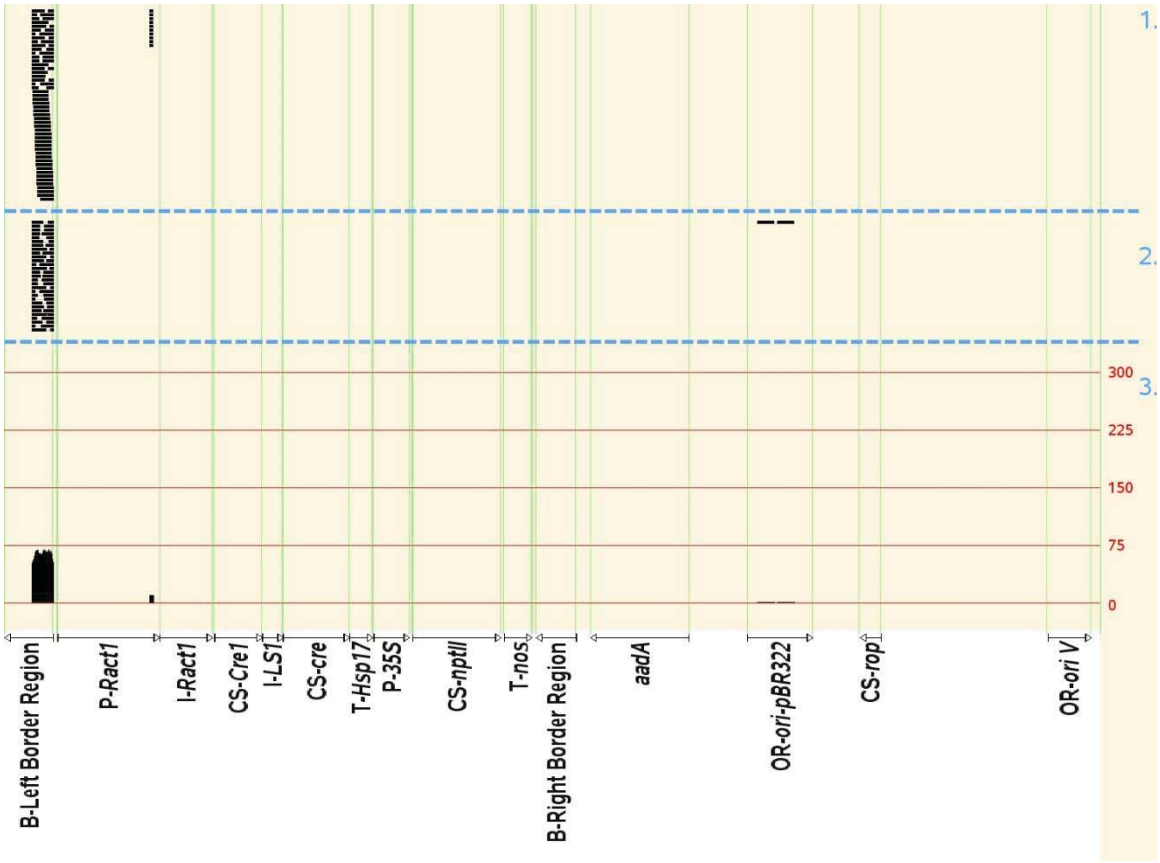

Figure 11. Read Mapping of MON 95379 (F4) Versus PV-ZMOO513642

Panel 1 shows the location of unpaired mapped reads. Panel 2 shows paired mapped reads and Panel 3 shows a representation of combined raw read depth for unpaired and paired reads across the reference sequence. Vertical lines show genetic element boundaries.

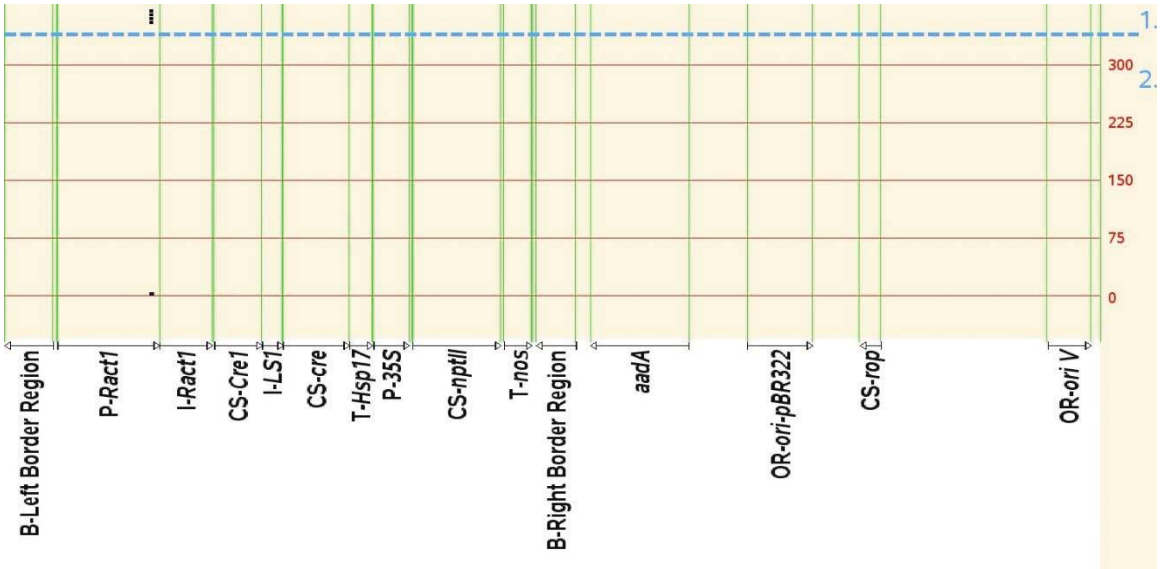

Figure 12. Read Mapping of Conventional Maize LH244 Versus PV-ZMOO513642

Panel 1 shows the location of unpaired mapped reads, there are no paired mapped reads, and Panel 2 shows a representation of combined raw read depth for unpaired and paired reads across the reference sequence.
Vertical lines show genetic element boundaries.

A.3(c)(iii) Full DNA sequence of each insertion site, including junction regions with the host DNA

Organisation and Sequence of the Insert and Adjacent DNA in MON 95379

The organisation of the elements within the DNA insert and the adjacent genomic DNA was assessed using directed DNA sequence analysis (refer to Figure 5, Step 4). PCR primers were designed to amplify two overlapping regions of the MON 95379 genomic DNA that span the entire length of the insert and the adjacent DNA flanking the insert (Figure 13). The amplified PCR products were subjected to DNA sequencing analyses. The results of this analysis confirm that the MON 95379 insert is 13322 bp and that each genetic element within the T-DNA is intact compared to PV-ZMIR522223, with the exception of the border regions. The right border region was absent and the left border region contained small terminal deletions with the remainder of the inserted border region being identical to the sequence in PV-ZMIR522223. The sequence and organisation of the insert was also shown to be identical to the corresponding T-DNA of PV-ZMIR522223 as intended. As noted, in Section A.3(c)(i), the selectable marker cassette (T-*TubA*, TS-*CTP2,* CS-*cp4 epsps*, and P-*TubA*) and one *lox*P site (bases 478 through 4893 of the PV-ZMIR522223 sequence) were excised by Cre recombinase, and as expected, are not present in the MON 95379 sequence. This analysis also shows that only T-DNA elements (described in Table 2) were present. In addition, 1000 base pairs flanking the 5′ end of the MON 95379 insert (Table 2, bases 1-1000) and 1000 base pairs flanking the 3′ end of the MON 95379 insert (Table 2, bases 14323-15322) were determined.

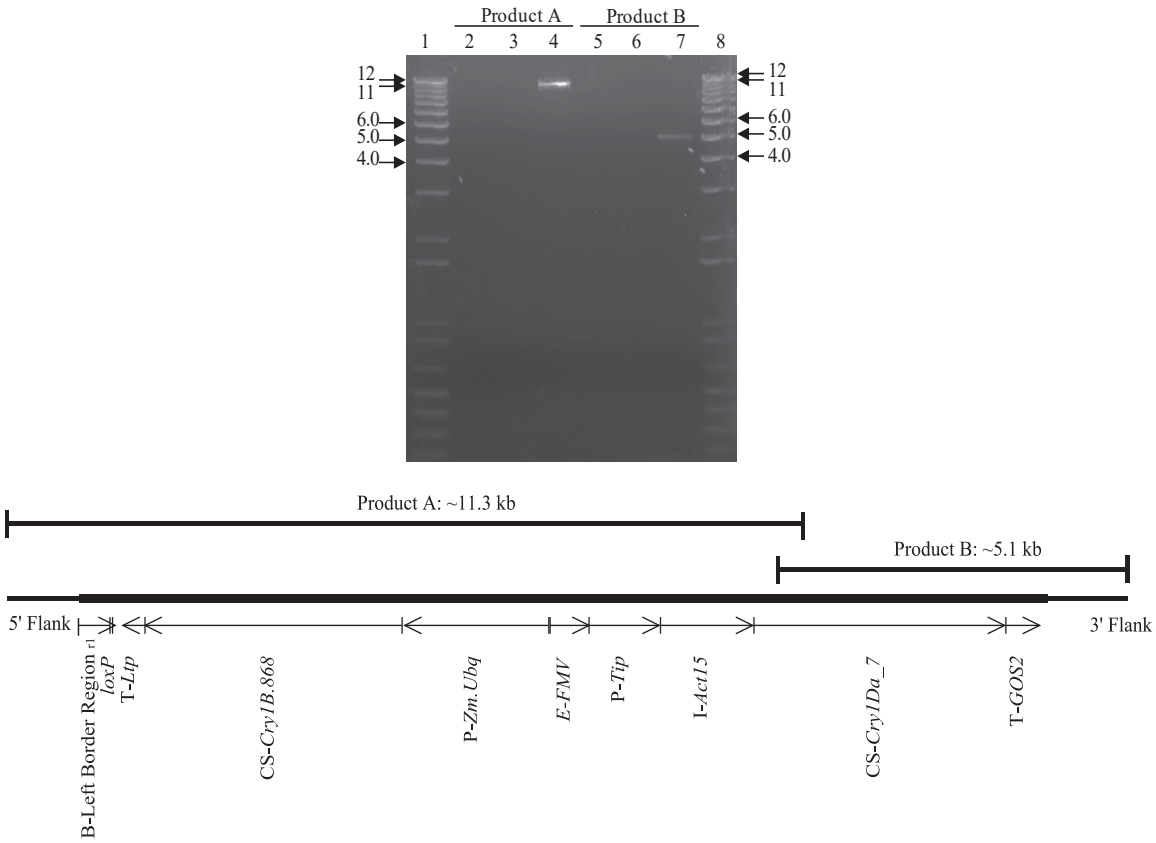

Figure 13. Overlapping PCR Analysis across the Insert in MON 95379

PCR was performed on both conventional control genomic DNA and genomic DNA of the F4 generation of MON 95379 using two pairs of primers to generate overlapping PCR fragments from MON 95379 for sequencing analysis. To verify the PCR products, 2 µl of each of the PCR reactions was loaded on the gel. The expected product size for each amplicon is provided in the illustration of the insert in MON 95379 that appears at the bottom of the figure. This figure is a representative of the data generated in the study. Lane designations are as follows:

Lane	
1	1 Kb Plus DNA Ladder
2	No template control
3	LH244 Conventional Control
4	MON 95379
5	No template control
6	LH244 Conventional Control
7	MON 95379
8	1 Kb Plus DNA Ladder

Arrows on the agarose gel photograph denote the size of the DNA, in kilobase pairs, obtained from the 1 Kb Plus DNA Ladder (Invitrogen) on the ethidium bromide stained gel.

[r1] Superscript in Left Border Regions indicate that the sequence in MON 95379 was truncated compared to the sequences in PV-ZMIR522223.

Sequencing of the MON 95379 Insertion Site

PCR and sequence analysis were performed on genomic DNA extracted from the conventional control to examine the insertion site in conventional maize (see Figure 5, Step 5). The PCR was performed with one primer specific to the genomic DNA sequence flanking the 5′ end of the MON 95379 insert paired with a second primer specific to the genomic DNA sequence flanking the 3′ end of the insert (Figure 14). A sequence comparison between the PCR product generated from the conventional control and the sequence generated from the 5′ and 3′ flanking sequences of MON 95379 indicates that 160 bases of maize genomic DNA were deleted during integration of the T-DNA. Such changes are common during plant transformation (Anderson *et al.*, 2016) and these changes presumably resulted from double stranded break repair mechanisms in the plant during *Agrobacterium*-mediated transformation process (Salomon and Puchta, 1998). The remainder of the maize genomic DNA sequences flanking the insert in MON 95379 are identical to the conventional control.

For details, please refer to Appendix 1 ([redacted]2020 (TRR0000070)).

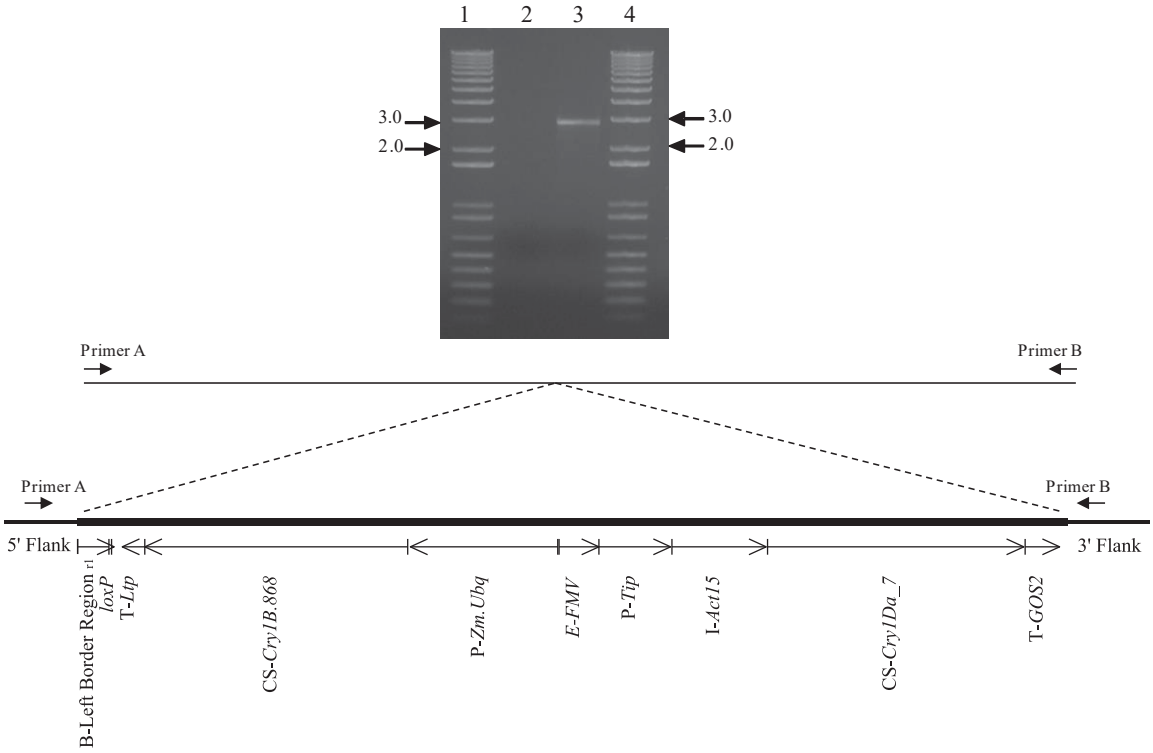

Figure 14. PCR Amplification of the MON 95379 Insertion Site

PCR analysis was performed to evaluate the insertion site. PCR was performed on conventional control DNA using Primer A, specific to the 5′ flanking sequence, and Primer B, specific to the 3′ flanking sequence of the insert in MON 95379. The DNA generated from the conventional control PCR was used for sequencing analysis. This illustration depicts the MON 95379 insertion site in the conventional control (upper panel) and the MON 95379 insert (lower panel). Approximately 2 µl of each of the PCR reactions was loaded on the gel. This figure is representative of the data generated in the study. Lane designations are as follows:

Lane	
1	1 Kb Plus DNA Ladder
2	No template control
3	LH244 Conventional Control
4	1 Kb Plus DNA Ladder

Arrows on the agarose gel photograph denote the size of the DNA, in kilobase pairs, obtained from the 1 Kb Plus DNA Ladder (Invitrogen) on the ethidium bromide stained gel.

[r1] Superscript in Left Border Regions indicate that the sequence in MON 95379 was truncated compared to the sequences in PV-ZMIR522223.

.

A.3(c)(iv) A map depicting the organisation of the inserted genetic material at each insertion site

PCR and DNA sequence analyses performed on MON 95379 and the conventional control determined the organisation of the genetic elements within the insert as given in Figure 14.

A.3(c)(v) Details of an analysis of the insert and junction regions for the occurrence of any open reading frames (ORFs)

Bioinformatic Assessment of Putative Open Reading Frames (ORFs) of MON 95379 Insert and Flanking Sequences

In addition to the bioinformatic analyses conducted on MON 95379 Cry1B.868 and Cry1Da_7 protein sequences (Sections B.2(a)(i) and B.2(b)(ii), respectively), bioinformatic analyses were also performed on the MON 95379 insert to assess the potential for allergenicity, toxicity, or biological activity of putative polypeptides encoded by all six reading frames present in the MON 95379 insert DNA, as well as ORFs present in the 5' and 3' flanking sequence junctions. These various bioinformatic evaluations are depicted in Figure 15. ORFs spanning the 5' and 3' maize genomic DNA-inserted DNA junctions were translated from stop codon to stop codon in all six reading frames (three forward reading frames and three reading frames in reverse orientation)[9]. Polypeptides of eight amino acids or greater from each reading frame were then compared to toxin, allergen and all proteins databases using bioinformatic tools. Similarly, the entire T-DNA sequence was translated in all six reading frames and the resulting deduced amino acid sequence was subjected to bioinformatic analyses. The data generated from these analyses confirm that even in the highly unlikely occurrence that a translation product other than MON 95379 Cry1B.868 and Cry1Da_7 proteins were derived from frames one to six of the insert DNA or the ORFs spanning the insert junctions, they would not share a sufficient degree of sequence similarity with other proteins to indicate they would be potentially allergenic, toxic, or have other safety implications. Therefore, there is no evidence for concern regarding the relatedness of the putative polypeptides for MON 95379 to known toxins, allergens, or biologically active putative peptides.

For details, please refer to Appendix 2 ([redacted] 2020 (TRR0000120)) and Appendix 3 ([redacted] 2020 (TRR0000119)).

[9] An evaluation of sequence translated from stop codon to stop codon represents the most conservative approach possible for flank junction analysis as it does not take into consideration that a start codon is necessary for the production of a protein sequence.

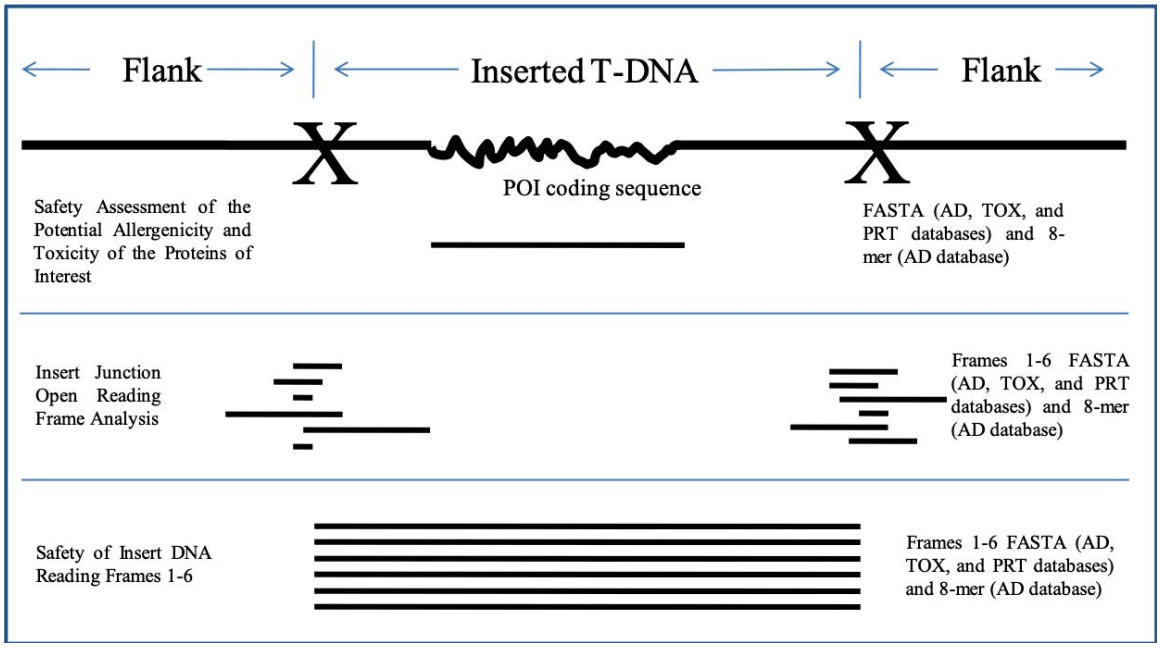

Figure 15. Schematic Summary of MON 95379 Bioinformatic Analyses

AD: AD_2020, TOX: TOX_2020, PRT: PRT_2020; 8-mer represents the eight amino acid sliding window search.

Bioinformatics Evaluation of the T-DNA Insert in MON 95379

Bioinformatic analyses were performed to assess the potential of toxicity, allergenicity or biological activity of any putative peptides encoded by translation of reading frames 1 through 6 of the inserted DNA in MON 95379 (Figure 15).

The FASTA sequence alignment tool was used to assess structural relatedness between the query sequences and any protein sequences in the AD_2020, TOX_2020, and PRT_2020 databases. Structural similarities shared between each putative polypeptide with each sequence in the database were examined. The extent of structural relatedness was evaluated by detailed visual inspection of the alignment, the calculated percent identity and alignment length to ascertain if alignments exceeded Codex (Codex Alimentarius, 2009) thresholds for FASTA searches of the AD_2020 database, and the *E*-score. Alignments having an *E*-score-less than 1×10^{-5} are deemed significant because they may reflect shared structure and function among sequences. In addition to structural similarity, each putative polypeptide was screened for short polypeptide matches using a pair-wise comparison algorithm. In these analyses, eight contiguous and identical amino acids were defined as immunologically relevant, where eight represents the typical minimum sequence length likely to represent an immunological epitope (Silvanovich *et al.*, 2006) and evaluated against the AD_2020 database.

The results of the search comparisons showed that no relevant structural similarity to known allergens and toxins were observed for any of the putative polypeptides when compared to proteins in the allergen (AD_2020) or toxin (TOX_2020) databases. Furthermore, no short (eight amino acid) polypeptide matches were shared between any of the putative polypeptides and proteins in the allergen database.

When the frames were used to query the PRT_2020 database, the results of these analyses positively identified the following genetic elements within the MON 95379 T-DNA: (1) frame 2 was observed to contain the sequence encoding the Cry1Da_7 protein present in

MON 95379; (2) frame 3 was observed to contain the enhancer from the 35S RNA of figwort mosaic virus (FMV) to enhance transcription in plant cells. Each of the genetic elements described are expected based on the known sequence of MON 95379 T-DNA. The positive identification of these elements does not indicate potential for adverse biological activity. No other relevant sequence similarities between the 6 reading frames translated from the MON 95379 T-DNA were observed with allergens, toxins or other biologically active proteins of concern.

Taken together, these data demonstrate the lack of relevant similarities between known allergens or toxins for putative peptides derived from all six reading frames from the inserted DNA sequence of MON 95379. As a result, in the unlikely event that a translation product other than Cry1B.868 and Cry1Da_7 proteins was derived from reading frames 1 to 6, these putative polypeptides are not expected to be cross-reactive allergens, toxins, or display adverse biological activity.

Bioinformatics Evaluation of the DNA Sequences Flanking the 5′ and 3′ Junctions of the MON 95379 Insert: Assessment of Putative Peptides

Analyses of putative polypeptides encoded by DNA spanning the 5' and 3' genomic junctions of the MON 95379 inserted DNA were performed using a bioinformatic comparison strategy. The purpose of the assessment is to evaluate the potential for novel open reading frames (ORFs) that may have homology to known allergens, toxins, or proteins that display adverse biological activity. Sequences spanning the 5' and 3' genomic DNA-insert DNA junctions, (Figure 15) were translated from stop codon (TGA, TAG, TAA) to stop codon in all six reading frames. Putative polypeptides from each reading frame, that were eight amino acids or greater in length, were compared to AD_2020, TOX_2020, and PRT_2020 databases using FASTA and to the AD_2020 database using an eight amino acid sliding window search. A total of 12 putative peptides were compared to allergen (AD_2020), toxin (TOX_2020), and all protein (PRT_2020) databases using bioinformatic tools.

The FASTA sequence alignment tool was used to assess the relatedness between the query sequences and any protein sequence in the AD_2020, TOX_2020, and PRT_2020 databases. Similarities shared between the sequence with each sequence in the database were examined. The extent of relatedness was evaluated by detailed visual inspection of the alignment, the calculated percent identity, and the *E*-score. Alignments having *E*-scores of ≤1e-5 (1×10^{-5}) are deemed significant because they may reflect shared structure and function among sequences. In addition to sequence similarity, sequences were screened for short peptide matches using a pair-wise comparison algorithm. In these analyses, eight contiguous and identical amino acids were defined as immunologically relevant, where eight represents the typical minimum sequence length likely to represent an immunological epitope (Silvanovich *et al.*, 2006).

The bioinformatic analysis performed using the 12 putative peptide sequences translated from junctions is theoretical as there is no reason to suspect, or evidence to indicate, the presence of transcripts spanning the flank junctions. The results of these bioinformatic analyses indicate that no structurally relevant sequence similarities were observed between the 12 putative flank junction derived sequences and allergens, toxins, or biologically active proteins. As a result, in the unlikely occurrence that any of the 12 peptides analyzed herein is found *in planta*, none would share significant similarity or identity to known allergens, toxins, or other biologically active proteins that could affect human or animal health.

A.3(d) A description of how the line or strain from which food is derived was obtained from the original tranformant (i.e. provide a family tree or describe the breeding process) including which generations have been used for each study

The MON 95379 transformation was conducted with inbred maize line LH244, a maize line assigned to Holden's Foundation Seeds, LLC in 2001 (U.S. Patent #6,252,148). LH244 is a medium season yellow dent maize line of Stiff Stalk background that is best adapted to the central regions of the U.S. corn belt.

Following transformation of immature LH244 embryos, selected transformants were self-pollinated to increase seed supplies. A Cre recombination system was used to remove the selectable marker starting with the selected events at the R2 generation. A selected inbred line homozygous for the presence of the T-DNA and lacking the selectable marker cassette was used to produce other MON 95379 materials for product testing, safety assessment studies, and commercial hybrid development. The non-transformed LH244 was used to produce conventional maize comparators (hereafter referred to as conventional controls) in the safety assessment of MON 95379.

For more details, see MON 95379 breeding history, Figure 8.

Please also refer to Section A.3(a).

A.3(e) Evidence of the stability of the genetic changes, including:

A.3(e)(i) The pattern of inheritance of the transferred gene(s) and the number of generations over which this has been monitored

In order to demonstrate the stability of the T-DNA present in MON 95379 through multiple breeding generations, NGS was performed using DNA obtained from five breeding generations of MON 95379. The breeding history of MON 95379 is presented in Figure 8, and the specific generations tested are indicated in the figure legend. The MON 95379 (F4) generation was used for the molecular characterisation analyses discussed in Sections A.3(c)(i) to A.3(c)(iii). To assess generational stability of the T-DNA, four additional generations were evaluated by NGS as previously described in Section A.3(c), and compared to the fully characterized F4 generation. The conventional controls used for the generational stability analysis included LH244, with similar background genetics to the F4 and F5 generations and represents the original transformation line; and LH244 × HCL617, a hybrid with similar background genetics to the F4F1, F5F1, F6F1 hybrids. Genomic DNA isolated from each of the selected generations of MON 95379 and conventional control was used for NGS, mapping, and subsequent junction identification (Table 5).

Table 5. Junction Sequences Detected

Sample	Junction Sequence Detected
MON 95379 (F4)	2
MON 95379 (F5)	2
MON 95379 (F4F1)	2
MON 95379 (F5F1)	2
MON 95379 (F6F1)	2
LH244	0
LH244 × HCL617	0

As shown by alignment to the full flank/insert sequence obtained from directed sequencing, a single conserved pair of junctions linked by contiguous known and expected DNA sequence is present in MON 95379 (F4). Two identical junctions are found in each of the breeding generations (F5, F4F1, F5F1, and F6F1), confirming the insertion of a single copy of PV-ZMIR522223 T-DNA at a single locus in the genome of MON 95379, and the consistency of these junctions in the mapping data across all generations tested demonstrates that this single locus is stably maintained throughout the MON 95379 breeding process.

These results demonstrate that the single locus of integration characterized in the F4 generation of MON 95379 is found in five breeding generations of MON 95379, confirming the stability of the insert. This comprehensive NGS and bioinformatic analysis of NGS data from multiple generations supports the conclusion that MON 95379 contains a single, stable insert T-DNA.

For details, please refer to Appendix 1 ([redacted], 2020 (TRR0000070)).

A.3(e)(ii) The pattern of inheritance and expression of the phenotype over several generations and, where appropriate, across different environments

Inheritance of the Genetic Insert in MON 95379

The MON 95379 T-DNA resides at a single locus within the maize genome and therefore should be inherited according to Mendelian principles of inheritance. During development of lines containing MON 95379, phenotypic and genotypic segregation data were recorded to assess the inheritance and stability of the MON 95379 T-DNA using Chi square (χ^2) analysis over several generations. The χ^2 analysis is based on comparing the observed segregation ratio to the expected segregation ratio according to Mendelian principles.

The MON 95379 breeding path for generating segregation data is described in Figure 16. The transformed R0 plant was self-pollinated to generate R1 seed. An individual homozygous positive plant for the MON 95379 T-DNA was identified in the R1 segregating population by Real-Time TaqMan®10PCR assay.

The homozygous positive R1 plant was self-pollinated to give rise to R2 seed. At the R2 generation, plants were crossed with a Cre recombinase expressing line. The Cre/*lox* technology enables the removal of DNA sequence positioned between two excision targeting sequences called *lox* sites (Hare and Chua, 2002; Zhang *et al.*, 2003). The Cre recombinase enzyme facilitates the excision of the selectable marker cassette which was inserted during the transformation as part of the T-DNA insertion that also included the gene of interest cassettes. After excision, a single *lox* site remains in the F_1 generation. The resulting F1 progeny were self-pollinated and the F2 generation were screened for the absence of the *cre* gene (and other sequences from plasmid PV-ZMOO513642), allowing for selection of lines lacking the Cre recombinase cassette from subsequent generations and the final product. The F2 plants lacking the *cre* gene were self-pollinated to produce F3 seed. The homozygous positive F3 plant was self-pollinated to give rise to F4 seed. The homozygous positive F4 plants were crossed via traditional breeding techniques to a proprietary elite inbred parent that does not contain the *cry1B.868* and *cry1Da_7* coding sequences to produce hemizygous F4F1 seed. The hemizygous F4F1 plants were self-pollinated to produce F4F2 seed. The F4F2 generation was tested for the presence of MON 95379 T-DNA by Real Time TaqMan® PCR assay for *cry1B.868*. Hemizygous positive F4F2 plants were self-pollinated to produce

10 TaqMan® is a registered trademark of Roche Molecular Systems, Inc.

F4F3 seed. The F4F3 generation was tested for the presence of the T-DNA by Real Time TaqMan® PCR assay for *cry1B.868*. Hemizygous positive F4F3 plants were self-pollinated to produce F4F4 seed. The F4F4 generation was tested for the presence of the T-DNA by Real Time TaqMan® PCR assay for *cry1B.868*.

The inheritance of the MON 95379 T-DNA was assessed in the F4F2, F4F3, and F4F4 generations. At all generations, the MON 95379 T-DNA was predicted to segregate at a 1:2:1 ratio (homozygous positive: hemizygous positive: homozygous negative) according to Mendelian inheritance principles.

A Pearson's chi square (χ^2) analysis was used to compare the observed segregation ratios of the MON 95379 T-DNA I coding sequence to the expected ratios.

The Chi square was calculated as:

$$\chi^2 = \sum [(| o - e |)^2 / e]$$

where o = observed frequency of the genotype or phenotype and e = expected frequency of the genotype or phenotype. The level of statistical significance was predetermined to be 5% ($\alpha = 0.05$).

The results of the χ^2 analysis of the segregating progeny of MON 95379 are presented in Table 6. The χ^2 value in the F4F2, F4F3, and F4F4 generations indicated no statistically significant difference between the observed and expected segregation ratios of MON 95379 T-DNA. These results support the conclusion that the MON 95379 T-DNA resides at a single locus within the maize genome and is inherited according to Mendelian principles of inheritance. These results are also consistent with the molecular characterisation data indicating that MON 95379 contains a single intact copy of the T-DNA inserted at a single locus in the maize genome (Sections A.3(c)(ii) and A.3(c)(iii).

For details, please also refer to Appendix 4 ([redacted] 2019 (MSL0030175)).

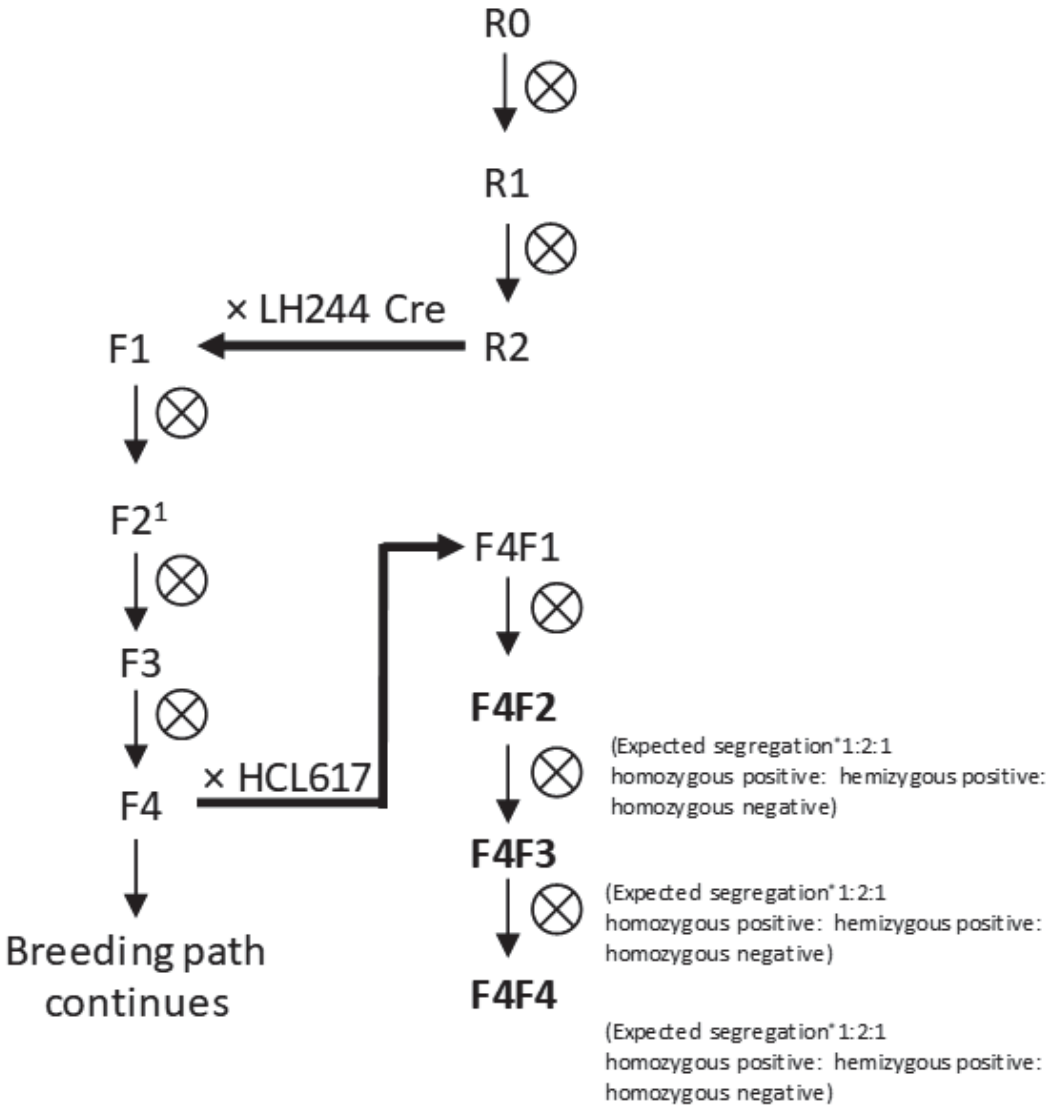

Figure 16. Breeding Path for Generating Segregation Data for MON 95379

*Chi-square analysis was conducted on segregation data from F4F2, F4F3, and F4F4 generations (bolded text).

⊗: Self-Pollinated

[1] The F2 generation was screened for plants lacking the *cre* gene cassette. Only those plants lacking the *cre* gene cassette were self-pollinated to create a F3 generation lacking the *cre* gene cassette.

Table 6. Segregation Results for MON 95379 from the F4F2, F4F3, and F4F4

					1:2:1 Segregation				
Generation	Total Plants	Observed # Plant Homozygous Positive	Observed # Plant Hemizygous Positive	Observed # Plant Homozygous Negative	Expected # Plant Homozygous Positive	Expected # Plant Hemizygous Positive	Expected # Plant Homozygous Negative	χ^2	Probability
F4F2	200	60	85	55	50	100	50	4.75	0.093
F4F3	247	62	125	60	61.75	123.5	61.75	0.07	0.966
F4F4	246	74	109	63	61.5	123	61.5	4.17	0.124

Expression of the genetic insert

In order to assess the presence of the Cry1B.868 and Cry1Da_7 proteins in MON 95379 across multiple breeding generations, western blot analysis of MON 95379 was conducted on grain tissue collected from generations F4, F4F1, F5, F5F1, and F6F1 of MON 95379, using grain tissue of the conventional control (LH244 × HCL617) as negative control.

The presence of the Cry1B.868 protein was demonstrated in five breeding generations of MON 95379 using western blot analysis. The *Bt*-produced Cry1B.868 protein reference standard (10 ng) was used as a reference for the positive identification of the Cry1B.868 protein (Figure 17, lane 3). The presence of the Cry1B.868 protein in grain tissue samples of MON 95379 was determined by visual comparison of the bands detected in five breeding generations (Figure 17, lanes 5-9) to the *Bt*-produced Cry1B.868 protein reference standard. The MON 95379-produced Cry1B.868 protein migrated indistinguishably from that of the *Bt*-produced protein standard analyzed on the same Western blot. As expected, the Cry1B.868 protein was not detected in the conventional control grain extract (Figure 17, lane 4).

The presence of the Cry1Da_7 protein was demonstrated in five breeding generations of MON 95379 using Western blot analysis. The *Bt*-produced Cry1Da_7 protein reference standard (0.2 ng) was used as a reference for the positive identification of the Cry1Da_7 protein (Figure 18, lane 3). The presence of the Cry1Da_7 protein in grain tissue samples of MON 95379 was determined by visual comparison of the bands detected in five breeding generations (Figure 18, lanes 5-9) to the *Bt*-produced Cry1Da_7 protein reference standard. The MON 95379-produced Cry1Da_7 protein migrated indistinguishably from that of the *Bt*-produced protein standard analyzed on the same Western blot. As expected, the Cry1Da_7 protein was not detected in the conventional control grain extract (Figure 18, lane 4).

For details, please also refer to Appendix 5 ([redacted] 2019 (MSL0030807)).

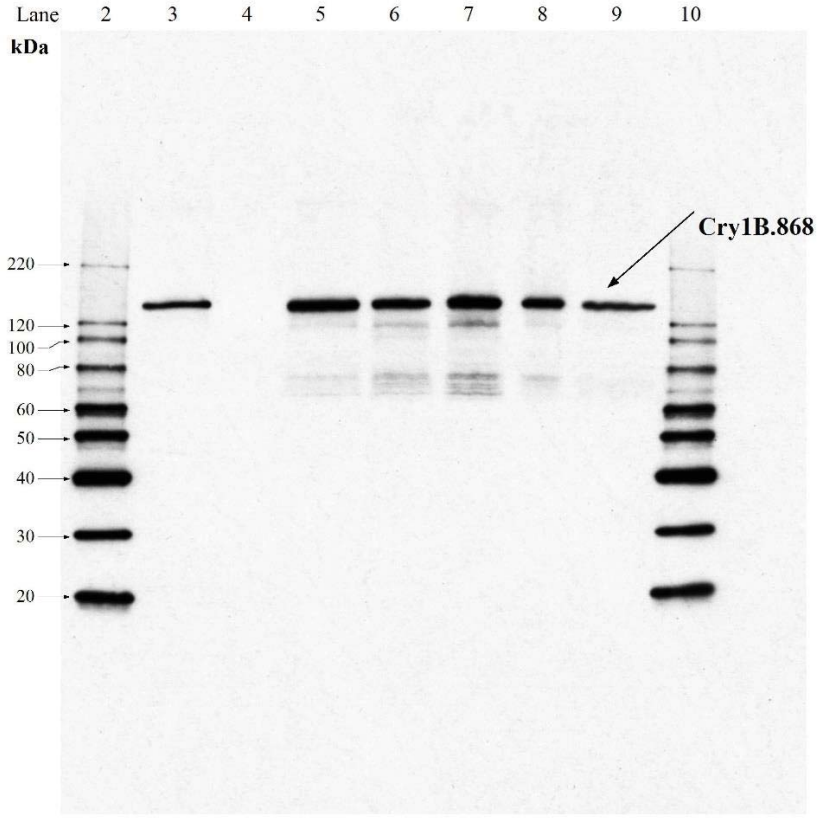

Figure 17. Presence of Cry1B.868 Protein in Multiple Generations of MON 95379

Blot probed with monoclonal anti-Cry1B.868 primary antibodies and HRP conjugated anti-mouse IgG secondary antibodies. Exposure time was 10 seconds. Lane 1 was cropped from the image. The MWs (kDa) of the MagicMark XP Western Standard were shown on the left.

Lane	Description	Amount Loaded
2	MagicMark XP Western Standard	4 µl
3	*Bt*-produced Cry1B.868 protein	10 ng
4	Conventional control	10 µl
5	MON 95379, F4	10 µl
6	MON 95379, F4F1	10 µl
7	MON 95379, F5	10 µl
8	MON 95379, F5F1	10 µl
9	MON 95379, F6F1	10 µl
10	MagicMark XP Western Standard	4 µl

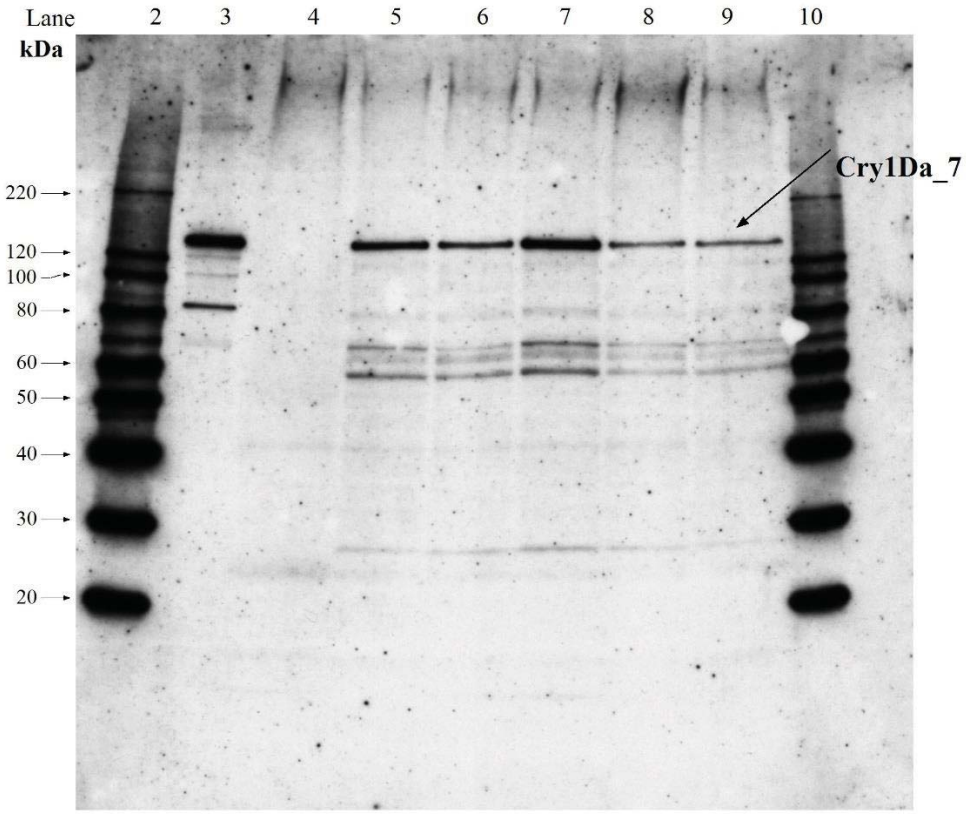

Figure 18. Presence of Cry1Da_7 Protein in Multiple Generations of MON 95379

Blot probed with monoclonal anti-Cry1Da primary antibodies and HPR conjugated anti-mouse IgG secondary antibodies. Exposure time was 30 seconds. Lane 1 was cropped from the image. The MWs (kDa) of the MagicMark XP Western Standard were shown on the left.

Lane	Description	Amount Loaded
2	MagicMark XP Western Standard (1/4 dilution)	2 µl
3	*Bt*-produced Cry1Da_7 protein	0.2 ng
4	Conventional control	20 µl
5	MON 95379, F4	20 µl
6	MON 95379, F4F1	20 µl
7	MON 95379, F5	20 µl
8	MON 95379, F5F1	20 µl
9	MON 95379, F6F1	20 µl
10	MagicMark XP Western Standard (1/4 dilution)	2 µl

A.3(f) An analysis of the expressed RNA transcripts, where RNA interference has been used

Not relevant for this product.

B. CHARACTERISATION AND SAFETY ASSESSMENT OF NEW SUBSTANCES

B.1 Characterisation and Safety Assessment of New Substances

B.1(a) Full description of the biochemical and phenotypic effects of all new substances (e.g. a protein or an untranslated RNA) that are expressed in the new GM organism, including their levels and site of accumulation, particularly in edible portions

Identity and Function of the Cry1B.868 and Cry1Da_7 Proteins from MON 95379

The MON 95379 Cry1B.868 and Cry1Da_7 proteins belong to the Cry three domain family of proteins that has a well-documented mode of action (Gill *et al.*, 1992; Schnepf *et al.*, 1998; Vachon *et al.*, 2012; OECD, 2007). Ingestion of Cry proteins by the target insect pest exposes the protein to the alkaline conditions and proteases in the insect midgut, resulting in proteolytic cleavage of the protein's protoxin domain, thus solubilizing the parasporal inclusions and converting the protein to the active insecticidal toxin. Following activation, this protease-resistant core protein is comprised of three distinct structural domains that function in a step-wise mechanism of binding to specific membrane-embedded receptors, oligomerization at the membrane interface, insertion into the plasma membrane and pore formation leading to loss of cell integrity followed by delayed development or insect death (Deist *et al.*, 2014; Bravo *et al.*, 2007).

Cry1B.868 is a protein that comprises a single polypeptide of 1199 amino acids with an apparent molecular weight of approximately 127 kDa. Like other Cry proteins, Cry1B.868 is first synthesized as a prototoxin that upon exposure to the midgut of target organisms is cleaved by digestive enzymes to yield an approximately 60 kDa activated protein (Bravo *et al.*, 2007). Cry1B.868 is a chimeric three domain protein that consists of domains I and II from Cry1Be, domain III from Cry1Ca, and the C-terminal domain from Cry1Ab (Figure 19). Cry1A, Cry1C and Cry1B proteins are from a family of insecticidal proteins derived from various subspecies of the soil bacterium *Bacillus thuringiensis* (*Bt*) which have been used extensively in formulation for commercial biopesticides (Betz *et al.*, 2000; EFSA, 2012; Bravo *et al.*, 2011). Cry1B.868 was designed using a domain exchange strategy to achieve high levels of activity against target lepidopteran insect pests. Domain exchange is a well-known mechanism in nature, resulting in diversities in Cry protein functional activity that have been described extensively in the literature (de Maagd *et al.*, 2001; de Maagd *et al.*, 2003). By utilizing modern molecular biological tools, a domain exchange strategy has previously been used successfully to switch the functional domains of Cry1 proteins to develop microbial biopesticides with improved specificity to lepidopteran insect pests. (Gao *et al.*, 2006; Baum, 1998; Baum *et al.*, 1999). Similarly, by exchanging Domain III, Cry1B.868 has been engineered to have an enhanced specificity for fall armyworm relative to Cry1Be (Wang *et al.*, 2019). Domains I and II of Cry1B.868 are 100% identical to the respective domains of Cry1Be. Domain III of Cry1B.868 is 100% identical to domain III of Cry1Ca. The C-terminal region of Cry1B.868 is 100% identical to that of Cry1Ab.

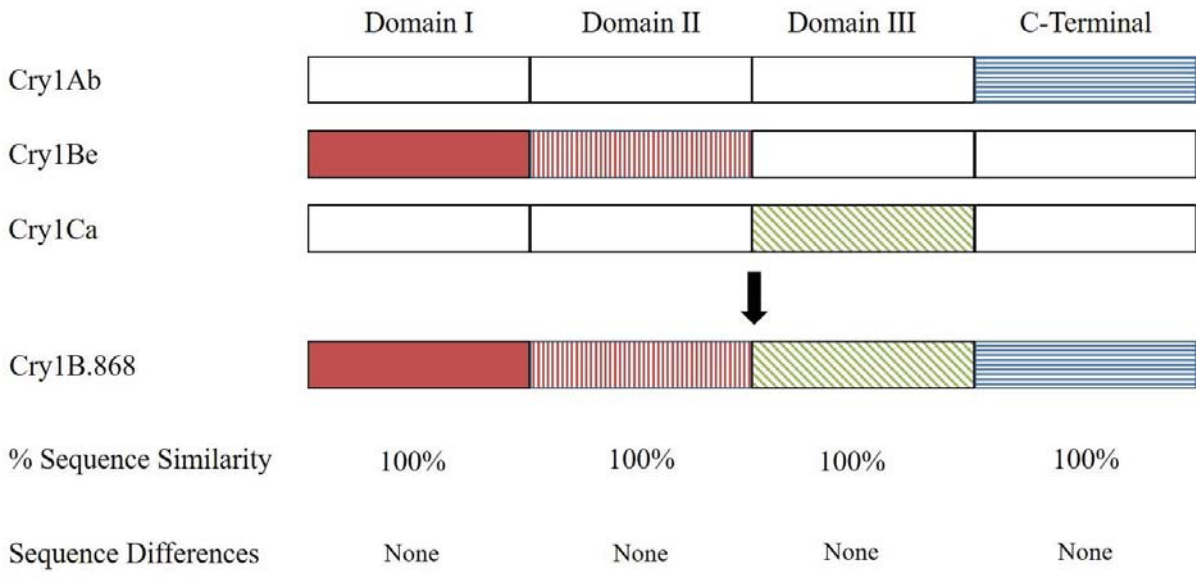

Figure 19. Schematic Representation of the Primary Domain Architecture of the Cry1B.868 Protein

The domain architecture of the chimeric Cry1B.868 protein is schematically presented. Different shades are used to differentiate the origin of domains. For simplicity, the lengths of the domains in this illustration are not in proportion to the lengths of amino acid sequence of the respective domains.

Cry1Da_7 in MON 95379 is a protein that comprises a single polypeptide of 1166 amino acids, with an apparent molecular weight of approximately 132 kDa. Like other Cry proteins, it is first synthesized as a prototoxin that upon exposure to the midgut of target organisms is cleaved by digestive enzymes to yield an approximately 60 kDa activated protein (Bravo *et al.*, 2007). Cry1Da_7 is a modified version of the Cry1Da protein that shares approximately 99.7% sequence identity to its parent protein (Figure 20). Cry1Da is an insecticidal protein derived from the soil bacterium *Bt*, which has been used extensively in the formulation of commercial biopesticides (EFSA, 2012; Bravo *et al.*, 2011). Cry1Da_7 has four distinct amino acid differences relative to Cry1Da. In Domain I, the protein has an additional alanine at position 2. This alanine was added to optimize the codon for translation of the protein *in planta*. In Domain II, there are three amino acid substitutions: serine 282 to valine, tyrosine 316 to serine, and isoleucine 368 to proline. These amino acid substitutions result in an improvement in activity towards corn earworm relative to Cry1Da while maintaining fall army worm activity (Wang *et al.*, 2019).

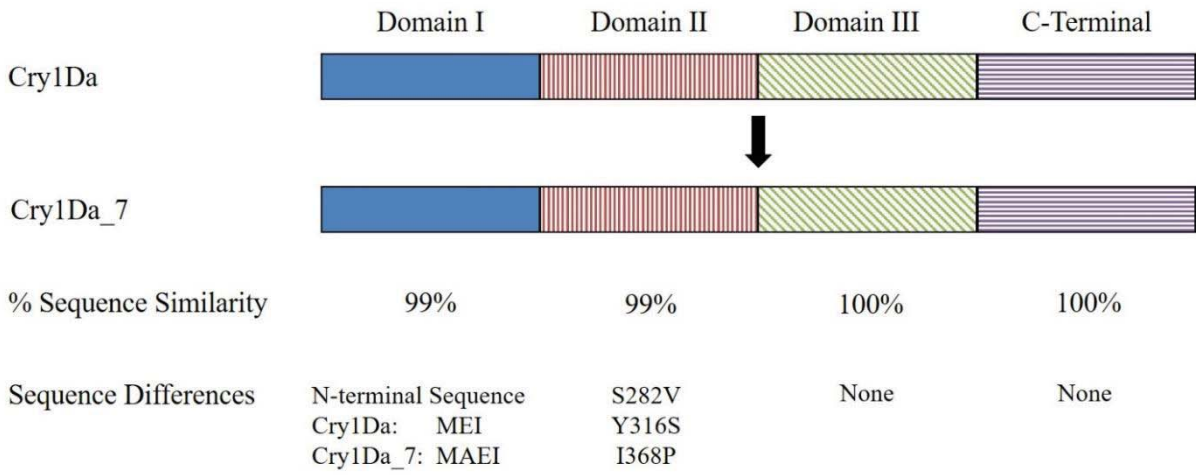

Figure 20. Schematic Representation of the Primary Domain Architecture of the Cry1Da_7 Protein

Domain architecture of the Cry1Da_7 protein, which differs from its parent protein by only four amino acids (an alanine is added in position two in Domain I and 3 single amino acid positions in Domain II; V = valine, S = serine, Y = tyrosine, P = proline, I = isoleucine). For simplicity, the lengths of the domains in this illustration are not in proportion to the lengths of amino acid sequence of the respective domains.

B.1(a)(i) Characterisation of the MON 95379 Cry1B.868 protein

Cry1B.868 Protein Identity and Equivalence

For the safety data generated using the *Bt*-produced Cry1B.868 protein to be applied to the MON 95379-produced Cry1B.868 protein (plant-produced Cry1B.868), the equivalence of the plant- and *Bt*-produced proteins must first be demonstrated. To assess the equivalence between the MON 95379-produced and *Bt*-produced Cry1B.868 proteins, a small quantity of the MON 95379-produced Cry1B.868 protein was purified from MON 95379 grain. The MON 95379-produced Cry1B.868 protein was characterized and the equivalence of the physicochemical characteristics and functional activity between the MON 95379-produced and *Bt*-produced Cry1B.868 proteins was assessed using a panel of analytical tests; as shown in Table 7. Taken together, these data provide a detailed characterisation of the MON 95379-produced Cry1B.868 protein and establish the equivalence of the MON 95379-produced and *Bt*-produced Cry1B.868 proteins.

For details, please refer to Appendix 6 ([redacted] 2020 (TRR0000416)).

Table 7. Summary of MON 95379 Cry1B.868 Protein Identity and Equivalence

Analytical Test Assessment	Section Cross Reference	Analytical Test Outcome
N-terminal sequence	B.1 (a)(i)(i)	The expected N-terminal sequence for MON 95379-produced Cry1B.868 protein was observed by Nano LC-MS/MS[1]
LC-MS/MS[1]	B.1 (a)(i)(ii)	Nano LC-MS/MS[1] analysis of trypsin or Asp-N digested peptides from MON 95379-produced Cry1B.868 protein yielded peptide masses consistent with expected peptide masses from the theoretical trypsin or Asp-N digest of the amino acid sequence
Western blot analysis	B.1 (a)(i)(iii)	MON 95379-produced Cry1B.868 protein identity was confirmed using a Western blot probed with antibodies specific for Cry1B.868 protein Immunoreactive properties of the MON 95379-produced Cry1B.868 and the *Bt*-produced Cry1B.868 proteins were shown to be equivalent
Apparent molecular weight (MW)	B.1 (a)(i)(iv)	Electrophoretic mobility and apparent molecular weight of the MON 95379-produced Cry1B.868 and the *Bt*-produced Cry1B.868 proteins were shown to be equivalent
Glycosylation analysis	B.1 (a)(i)(v)	Glycosylation status of MON 95379-produced Cry1B.868 and *Bt*-produced Cry1B.868 proteins were shown to be equivalent
Functional activity	B.1 (a)(i)(vi)	Functional activity of the MON 95379-produced Cry1B.868 and the *Bt*-produced Cry1B.868 proteins were shown to be equivalent by insect bioassay

[1] Nano LC-MS/MS = Nanoscale liquid chromatography-tandem mass spectrometry

A summary of the data obtained to support the characterisation of the MON 95379-produced Cry1B.868 and a conclusion of protein equivalence is below.

B.1(a)(i)(i) Results of the N-terminal sequencing analysis

The identification of N-terminal sequence was conducted by LC-MS/MS analysis of peptide fragments produced through enzymatic digestion of the MON 95379-produced Cry1B.868 protein with Asp-N. The expected N-terminal sequence for the Cry1B.868 protein deduced from the *cry1B.868* gene present in maize of MON 95379 was observed, except that the N-terminal methionine was cleaved *in vivo* from the MON 95379-produced Cry1B.868 by methionine aminopeptidase (see Experimental Sequence, Figure 21). The cleavage of the N-terminal methionine from proteins *in vivo* by methionine aminopeptidase is common in many organisms (Bradshaw *et al.*, 1998; Wang *et al.*, 2016). The N-terminal sequence for MON 95379-produced Cry1B.868 protein was consistent with the N-terminal sequence for the *Bt*-produced Cry1B.868 protein observed by LC-MS/MS (Figure 21). An additional minor form of the MON 95379-produced Cry1B.868 protein with the N-terminal methionine was also observed. Hence, the sequence information confirms the identity of the Cry1B.868 protein isolated from the grain of MON 95379.

Amino Acids Residue # from the N-terminus	→	1	2	3	4	5	6	7	8	9	10	11	12	13	14	15	16
Bt-produced Cry1B.868 sequence	→	-	T	S	N	R	K	N	E	N	E	I	I	N	A	L	S
			|	|	|	|	|	|	|	|	|	|	|	|	|	|	|	|
Expected Cry1B.868 Sequence	→	M	T	S	N	R	K	N	E	N	E	I	I	N	A	L	S
			|	|	|	|	|	|	|	|	|	|	|	|	|	|	|	|
MON 95379 Experimental Sequence	→	-	T	S	N	R	K	N	E	N	E	I	I	N	A	L	S

Figure 21. N-Terminal Sequence of the MON 95379-Produced Cry1B.868 Protein

The experimental sequence obtained from the MON 95379-produced Cry1B.868 was compared to the expected sequence deduced from the *cry1B.868* gene present in MON 95379. *Bt*-produced Cry1B.868 protein sequence above was derived from the reference substance Certificate of Analysis (COA) (lot 7565). The single-letter International Union of Pure and Applied Chemistry - International Union of Biochemistry (IUPAC-IUB) amino acid code is M, methionine; T, Threonine; S, Serine; N, Asparagine; R, Arginine; K, Lysine; E, Glutamic acid; I, Isoleucine; A, Alanine; L, Leucine.

B.1(a)(i)(ii) Results of nano LC-MS/MS mass fingerprint analysis

Peptide mass fingerprint analysis is a standard technique used for confirming the identity of proteins. The ability to identify a protein using this method is dependent upon matching a sufficient number of observed tryptic peptide fragment masses with predicted tryptic peptide fragment masses. In general, protein identification made by peptide mapping is considered to be reliable if > 40% of the protein sequence was identified by matching experimental masses observed for the tryptic peptide fragments to the expected masses for the fragments (Biron *et al.*, 2006; Krause *et al.*, 1999). The identity of the MON 95379-produced Cry1B.868 protein was confirmed by LC-MS/MS analysis of peptide fragments produced through enzymatic digestion of the MON 95379-produced Cry1B.868 protein.

There were 110 unique peptides identified that correspond to the masses expected to be produced by trypsin digestion of the MON 95379-produced Cry1B.868 protein (Table 8). The identified peptides were used to assemble a sequence coverage map of the entire Cry1B.868 protein (Figure 22). The experimentally determined coverage of the MON 95379-produced Cry1B.868 protein was 91% (Figure 22A, 1088 out of 1199 amino acids). This analysis further confirms the identity of MON 95379-produced Cry1B.868 protein.

There were 145 unique peptides identified that correspond to the masses expected to be produced by trypsin digestion of the *Bt*-produced Cry1B.868 protein (Table 9) by LC-MS/MS analysis during the protein characterisation. The identified peptides were used to assemble a coverage map of the entire Cry1B.868 protein (Figure 22). The experimentally determined coverage of the *Bt*-produced Cry1B.868 protein was 96% (Figure 22B, 1156 out of 1199 amino acids).

Table 8. Summary of the Tryptic Masses Identified for the MON 95379-Produced Cry1B.868 Using LC-MS/MS[1]

Experimental Mass[2]	Calculated Mass[3]	Difference[4]	Fragment[5]	Sequence[6]
3136.5591	3136.5571	0.0020	6 - 34	KNEN...TDAR
3008.4627	3008.4621	0.0006	7 - 34	NENE...TDAR
3261.5882	3261.5823	0.0059	35 - 65	IEDS...IAGR
2935.6012	2935.6000	0.0012	66 - 92	ILGV...LWPR
2136.1137	2136.1116	0.0021	93 - 109	GRDP...QLIR
1922.9901	1922.9890	0.0011	95 - 109	DPWE...QLIR
974.4775	974.4781	-0.0006	110 - 117	QQVTENTR
1601.8130	1601.8121	0.0009	110 - 123	QQVT...ALAR
645.3443	645.3446	-0.0003	118 - 123	DTALAR
990.5252	990.5247	0.0005	124 - 132	LQGL...NSFR
1650.7638	1650.7638	0.0000	133 - 145	AYQQ...LENR
2107.9605	2107.9559	0.0046	133 - 149	AYQQ...DDAR
2800.4884	2800.4873	0.0011	152 - 175	SVLY...FAIR
2518.4144	2518.4093	0.0051	176 - 197	NQEV...LLLR
1983.9540	1983.9538	0.0002	198 - 215	DASL...EIQR
629.2809	629.2809	0.0000	216 - 219	YYER
502.2752	502.2751	0.0001	220 - 223	QVEK
1249.6222	1249.6203	0.0019	234 - 243	WYNT...NNLR
1032.4997	1032.4988	0.0009	244 - 252	GTNA...SWLR
726.3454	726.3449	0.0005	253 - 257	YNQFR
2263.2201	2263.2212	-0.0011	258 - 277	RDLT...YDTR
2107.1237	2107.1201	0.0036	259 - 277	DLTL...YDTR
1379.6874	1379.6867	0.0007	278 - 289	VYPM...QLTR
1062.5349	1062.5346	0.0003	290 - 298	EIYT...PIGR
5243.6491	5243.6469	0.0022	299 - 346	TNAP...VLSR
1840.8100	1840.8104	-0.0004	347 - 360	WSNT...VGHR
503.2703	503.2703	0.0000	361 - 364	LESR
2619.2933	2619.2889	0.0044	368 - 392	GSLS...FTSR
551.2703	551.2704	-0.0001	393 - 396	DVYR
2888.5213	2888.5185	0.0028	393 - 418	DVYR...PWAR
2355.2594	2355.2587	0.0007	397 - 418	TESF...PWAR
621.3022	621.3023	-0.0001	419 - 422	FNWR
1415.7410	1415.7422	-0.0012	419 - 429	FNWR...NSLR
812.4502	812.4504	-0.0002	423 - 429	NPLNSLR
4407.0833	4407.0819	0.0014	430 - 468	GSLL...YSHR
601.3545	601.3547	-0.0002	469 - 473	LSNIR
872.5075	872.5080	-0.0005	474 - 481	LISGNTLR
1115.5512	1115.5512	0.0000	482 - 490	APVY...WTHR
447.2077	447.2077	0.0000	491 - 494	SADR
2158.1219	2158.1230	-0.0011	491 - 510	SADR...PLVK
1728.9273	1728.9258	0.0015	495 - 510	TNTI...PLVK
2089.1224	2089.1168	0.0056	495 - 513	TNTI...KGFR

Experimental Mass[2]	Calculated Mass[3]	Difference[4]	Fragment[5]	Sequence[6]
2349.2223	2349.2230	-0.0007	511 - 533	GFRV...DILR
1989.0345	1989.0320	0.0025	514 - 533	VWGG...DILR
2145.1336	2145.1331	0.0005	514 - 534	VWGG...ILRR
2405.2430	2405.2452	-0.0022	534 - 554	RNTF...ITQR
2249.1461	2249.1441	0.0020	535 - 554	NTFG...ITQR
582.2760	582.2762	-0.0002	561 - 565	YASSR
2325.2765	2325.2726	0.0039	569 - 592	VIVL...PLQK
1249.5978	1249.5972	0.0006	593 - 603	TMEI...LTSR
1379.6156	1379.6146	0.0010	607 - 617	YTDF...FSFR
2890.4515	2890.4600	-0.0085	618 - 645	ANPD...YIDK
4906.4687	4906.4651	0.0036	618 - 663	ANPD...DLER
2034.0166	2034.0157	0.0009	646 - 663	IEII...DLER
1947.0454	1947.0425	0.0029	664 - 681	AQKA...IGLK
1619.8520	1619.8519	0.0001	667 - 681	AVNE...IGLK
732.4017	732.4017	0.0000	709 - 714	KELSEK
604.3070	604.3068	0.0002	710 - 714	ELSEK
774.3987	774.3984	0.0003	720 - 725	RLSDER
618.2979	618.2973	0.0006	721 - 725	LSDER
1715.8592	1715.8591	0.0001	721 - 734	LSDE...PNFR
1115.5730	1115.5723	0.0007	726 - 734	NLLQ...PNFR
458.2602	458.2601	0.0001	735 - 738	GINR
530.2812	530.2813	-0.0001	739 - 742	QLDR
1551.7420	1551.7417	0.0003	746 - 760	GSTD...DVFK
4150.9422	4150.9245	0.0177	746 - 781	GSTD...LYQK
590.2911	590.2911	0.0000	782 - 786	IDESK
509.2598	509.2598	0.0000	789 - 792	AYTR
578.3175	578.3176	-0.0001	793 - 796	YQLR
1825.9111	1825.9098	0.0013	797 - 811	GYIE...YLIR
494.2489	494.2489	0.0000	812 - 815	YNAK
2819.4554	2819.4606	-0.0052	812 - 838	YNAK...PIGK
2343.2223	2343.2223	0.0000	816 - 838	HETV...PIGK
1024.5414	1024.5414	0.0000	869 - 877	IKTQ...GHAR
783.3622	783.3624	-0.0002	871 - 877	TQDGHAR
2097.1480	2097.1470	0.0010	878 - 896	LGNL...ALAR
502.2863	502.2863	0.0000	899 - 902	RAEK
474.2802	474.2802	0.0000	900 - 903	AEKK
1550.7981	1550.7980	0.0001	909 - 920	EKLE...IVYK
1293.6601	1293.6605	-0.0004	911 - 920	LEWE...IVYK
1969.9390	1969.9381	0.0009	921 - 937	EAKE...QYDR
1641.7639	1641.7635	0.0004	924 - 937	ESVD...QYDR
1610.8088	1610.8086	0.0002	938 - 952	LQAD...AADK
1766.9090	1766.9097	-0.0007	938 - 953	LQAD...ADKR
766.4563	766.4562	0.0001	953 - 958	RVHSIR
610.3547	610.3551	-0.0004	954 - 958	VHSIR

Experimental Mass[2]	Calculated Mass[3]	Difference[4]	Fragment[5]	Sequence[6]
2615.3490	2615.3482	0.0008	959 - 982	EAYL...LEGR
1302.6615	1302.6608	0.0007	983 - 993	IFTA...YDAR
1756.9508	1756.9512	-0.0004	983 - 997	IFTA...NVIK
472.3006	472.3009	-0.0003	994 - 997	NVIK
2078.9832	2078.9844	-0.0012	994 - 1011	NVIK...WNVK
1624.6944	1624.6940	0.0004	998 - 1011	NGDF...WNVK
1432.6460	1432.6443	0.0017	1012 - 1023	GHVD...NNHR
1955.0016	1955.0000	0.0016	1024 - 1040	SVLV...QEVR
620.3647	620.3646	0.0001	1046 - 1050	GYILR
580.3217	580.3221	-0.0004	1051 - 1055	VTAYK
2969.3562	2969.3600	-0.0038	1051 - 1076	VTAY...DELK
2407.0481	2407.0485	-0.0004	1056 - 1076	EGYG...DELK
6460.6970	6460.6802	0.0168	1056 - 1110	EGYG...YTSR
4071.6560	4071.6422	0.0138	1077 - 1110	FSNC...YTSR
2742.1708	2742.1681	0.0027	1111 - 1135	NRGY...YEEK
2472.0260	2472.0241	0.0019	1113 - 1135	GYDG...YEEK
3135.3217	3135.3217	0.0000	1113 - 1141	GYDG...TDGR
681.3079	681.3082	-0.0003	1136 - 1141	AYTDGR
837.4118	837.4093	0.0025	1136 - 1142	AYTDGRR
2730.2378	2730.2344	0.0034	1142 - 1165	RDNP...YVTK
2574.1331	2574.1333	-0.0002	1143 - 1165	DNPC...YVTK
1600.7776	1600.7773	0.0003	1151 - 1165	GYGD...YVTK
1269.5754	1269.5765	-0.0011	1166 - 1175	ELEY...ETDK
4001.9276	4001.9271	0.0005	1166 - 1199	ELEY...LMEE

[1]All imported values were rounded to 4 decimal places.
[2]Only experimental masses that matched calculated masses with the highest scores are listed in the table.
[3] The calculated mass is the exact molecular mass calculated from the matched peptide sequence.
[4] The calculated difference = experimental mass – calculated mass.
[5] Position refers to amino acid residues within the predicted MON 95379-produced Cry1B.868 sequence as depicted in Figure 22, Panel A.
[6] For peptide matches greater than nine amino acids in length, the first 4 residues and last 4 residues are show separated by three dots (...).

Table 9. Summary of the Tryptic Masses Identified for the *Bt*-Produced Cry1B.868 Using LC-MS/MS[1]

Experimental Mass[2]	Calculated Mass[3]	Difference[4]	Fragment[5]	Sequence[6]
3594.7858	3594.7808	0.0050	2 - 34	TSNR...TDAR
3136.5591	3136.5571	0.0020	6 - 34	KNEN...TDAR
3008.4640	3008.4621	0.0019	7 - 34	NENE...TDAR
3260.6014	3260.5983	0.0031	35 - 65	IEDS...IAGR
6178.1936	6178.1878	0.0058	35 - 92	IEDS...LWPR
2935.6029	2935.6000	0.0029	66 - 92	ILGV...LWPR
2136.1155	2136.1116	0.0039	93 - 109	GRDP...QLIR
3092.5798	3092.5792	0.0006	93 - 117	GRDP...ENTR
1922.9911	1922.9890	0.0021	95 - 109	DPWE...QLIR
974.4786	974.4781	0.0005	110 - 117	QQVTENTR
1601.8121	1601.8121	0.0000	110 - 123	QQVT...ALAR
645.3440	645.3446	-0.0006	118 - 123	DTALAR
990.5245	990.5247	-0.0002	124 - 132	LQGL...NSFR
1650.7633	1650.7638	-0.0005	133 - 145	AYQQ...LENR
2107.9515	2107.9559	-0.0044	133 - 149	AYQQ...DDAR
2365.1092	2365.1047	0.0045	133 - 151	AYQQ...ARTR
3057.6331	3057.6361	-0.0030	150 - 175	TRSV...FAIR
2800.4818	2800.4873	-0.0055	152 - 175	SVLY...FAIR
7266.8344	7266.8293	0.0051	152 - 215	SVLY...EIQR
2518.4161	2518.4093	0.0068	176 - 197	NQEV...LLLR
4484.3640	4484.3526	0.0114	176 - 215	NQEV...EIQR
1983.9531	1983.9538	-0.0007	198 - 215	DASL...EIQR
1113.5454	1113.5454	0.0000	216 - 223	YYERQVEK
1319.5563	1319.5564	-0.0001	224 - 233	TREY...YCAR
1062.4082	1062.4076	0.0006	226 - 233	EYSDYCAR
1249.6207	1249.6203	0.0004	234 - 243	WYNT...NNLR
2264.1086	2264.1086	0.0000	234 - 252	WYNT...SWLR
1032.4995	1032.4988	0.0007	244 - 252	GTNA...SWLR
1896.9329	1896.9343	-0.0014	244 - 258	GTNA...QFRR
882.4483	882.4460	0.0023	253 - 258	YNQFRR
2263.2196	2263.2212	-0.0016	258 - 277	RDLT...YDTR
2107.1212	2107.1201	0.0011	259 - 277	DLTL...YDTR
3468.7981	3468.7963	0.0018	259 - 289	DLTL...QLTR
4513.3151	4513.3203	-0.0052	259 - 298	DLTL...PIGR
1379.6881	1379.6867	0.0014	278 - 289	VYPM...QLTR
1062.5338	1062.5346	-0.0008	290 - 298	EIYT...PIGR
5243.6491	5243.6469	0.0022	299 - 346	TNAP...VLSR
7066.4556	7066.4467	0.0089	299 - 360	TNAP...VGHR
1840.8100	1840.8104	-0.0004	347 - 360	WSNT...VGHR
2326.0712	2326.0701	0.0011	347 - 364	WSNT...LESR
2989.5168	2989.5217	-0.0049	365 - 392	TIRG...FTSR
2619.2933	2619.2889	0.0044	368 - 392	GSLS...FTSR

Experimental Mass[2]	Calculated Mass[3]	Difference[4]	Fragment[5]	Sequence[6]
3152.5479	3152.5487	-0.0008	368 - 396	GSLS...DVYR
5489.7927	5489.7968	-0.0041	368 - 418	GSLS...PWAR
2888.5197	2888.5185	0.0012	393 - 418	DVYR...PWAR
2355.2601	2355.2587	0.0014	397 - 418	TESF...PWAR
1415.7423	1415.7422	0.0001	419 - 429	FNWR...NSLR
5804.8251	5804.8135	0.0116	419 - 468	FNWR...YSHR
812.4504	812.4504	0.0000	423 - 429	NPLNSLR
5201.5275	5201.5218	0.0057	423 - 468	NPLN...YSHR
4407.0847	4407.0819	0.0028	430 - 468	GSLL...YSHR
1455.8525	1455.8521	0.0004	469 - 481	LSNI...NTLR
2553.3958	2553.3928	0.0030	469 - 490	LSNI...WTHR
872.5078	872.5080	-0.0002	474 - 481	LISGNTLR
1970.0517	1970.0486	0.0031	474 - 490	LISG...WTHR
1115.5515	1115.5512	0.0003	482 - 490	APVY...WTHR
2158.1246	2158.1230	0.0016	491 - 510	SADR...PLVK
1728.9264	1728.9258	0.0006	495 - 510	TNTI...PLVK
2089.1186	2089.1168	0.0018	495 - 513	TNTI...KGFR
4060.1354	4060.1382	-0.0028	495 - 533	TNTI...DILR
2349.2274	2349.2230	0.0044	511 - 533	GFRV...DILR
2505.3200	2505.3241	-0.0041	511 - 534	GFRV...ILRR
1989.0338	1989.0320	0.0018	514 - 533	VWGG...DILR
2145.1384	2145.1331	0.0053	514 - 534	VWGG...ILRR
2405.2503	2405.2452	0.0051	534 - 554	RNTF...ITQR
2249.1415	2249.1441	-0.0026	535 - 554	NTFG...ITQR
2325.2740	2325.2726	0.0014	569 - 592	VIVL...PLQK
1249.5969	1249.5972	-0.0003	593 - 603	TMEI...LTSR
1783.8307	1783.8318	-0.0011	604 - 617	TFRY...FSFR
1379.6152	1379.6146	0.0006	607 - 617	YTDF...FSFR
2890.4637	2890.4600	0.0037	618 - 645	ANPD...YIDK
4906.4672	4906.4651	0.0021	618 - 663	ANPD...DLER
5233.6603	5233.6557	0.0046	618 - 666	ANPD...RAQK
1947.0437	1947.0425	0.0012	664 - 681	AQKA...IGLK
1619.8526	1619.8519	0.0007	667 - 681	AVNE...IGLK
3243.4239	3243.4224	0.0015	682 - 708	TDVT...LDEK
3371.5164	3371.5174	-0.0010	682 - 709	TDVT...DEKK
3957.8241	3957.8136	0.0105	682 - 714	TDVT...LSEK
732.4015	732.4017	-0.0002	709 - 714	KELSEK
831.4702	831.4702	0.0000	710 - 716	ELSEKVK
774.3982	774.3984	-0.0002	720 - 725	RLSDER
1871.9588	1871.9602	-0.0014	720 - 734	RLSD...PNFR
1715.8591	1715.8591	0.0000	721 - 734	LSDE...PNFR
2156.1103	2156.1086	0.0017	721 - 738	LSDE...GINR
1115.5726	1115.5723	0.0003	726 - 734	NLLQ...PNFR
1555.8231	1555.8219	0.0012	726 - 738	NLLQ...GINR

Experimental Mass[2]	Calculated Mass[3]	Difference[4]	Fragment[5]	Sequence[6]
970.5311	970.5308	0.0003	735 - 742	GINRQLDR
929.4830	929.4831	-0.0001	739 - 745	QLDRGWR
4549.1413	4549.1424	-0.0011	743 - 781	GWRG...LYQK
1551.7441	1551.7417	0.0024	746 - 760	GSTD...DVFK
4149.9435	4149.9405	0.0030	746 - 781	GSTD...LYQK
2616.2074	2616.2094	-0.0020	761 - 781	ENYV...LYQK
831.4697	831.4702	-0.0005	782 - 788	IDESKLK
1322.7212	1322.7194	0.0018	782 - 792	IDES...AYTR
750.4382	750.4388	-0.0006	787 - 792	LKAYTR
1069.5662	1069.5668	-0.0006	789 - 796	AYTRYQLR
1825.9099	1825.9098	0.0001	797 - 811	GYIE...YLIR
2302.1537	2302.1481	0.0056	797 - 815	GYIE...YNAK
4627.3601	4627.3598	0.0003	797 - 838	GYIE...PIGK
2819.4571	2819.4606	-0.0035	812 - 838	YNAK...PIGK
2343.2218	2343.2223	-0.0005	816 - 838	HETV...PIGK
3520.6328	3520.6293	0.0035	839 - 868	CAHH...VIFK
1024.5414	1024.5414	0.0000	869 - 877	IKTQ...GHAR
783.3623	783.3624	-0.0001	871 - 877	TQDGHAR
2862.5031	2862.4988	0.0043	871 - 896	TQDG...ALAR
2097.1474	2097.1470	0.0004	878 - 896	LGNL...ALAR
1706.8983	1706.8991	-0.0008	908 - 920	REKL...IVYK
1550.8030	1550.7980	0.0050	909 - 920	EKLE...IVYK
1878.9717	1878.9727	-0.0010	909 - 923	EKLE...KEAK
1293.6614	1293.6605	0.0009	911 - 920	LEWE...IVYK
1621.8354	1621.8351	0.0003	911 - 923	LEWE...KEAK
1969.9380	1969.9381	-0.0001	921 - 937	EAKE...QYDR
1641.7602	1641.7635	-0.0033	924 - 937	ESVD...QYDR
3390.6601	3390.6626	-0.0025	924 - 953	ESVD...ADKR
1610.8082	1610.8086	-0.0004	938 - 952	LQAD...AADK
1766.9128	1766.9097	0.0031	938 - 953	LQAD...ADKR
766.4567	766.4562	0.0005	953 - 958	RVHSIR
4492.3474	4492.3430	0.0044	954 - 993	VHSI...YDAR
2615.3494	2615.3482	0.0012	959 - 982	EAYL...LEGR
3900.0148	3899.9985	0.0163	959 - 993	EAYL...YDAR
1302.6617	1302.6608	0.0009	983 - 993	IFTA...YDAR
1756.9504	1756.9512	-0.0008	983 - 997	IFTA...NVIK
1432.6447	1432.6443	0.0004	1012 - 1023	GHVD...NNHR
3369.6337	3369.6338	-0.0001	1012 - 1040	GHVD...QEVR
1954.9977	1955.0000	-0.0023	1024 - 1040	SVLV...QEVR
2524.2738	2524.2744	-0.0006	1024 - 1045	SVLV...CPGR
1189.6406	1189.6390	0.0016	1041 - 1050	VCPG...YILR
1182.6760	1182.6761	-0.0001	1046 - 1055	GYIL...TAYK
2968.3764	2968.3760	0.0004	1051 - 1076	VTAY...DELK
4069.6770	4069.6742	0.0028	1077 - 1110	FSNC...YTSR

Experimental Mass[2]	Calculated Mass[3]	Difference[4]	Fragment[5]	Sequence[6]
4339.8198	4339.8182	0.0016	1077 - 1112	FSNC...SRNR
2742.1699	2742.1681	0.0018	1111 - 1135	NRGY...YEEK
3405.4638	3405.4657	-0.0019	1111 - 1141	NRGY...TDGR
2472.0208	2472.0241	-0.0033	1113 - 1135	GYDG...YEEK
3135.3206	3135.3217	-0.0011	1113 - 1141	GYDG...TDGR
3291.4220	3291.4228	-0.0008	1113 - 1142	GYDG...DGRR
681.3083	681.3082	0.0001	1136 - 1141	AYTDGR
837.4092	837.4093	-0.0001	1136 - 1142	AYTDGRR
1146.4839	1146.4836	0.0003	1142 - 1150	RDNP...ESNR
2729.2520	2729.2504	0.0016	1142 - 1165	RDNP...YVTK
990.3831	990.3825	0.0006	1143 - 1150	DNPCESNR
2573.1489	2573.1493	-0.0004	1143 - 1165	DNPC...YVTK
1600.7778	1600.7773	0.0005	1151 - 1165	GYGD...YVTK
1269.5777	1269.5765	0.0012	1166 - 1175	ELEY...ETDK
4001.9221	4001.9271	-0.0050	1166 - 1199	ELEY...LMEE

[1] All imported values were rounded to 4 decimal places.
[2] Only experimental masses that matched calculated masses with the highest scores are listed in table.
[3] The calculated mass is the exact molecular mass calculated from the matched peptide sequence.
[4] The calculated difference = experimental mass – calculated mass.
[5] Position refers to amino acid residues within the predicted *Bt*-produced Cry1B.868 sequence as depicted in Figure 22, Panel B.
[6] For peptide matches greater than nine amino acids in length the first 4 residues and last 4 residues are shown separated by dots (…).

(A)

```
   1 MTSNRKNENE IINALSIPAV SNHSAQMNLS TDARIEDSLC IAEGNNIDPF
  51 VSASTVQTGI NIAGRILGVL GVPFAGQIAS FYSFLVGELW PRGRDPWEIF
 101 LEHVEQLIRQ QVTENTRDTA LARLQGLGNS FRAYQQSLED WLENRDDART
 151 RSVLYTQYIA LELDFLNAMP LFAIRNQEVP LLMVYAQAAN LHLLLLRDAS
 201 LFGSEFGLTS QEIQRYYERQ VEKTREYSDY CARWYNTGLN NLRGTNAESW
 251 LRYNQFRRDL TLGVLDLVAL FPSYDTRVYP MNTSAQLTRE IYTDPIGRTN
 301 APSGFASTNW FNNNAPSFSA IEAAVIRPPH LLDFPEQLTI FSVLSRWSNT
 351 QYMNYWVGHR LESRTIRGSL STSTHGNTNT SINPVTLQFT SRDVYRTESF
 401 AGINILLTTP VNGVPWARFN WRNPLNSLRG SLLYTIGYTG VGTQLFDSET
 451 ELPPETTERP NYESYSHRLS NIRLISGNTL RAPVYSWTHR SADRTNTISS
 501 DSINQIPLVK GFRVWGGTSV ITGPGFTGGD ILRRNTFGDF VSLQVNINSP
 551 ITQRYRLRFR YASSRDARVI VLTGAASTGV GGQVSVNMPL QKTMEIGENL
 601 TSRTFRYTDF SNPFSFRANP DIIGISEQPL FGAGSISSGE LYIDKIEIIL
 651 ADATFEAESD LERAQKAVNE LFTSSNQIGL KTDVTDYHID QVSNLVECLS
 701 DEFCLDEKKE LSEKVKHAKR LSDERNLLQD PNFRGINRQL DRGWRGSTDI
 751 TIQGGDDVFK ENYVTLLGTF DECYPTYLYQ KIDESKLKAY TRYQLRGYIE
 801 DSQDLEIYLI RYNAKHETVN VPGTGSLWPL SAPSPIGKCA HHSHHFSLDI
 851 DVGCTDLNED LGVWVIFKIK TQDGHARLGN LEFLEEKPLV GEALARVKRA
 901 EKKWRDKREK LEWETNIVYK EAKESVDALF VNSQYDRLQA DTNIAMIHAA
 951 DKRVHSIREA YLPELSVIPG VNAAIFEELE GRIFTAFSLY DARNVIKNGD
1001 FNNGLSCWNV KGHVDVEEQN NHRSVLVVPE WEAEVSQEVR VCPGRGYILR
1051 VTAYKEGYGE GCVTIHEIEN NTDELKFSNC VEEEVYPNNT VTCNDYTATQ
1101 EEYEGTYTSR NRGYDGAYES NSSVPADYAS AYEEKAYTDG RRDNPCESNR
1151 GYGDYTPLPA GYVTKELEYF PETDKVWIEI GETEGTFIVD SVELLLMEE
```

(B)

```
   1 MTSNRKNENE IINALSIPAV SNHSAQMNLS TDARIEDSLC IAEGNNIDPF
  51 VSASTVQTGI NIAGRILGVL GVPFAGQIAS FYSFLVGELW PRGRDPWEIF
 101 LEHVEQLIRQ QVTENTRDTA LARLQGLGNS FRAYQQSLED WLENRDDART
 151 RSVLYTQYIA LELDFLNAMP LFAIRNQEVP LLMVYAQAAN LHLLLLRDAS
 201 LFGSEFGLTS QEIQRYYERQ VEKTREYSDY CARWYNTGLN NLRGTNAESW
 251 LRYNQFRRDL TLGVLDLVAL FPSYDTRVYP MNTSAQLTRE IYTDPIGRTN
 301 APSGFASTNW FNNNAPSFSA IEAAVIRPPH LLDFPEQLTI FSVLSRWSNT
 351 QYMNYWVGHR LESRTIRGSL STSTHGNTNT SINPVTLQFT SRDVYRTESF
 401 AGINILLTTP VNGVPWARFN WRNPLNSLRG SLLYTIGYTG VGTQLFDSET
 451 ELPPETTERP NYESYSHRLS NIRLISGNTL RAPVYSWTHR SADRTNTISS
 501 DSINQIPLVK GFRVWGGTSV ITGPGFTGGD ILRRNTFGDF VSLQVNINSP
 551 ITQRYRLRFR YASSRDARVI VLTGAASTGV GGQVSVNMPL QKTMEIGENL
 601 TSRTFRYTDF SNPFSFRANP DIIGISEQPL FGAGSISSGE LYIDKIEIIL
 651 ADATFEAESD LERAQKAVNE LFTSSNQIGL KTDVTDYHID QVSNLVECLS
 701 DEFCLDEKKE LSEKVKHAKR LSDERNLLQD PNFRGINRQL DRGWRGSTDI
 751 TIQGGDDVFK ENYVTLLGTF DECYPTYLYQ KIDESKLKAY TRYQLRGYIE
 801 DSQDLEIYLI RYNAKHETVN VPGTGSLWPL SAPSPIGKCA HHSHHFSLDI
 851 DVGCTDLNED LGVWVIFKIK TQDGHARLGN LEFLEEKPLV GEALARVKRA
 901 EKKWRDKREK LEWETNIVYK EAKESVDALF VNSQYDRLQA DTNIAMIHAA
 951 DKRVHSIREA YLPELSVIPG VNAAIFEELE GRIFTAFSLY DARNVIKNGD
1001 FNNGLSCWNV KGHVDVEEQN NHRSVLVVPE WEAEVSQEVR VCPGRGYILR
1051 VTAYKEGYGE GCVTIHEIEN NTDELKFSNC VEEEVYPNNT VTCNDYTATQ
1101 EEYEGTYTSR NRGYDGAYES NSSVPADYAS AYEEKAYTDG RRDNPCESNR
1151 GYGDYTPLPA GYVTKELEYF PETDKVWIEI GETEGTFIVD SVELLLMEE
```

Figure 22. Peptide Map of the MON 95379-Produced Cry1B.868 and *Bt*-Produced Cry1B.868 Proteins

(A). The amino acid sequence of the MON 95379-produced Cry1B.868 protein was deduced from the *cry1B.868* gene present in MON 95379. Boxed regions correspond to peptides that were identified from the MON 95379-produced Cry1B.868 protein sample using LC-MS/MS. In total, 91% coverage (1088 out of 1199 amino acids) of the expected protein sequence was covered by the identified peptides. Gray highlighted regions correspond to the receptor binding domain.

(B). The amino acid sequence of the *Bt*-produced Cry1B.868 protein was deduced from the *cry1B.868* gene that is contained on the expression plasmid pMON236906. Boxed regions correspond to peptides that were identified from the *Bt*-produced Cry1B.868 protein sample using LC-MS/MS. In total, 96% coverage (1156 out of 1199 amino acids) of the expected protein sequence was covered by the identified peptides. Gray highlighted regions correspond to the receptor binding domain.

B.1(a)(i)(iii) Results of western blot analysis of the Cry1B.868 protein isolated from the grain of MON 95379 and immunoreactivity comparison to *Bt*-produced Cry1B.868

Western blot analysis was conducted using rabbit anti-Cry1B.868 polyclonal antibody as additional means to confirm the identity of the Cry1B.868 protein isolated from the grain of MON 95379 and to assess the equivalence of the immunoreactivity of the MON 95379-produced and *Bt*-produced Cry1B.868 proteins.

The results showed that immunoreactive bands with the same electrophoretic mobility were present in all lanes loaded with the MON 95379-produced and *Bt*-produced Cry1B.868 proteins (Figure 23). For each amount loaded, comparable signal intensity was observed between the MON 95379-produced and *Bt*-produced Cry1B.868 protein bands. As expected, the signal intensity increased with the increasing amounts of protein loaded, thus, supporting identification of MON 95379-produced Cry1B.868 protein.

To compare the immunoreactivity of the MON 95379-produced and *Bt*-produced Cry1B.868 proteins, densitometric analysis was conducted on the bands that migrated at the expected apparent MW for Cry1B.868 proteins (~ 130 kDa). The signal intensity (reported in OD) of the band of interest in lanes loaded with MON 95379-produced and *Bt*-produced Cry1B.868 proteins was measured. Because the mean signal intensity of the MON 95379-produced Cry1B.868 protein was within 35% of the mean signal intensity of the *Bt*-produced Cry1B.868 protein (Table 10), the MON 95379-produced Cry1B.868 and *Bt*-produced Cry1B.868 proteins were determined to have equivalent immunoreactivity.

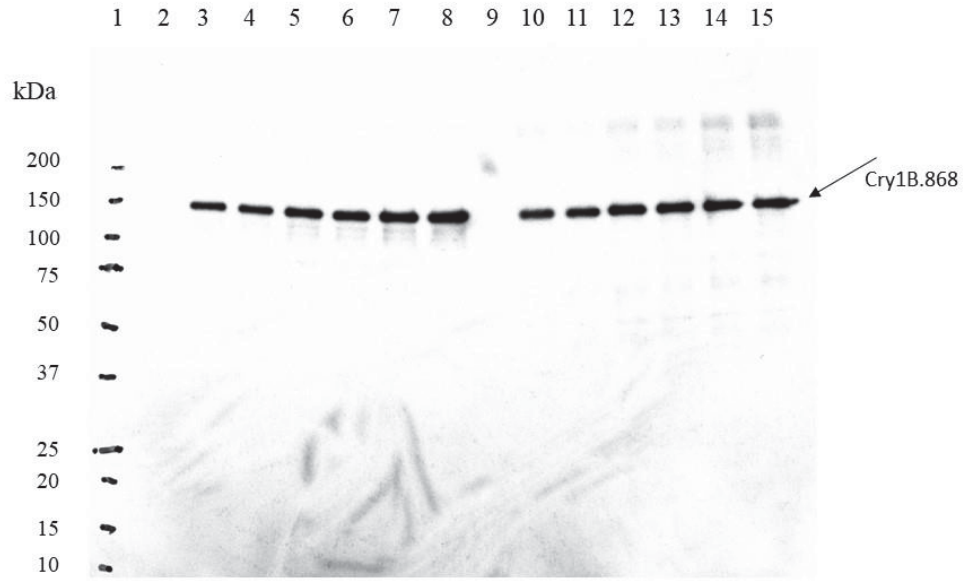

Figure 23. Western Blot Analysis and Immunoreactivity of MON 95379-Produced and *Bt*-Produced Cry1B.868 Proteins

Aliquots of the MON 95379-produced and *Bt*-produced Cry1B.868 proteins were subjected to SDS-PAGE and electro-transferred to a PVDF membrane. Proteins were detected using rabbit anti-Cry1B.868 polyclonal antibodies as the primary antibodies. Immunoreactive bands were visualized using HRP-conjugated secondary antibodies and an ECL system. The 1-minute exposure is shown. The approximate MW (kDa) of the standards are shown on the left. Lane designations are as follows:

Lane	Sample	Amount (ng)
1	Precision Plus Protein™ Standards	-
2	Blank	-
3	MON 95379-produced Cry1B.868	5
4	MON 95379-produced Cry1B.868	5
5	MON 95379-produced Cry1B.868	10
6	MON 95379-produced Cry1B.868	10
7	MON 95379-produced Cry1B.868	15
8	MON 95379-produced Cry1B.868	15
9	Blank	-
10	*Bt*-produced Cry1B.868	5
11	*Bt*-produced Cry1B.868	5
12	*Bt*-produced Cry1B.868	10
13	*Bt*-produced Cry1B.868	10
14	*Bt*-produced Cry1B.868	15
15	*Bt*-produced Cry1B.868	15

Table 10. Immunoreactivity of the MON 95379-Produced and *Bt*-Produced Cry1B.868 Proteins

Mean Signal Intensity from MON 95379-Produced Cry1B.868 [1] (OD)	Mean Signal Intensity from *Bt*-Produced Cry1B.868 [1] (OD)	Acceptance Limits[2] (OD)
2156.21	2527.92	1643.15 – 3412.69

[1] Each value represents the mean of six values (n = 6).
[2] The acceptance limits are for the MON 95379-produced Cry1B.868 protein and are based on the interval between -35% (2527.92 x 0.65 = 1643.15) and +35 % (2527.92 x 1.35 = 3412.69) of the mean of the *Bt*-produced Cry1B.868 signal intensity across all loads.

B.1(a)(i)(iv) Results of the Cry1B.868 protein molecular weight and purity analysis

For apparent MW and purity determination, the MON 95379-produced Cry1B.868 and the *Bt*-produced Cry1B.868 proteins were subjected to SDS-PAGE. Following electrophoresis, the gel was stained with Brilliant Blue G-Colloidal stain and analyzed by densitometry. The MON 95379-produced Cry1B.868 protein (Figure 24, lanes 3-8) migrated to the same position on the gel as the *Bt*-produced Cry1B.868 protein (Figure 24, lane 2) and the apparent MW was calculated to be 126.8 kDa (Table 11) Because the experimentally determined apparent MW of the MON 95379-produced Cry1B.868 protein was within the acceptance limits for equivalence (Table 12), the MON 95379-produced Cry1B.868 and *Bt*-produced Cry1B.868 proteins were determined to have equivalent apparent molecular weights.

The purity of the MON 95379-produced Cry1B.868 protein was calculated based on the six lanes loaded on the gel (Figure 24, lanes 3-8). The average purity was determined to be 97% (Table 11).

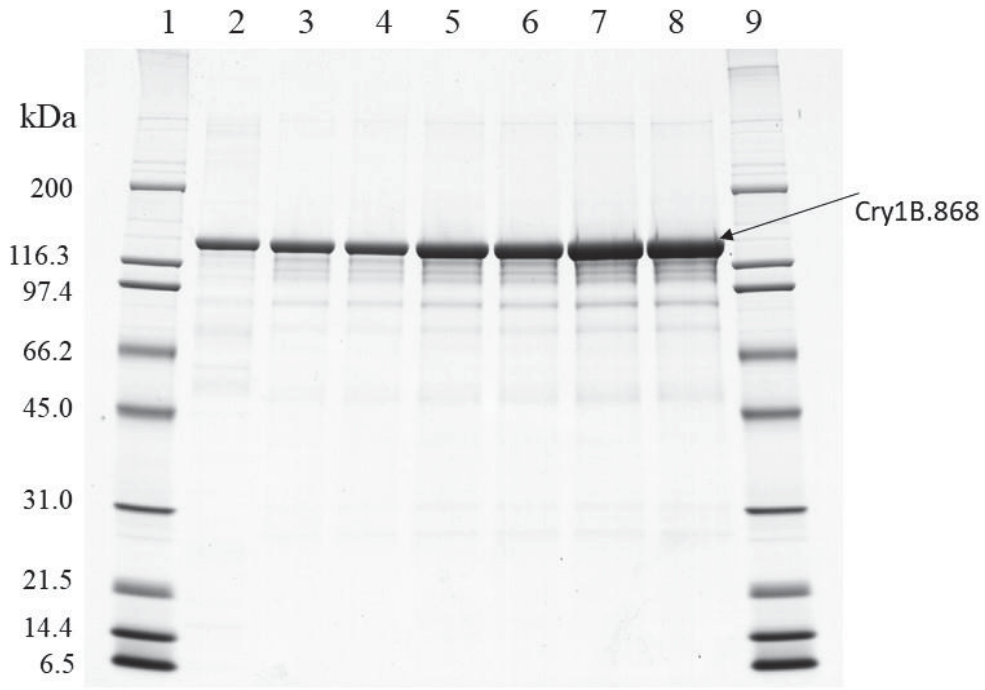

Figure 24. Purity and Apparent Molecular Weight Analysis of the MON 95379-Produced Cry1B.868 Protein

Aliquots of the MON 95379-produced and the *Bt*-produced Cry1B.868 proteins were subjected to SDS-PAGE and the gel was stained with Brilliant Blue G-Colloidal stain. The MWs (kDa) are shown on the left and correspond to the standards loaded in lanes 1 and 9. Lane 10 was cropped from the image. The intact Cry1B.868 protein is indicated with an arrow in the image. Lane designations are as follows:

Lane	Sample	Amount (µg)
1	Broad Range MW Standard	5.0
2	*Bt*-produced Cry1B.868	1.0
3	MON 95379-produced Cry1B.868	1.0
4	MON 95379-produced Cry1B.868	1.0
5	MON 95379-produced Cry1B.868	2.0
6	MON 95379-produced Cry1B.868	2.0
7	MON 95379-produced Cry1B.868	3.0
8	MON 95379-produced Cry1B.868	3.0
9	Broad Range MW Standard	5.0
10	Blank	

Table 11. Apparent Molecular Weight and Purity Analysis of the MON 95379-Produced Cry1B.868 Protein

	Apparent MW[1] (kDa)	Purity[2] (%)
Average (n=6)	126.8	97

[1]Final MW was rounded to one decimal place.
[2]Average % purity was rounded to the nearest whole number.

Table 12. Apparent Molecular Weight Comparison Between the MON 95379-Produced Cry1B.868 and *Bt*-Produced Cry1B.868 Proteins

Apparent MW of MON 95379-Produced Cry1B.868 Protein (kDa)	Apparent MW of Bt-Produced Cry1B.868 Protein[1] (kDa)	Acceptance Limits[2] (kDa)
126.8	129.6	118.5 – 140.7

[1] As reported on the COA of the *Bt*-produced Cry1B.868 protein (lot 7565).
[2] Data obtained for the *Bt*-produced Cry1B.868 protein were used to generate the prediction interval. Values in this column represent a 95% prediction interval developed from eight individual assays with *Bt*-produced Cry1B.868 protein (Appendix 1).

B.1(a)(i)(v) Cry1B.868 glycosylation analysis

Some eukaryotic proteins are post-translationally modified by the addition of carbohydrate moieties (Rademacher *et al.*, 1988). To test whether the Cry1B.868 protein was glycosylated when expressed in the maize grain of MON 95379, the MON 95379-produced Cry1B.868 protein was analyzed using an ECL™ glycoprotein detection method. Transferrin, a glycosylated protein, was used as a positive control in the assay. To assess equivalence of the MON 95379-produced and *Bt*-produced Cry1B.868 proteins, the *Bt*-produced Cry1B.868 protein was also analyzed.

A clear glycosylation signal was observed at the expected molecular weight (~ 80 kDa) in the lanes containing the positive control (transferrin) and the band intensity increased with increasing concentration (Figure 25A). In contrast, no glycosylation signal was observed in the lanes containing the *Bt*-produced Cry1B.868 protein or MON 95379-produced Cry1B.868 protein (Figure 25A).

To confirm that MON 95379-produced Cry1B.868 and *Bt*-produced Cry1B.868 proteins were appropriately loaded for glycosylation analysis, a second membrane with identical loadings and transfer time was stained with Coomassie Blue R250 for protein detection. Both the MON 95379-produced and *Bt*-produced Cry1B.868 proteins were detected (Figure 25B). These data indicate that the glycosylation status of MON 95379-produced Cry1B.868 protein is equivalent to that of the *Bt*-produced Cry1B.868 protein and that neither is glycosylated.

A. B.

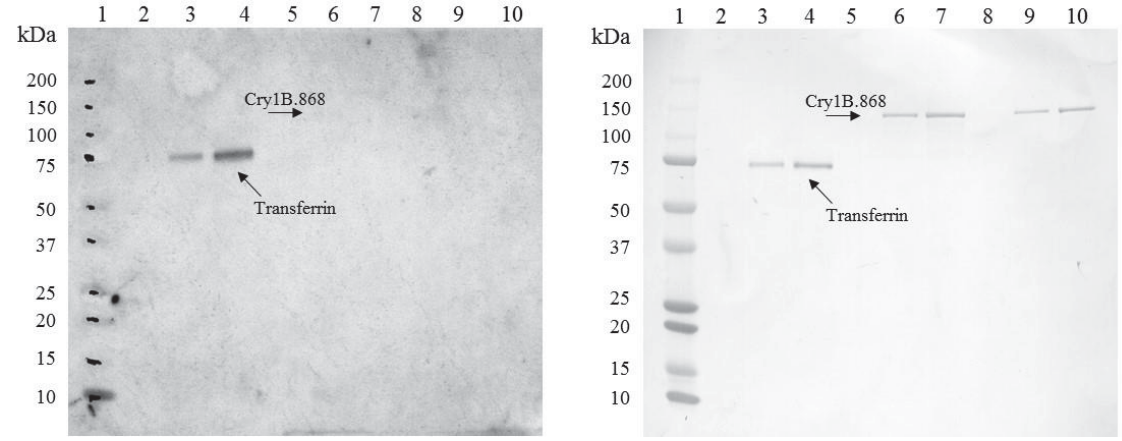

Figure 25. Glycosylation Analysis of the MON 95379-Produced and *Bt*-Produced Cry1B.868 Proteins

Aliquots of the transferrin (positive control), MON 95379-produced and *Bt*-produced Cry1B.868 proteins were subjected to SDS-PAGE and electro-transferred to a PVDF membrane. The MWs (kDa) correspond to the Precision Plus Protein™ Standards. The arrows show the expected migration of the MON 95379-produced and *Bt*-produced Cry1B.868 proteins and transferrin. (A) Where present, the labeled carbohydrate moieties were detected by addition of streptavidin conjugated to HRP followed by a luminol-based detection using ECL reagents and exposure to Hyperfilm™. The 1.5-minute exposure is shown. (B) An equivalent blot was stained with Coomassie Blue R250 to confirm the presence of proteins. Lane designations are as follows:

Lane	Sample	Amount (ng)
1	Precision Plus Protein™ Standards	-
2	Blank	-
3	Transferrin (positive control)	100
4	Transferrin (positive control)	200
5	Blank	-
6	MON 95379-produced Cry1B.868	100
7	MON 95379-produced Cry1B.868	200
8	Blank	-
9	*Bt*-produced Cry1B.868	100
10	*Bt*-produced Cry1B.868	200

B.1(a)(i)(vi) Cry1B.868 functional activity

The MON 95379-produced Cry1B.868 and *Bt*-produced Cry1B.868 proteins were considered to have equivalent functional activity if the activities of both proteins (measured by EC_{50} values) were within the acceptance limits of 0.024 to 0.272 µg of Cry1B.868 protein/mL diet, which is the prediction interval calculated from a data set of *Bt*-produced Cry1B.868 protein activity.

The experimentally determined functional activity for the MON 95379-produced and *Bt*-produced Cry1B.868 proteins are presented in (Table 13). The mean EC_{50}s values of MON 95379-produced and *Bt*-produced Cry1B.868 proteins were 0.15 and 0.20 µg of Cry1B.868 protein/mL diet, respectively. Because both EC_{50}s fall within the preset acceptance limits (Table 13), the MON 95379-produced Cry1B.868 protein was considered to have equivalent functional activity to that of the *Bt*-produced Cry1B.868 protein.

Table 13. Functional Activity of MON 95379-Produced and *Bt*-Produced Cry1B.868 Proteins

Replicates	MON 95379-Produced Cry1B.868 EC_{50} [1] (µg protein/ml diet)	Bt-Produced Cry1B.868 EC_{50} [1] (µg protein/ml diet)	EC_{50} Acceptance Limits[2] (µg protein/ml diet)
1	0.18	0.25	
2	0.15	0.21	0.024 – 0.272
3	0.12	0.14	
Mean	0.15	0.20	-

[1] Value refers to mean calculated based on three independent assays (n=3).
[2] Data obtained for the *Bt*-produced Cry1B.868 proteins were used to generate a prediction interval for setting the acceptance limits. Values in this column represent a 95% prediction interval developed from 24 individual bioassays with *Bt*-produced Cry1B.868 protein (Appendix 6).

B.1(a)(i)(vii) MON 95379 Cry1B.868 protein identity and equivalence conclusion

The MON 95379-produced Cry1B.868 protein purified from MON 95379 grain was characterized, and a comparison of the physicochemical and functional properties between the MON 95379-produced and the *Bt*-produced Cry1B.868 proteins was conducted following a panel of analytical tests: 1) N-terminal sequence analysis established the same identity for the MON 95379-produced and the *Bt*-produced Cry1B.868 proteins; 2) Nano LC-MS/MS analysis yielded peptide masses consistent with the expected peptide masses from the theoretical trypsin digest of the *cry1B.868* gene product present in MON 95379; 3) the MON 95379-produced and the *Bt*-produced Cry1B.868 proteins were both detected on a western blot probed with antibodies specific for Cry1B.868 protein and the immunoreactive properties of both proteins was shown to be equivalent; 4) the electrophoretic mobility and apparent molecular weight of the MON 95379-produced and the *Bt*-produced Cry1B.868 proteins were shown to be equivalent; 5) the glycosylation status of MON 95379-produced

and the *Bt*-produced Cry1B.868 proteins was determined to be equivalent; and 6) the functional activity of the MON 95379-produced and the *Bt*-produced Cry1B.868 was demonstrated to be equivalent. These results demonstrate that the MON 95379-produced and the *Bt*-produced Cry1B.868 protein are equivalent.

The ability of the Cry1B.868 to bind to its target receptor is dependent on the confirmation of the Cry1B.868 receptor binding domain. Protein structure, or confirmation, is determined by the specific sequence of amino acids that comprise the different structural and functional elements. It can inferred that once properly folded, proteins that possess equivalent amino acid sequences would have equivalent functional activity or receptor binding. The MON 95379- and *Bt*-produced Cry1B.868 proteins possess equivalent amino sequences, and thereby equivalent receptor binding domains, as evidenced by the very high amino acid sequence similarity seen by mass fingerprint analysis where >90% coverage was observed. The equivalency of the protein sequences was also confirmed indirectly through sequencing the of genes of the expressed MON 95379- and *Bt*-produced Cry1B.868 proteins. Finally, the equivalent functional activity of the protein isolated from both sources indicates that the confirmation of the receptor binding domains in both proteins are equivalent.

Taken together, the equivalency data provided in support of MON 95379 Cry1B.868 confirms that the *Bt*-produced Cry1B.868 protein is appropriate surrogate for use in the evaluation of the safety of the MON 95379-produced Cry1B.868 protein.

For details, please also refer to Appendix 6 ([redacted]., 2020 (TRR0000416)).

B.1(a)(ii) Characterisation of the MON 95379 Cry1Da_7 protein

Cry1Da_7 Protein Identity and Equivalence

For the safety data generated using the *Bt*-produced Cry1Da_7 protein to be applied to the MON 95379-produced Cry1Da_7 protein (plant-produced Cry1Da_7), the equivalence of the plant- and *Bt*-produced proteins must first be demonstrated. To assess the equivalence between the MON 95379-produced and *Bt*-produced Cry1Da_7 proteins, a small quantity of the MON 95379-produced Cry1Da_7 protein was purified from MON 95379 grain. The MON 95379-produced Cry1Da_7 protein was characterized and the equivalence of the physicochemical characteristics and functional activity between the MON 95379-produced and *Bt*-produced Cry1Da_7 proteins was assessed using a panel of analytical tests; as shown in Table 14. Taken together, these data provide a detailed characterisation of the MON 95379-produced Cry1Da_7 protein and establish the equivalence of the MON 95379-produced and *Bt*-produced Cry1Da_7 proteins.

For details, please also refer to Appendix 7 ([redacted], 2020 (MSL0030547)).

Table 14. Summary of MON 95379 Cry1Da_7 Protein Identity and Equivalence

Analytical Test Assessment	Section Cross Reference	Analytical Test Outcome
N-terminal sequence	B.1 (a)(ii)(i)	The expected N-terminal sequence for MON 95379-produced Cry1Da_7 protein was observed by Nano LC-MS/MS[1]
Nano LC-MS/MS[1]	B.1 (a)(ii)(ii)	Nano LC-MS/MS[1] analysis of trypsin digested peptides from MON 95379-produced Cry1Da_7 protein yielded peptide masses consistent with expected peptide masses from the theoretical trypsin digest of the amino acid sequence
Western blot analysis	B.1 (a)(ii)(iii)	MON 95379-produced Cry1Da_7 protein identity was confirmed using a western blot probed with antibodies specific for Cry1Da_7 protein Immunoreactive properties of the MON 95379-produced Cry1Da_7 and the *Bt*-produced Cry1Da_7 proteins were shown to be equivalent
Apparent molecular weight (MW)	B.1 (a)(ii)(iv)	Electrophoretic mobility and apparent molecular weight of the MON 95379-produced Cry1Da_7 and the *Bt*-produced Cry1Da_7 proteins were shown to be equivalent
Glycosylation analysis	B.1 (a)(ii)(v)	Glycosylation status of MON 95379-produced Cry1Da_7 and *Bt*-produced Cry1Da_7 proteins were shown to be equivalent
Functional activity	B.1 (a)(ii)(vi)	Functional activity of the MON 95379-produced Cry1Da_7 and the *Bt*-produced Cry1Da_7 proteins were shown to be equivalent by insect bioassay.

[1] Nano LC-MS/MS = Nanoscale liquid chromatography-tandem mass spectrometry

A summary of the data obtained to support a conclusion of protein equivalence is below.

B.1(a)(ii)(i) Results of the N-terminal sequencing analysis

The expected N-terminal sequence for the Cry1Da_7 protein deduced from the *cry1Da_7* gene present in maize of MON 95379 was observed by LC-MS/MS, except that the N-terminal methionine was cleaved *in vivo* from MON 95379 produced Cry1Da_7 by methionine aminopeptidase or other aminopeptidases (see Experimental Sequence, Figure 26). The cleavage of the N-terminal methionine from proteins *in vivo* by methionine aminopeptidase is common in many organisms (Bradshaw *et al.*, 1998; Wang *et al.*, 2016). The N-terminal sequence for MON 95379-produced Cry1Da_7 protein was consistent with the N-terminal sequence for the *Bt*-produced Cry1Da_7 protein observed by LC-MS/MS (Figure 26). Hence, the sequence information confirms the identity of the Cry1Da_7 protein isolated from the grain of MON 95379.

Amino Acids Residue # from the N-terminus	→	1	2	3	4	5	6	7	8	9	10	11	12	13	14	15	16
Bt-produced Cry1Da_7 sequence	→	-	A	E	I	N	N	Q	N	Q	C	V	P	Y	N	C	L
Expected Cry1Da_7 Sequence	→	M	A	E	I	N	N	Q	N	Q	C	V	P	Y	N	C	L
MON 95379 Experimental Sequence	→	-	A	E	I	N	N	Q	N	Q	C	V	P	Y	N	C	L

Figure 26. N-terminal Sequence of the MON 95379-Produced Cry1Da_7 Protein

The experimental sequence obtained from the MON 95379-produced Cry1Da_7 was compared to the expected sequence deduced from the *cry1Da_7* gene present in MON 95379. *Bt*-produced Cry1Da_7 protein sequence above was derived from the reference substance COA (lot 7799). The single letter International Union of Pure and Applied Chemistry - International Union of Biochemistry (IUPAC-IUB) amino acid code is M, Methionine; A, Alanine; E, Glutamic acid; I, Isoleucine; N, Asparagine; Q, Glutamine; C, Cysteine; V, Valine; P, Proline; Y, Tyrosine; L, Leucine.

B.1(a)(ii)(ii) Results of nano LC-MS/MS mass fingerprint analysis

The identity of the MON 95379-produced Cry1Da_7 protein was confirmed by LC-MS/MS analysis of peptide fragments produced by the trypsin digestion of the MON 95379-produced Cry1Da_7 protein.

There were 113 unique peptides identified that corresponded to the masses expected to be produced by trypsin digestion of the MON 95379-produced Cry1Da_7 protein (Table 15). The identified masses were used to assemble a coverage map of the entire Cry1Da_7 protein (Figure 27A). The experimentally determined coverage of the MON 95379-produced Cry1Da_7 protein was 89% (Figure 27A, 1049 out of 1166 amino acids). This analysis further confirms the identity of MON 95379-produced Cry1Da_7 protein.

There were 136 unique peptides identified that corresponded to the masses expected to be produced by trypsin digestion of the *Bt*-produced Cry1Da_7 protein (Table 16) by

LC-MS/MS analysis during the protein characterisation. The identified masses were used to assemble a coverage map of the entire Cry1Da_7 protein (Figure 27B). The experimentally determined coverage of the *Bt*-produced Cry1Da_7 protein was 89% (Figure 27B, 1049 out of 1166 amino acids). This analysis further confirms the identity of *Bt*-produced Cry1Da_7 protein.

Table 15. Summary of the Tryptic Masses Identified for the MON 95379-Produced Cry1Da_7 Using LC-MS/MS[1]

Experimental Mass[2]	Calculated Mass[3]	Difference[4]	Fragment[5]	Sequence[6]
2304.0267	2304.0263	0.0004	2 - 20	AEIN...SNPK
3243.5301	3243.5288	0.0013	2 - 28	AEIN...GEER
957.5145	957.5131	0.0014	21 - 28	EIILGEER
763.3866	763.3864	0.0002	88 - 93	IEEFAR
687.3664	687.3664	0.0000	94 - 99	NQAISR
1035.5602	1035.5600	0.0002	100 - 108	LEGL...NLYK
535.3120	535.3118	0.0002	109 - 112	VYVR
1745.8390	1745.8373	0.0017	113 - 127	AFSD...PALR
2291.0670	2291.0640	0.0030	113 - 131	AFSD...EEMR
882.4554	882.4559	-0.0005	120 - 127	DPTNPALR
1427.6810	1427.6827	-0.0017	120 - 131	DPTN...EEMR
2063.0863	2063.0874	-0.0011	132 - 149	IQFN...PLFR
2712.5042	2712.4962	0.0080	150 - 173	VQNY...SILR
3601.9240	3601.9256	-0.0016	150 - 181	VQNY...FGER
907.4401	907.4400	0.0001	174 - 181	DVSVFGER
1309.6070	1309.6051	0.0019	182 - 192	WGYD...INNR
2868.3482	2868.3501	-0.0019	193 - 216	YSDL...QGLR
3024.4491	3024.4512	-0.0021	193 - 217	YSDL...GLRR
629.3609	629.3609	0.0000	217 - 221	RLEGR
1311.6614	1311.6612	0.0002	222 - 231	FLSD...VYNR
1614.8294	1614.8307	-0.0013	222 - 233	FLSD...NRFR
2379.2982	2379.2951	0.0031	234 - 253	RQLT...YDIR
2223.1952	2223.1940	0.0012	235 - 253	QLTI...YDIR
1391.7412	1391.7409	0.0003	254 - 265	TYPI...QLTR
3409.7462	3409.7445	0.0017	266 - 296	EVYL...AIIR
2295.1538	2295.1535	0.0003	297 - 316	SPHL...SLAR
1492.7231	1492.7211	0.0020	317 - 329	SAYW...NSFR
975.5357	975.5349	0.0008	330 - 338	TGTT...NLIR
691.3647	691.3653	-0.0006	339 - 344	SPLYGR
2170.1388	2170.1382	0.0006	345 - 364	EGNT...PIFR
2978.4638	2978.4621	0.0017	365 - 392	TLSY...TISR
537.2912	537.2911	0.0001	393 - 396	SIYR
665.3863	665.3860	0.0003	393 - 397	SIYRK
2841.3900	2841.3933	-0.0033	397 - 423	KSGP...YSHR
2713.2996	2713.2984	0.0012	398 - 423	SGPI...YSHR
1145.5647	1145.5652	-0.0005	424 - 432	LCHA...FLER
528.3017	528.3020	-0.0003	433 - 437	ISGPR
1273.6564	1273.6568	-0.0004	438 - 448	IAGT...WTHR
1230.5843	1230.5840	0.0003	449 - 460	SASP...SPSR
983.5802	983.5804	-0.0002	461 - 468	ITQIPWVK

Experimental Mass[2]	Calculated Mass[3]	Difference[4]	Fragment[5]	Sequence[6]
2119.2160	2119.2153	0.0007	461 - 480	ITQI...SVIK
1153.6452	1153.6455	-0.0003	469 - 480	AHTL...SVIK
2325.2455	2325.2441	0.0014	469 - 492	AHTL...ILTR
1189.6101	1189.6092	0.0009	481 - 492	GPGF...ILTR
1076.5298	1076.5284	0.0014	493 - 502	NSMG...GTLR
679.3655	679.3653	0.0002	503 - 508	VTFTGR
1699.9055	1699.9046	0.0009	503 - 516	VTFT...YYIR
1038.5499	1038.5498	0.0001	509 - 516	LPQSYYIR
1082.5652	1082.5621	0.0031	517 - 525	FRYA...VANR
779.3924	779.3926	-0.0002	519 - 525	YASVANR
566.2813	566.2813	0.0000	526 - 530	SGTFR
1469.7206	1469.7191	0.0015	531 - 543	YSQP...SFPK
2628.2534	2628.2530	0.0004	531 - 554	YSQP...LTSR
1176.5445	1176.5445	0.0000	544 - 554	TMDA...LTSR
1724.8899	1724.8886	0.0013	555 - 569	SFAH...TFSR
2044.9717	2044.9742	-0.0025	570 - 586	AQEE...YIDR
2142.0511	2142.0521	-0.0010	587 - 604	IEFI...DLER
1931.0804	1931.0840	-0.0036	605 - 622	AQKV...LGLK
1603.8943	1603.8934	0.0009	608 - 622	VVNA...LGLK
3185.4190	3185.4169	0.0021	623 - 649	TDVT...LDEK
3341.5160	3341.5180	-0.0020	623 - 650	TDVT...DEKR
774.3980	774.3984	-0.0004	661 - 666	RLSDER
618.2972	618.2973	-0.0001	662 - 666	LSDER
1715.8601	1715.8591	0.0010	662 - 675	LSDE...PNFR
1115.5731	1115.5723	0.0008	667 - 675	NLLQ...PNFR
458.2603	458.2601	0.0002	676 - 679	GINR
514.2499	514.2500	-0.0001	680 - 683	QPDR
1551.7422	1551.7417	0.0005	687 - 701	GSTD...DVFK
4133.9082	4133.9092	-0.0010	687 - 722	GSTD...LYQK
2600.1822	2600.1781	0.0041	702 - 722	ENYV...LYQK
831.4703	831.4702	0.0001	723 - 729	IDESKLK
1322.7187	1322.7194	-0.0007	723 - 733	IDES...AYTR
578.3178	578.3176	0.0002	734 - 737	YQLR
1825.9126	1825.9098	0.0028	738 - 752	GYIE...YLIR
494.2490	494.2489	0.0001	753 - 756	YNAK
3631.7841	3631.7841	0.0000	753 - 785	YNAK...EPNR
3155.5468	3155.5458	0.0010	757 - 785	HEIV...EPNR
2050.8506	2050.8560	-0.0054	786 – 801	CAPH...CSCR
2480.0419	2480.0420	-0.0001	786 - 805	CAPH...DGEK
1024.5408	1024.5414	-0.0006	836 - 844	IKTQ...GHAR

Experimental Mass[2]	Calculated Mass[3]	Difference[4]	Fragment[5]	Sequence[6]
783.3623	783.3624	-0.0001	838 - 844	TQDGHAR
2111.1646	2111.1626	0.0020	845 - 863	LGNL...ALAR
1592.8764	1592.8774	-0.0010	875 - 887	RETL...IVYK
1436.7744	1436.7762	-0.0018	876 - 887	ETLQ...IVYK
1764.9519	1764.9509	0.0010	876 - 890	ETLQ...KEAK
1969.9379	1969.9381	-0.0002	888 - 904	EAKE...QYDR
1641.7638	1641.7635	0.0003	891 - 904	ESVD...QYDR
1610.8084	1610.8086	-0.0002	905 - 919	LQAD...AADK
1766.9092	1766.9097	-0.0005	905 - 920	LQAD...ADKR
2956.5439	2956.5545	-0.0106	924 - 949	IREA…LEER
2687.3701	2687.3694	0.0007	926 - 949	EAYL...LEER
1302.6612	1302.6608	0.0004	950 - 960	IFTA...YDAR
486.3167	486.3166	0.0001	961 - 964	NIIK
1649.7636	1649.7620	0.0016	965 - 978	NGDF...WNVK
1446.6600	1446.6600	0.0000	979 - 990	GHVE...NNHR
1969.0179	1969.0156	0.0023	991 - 1007	SVLV...QEVR
587.2851	587.2850	0.0001	1008 - 1012	VCPGR
1189.6378	1189.6390	-0.0012	1008 - 1017	VCPG...YILR
620.3646	620.3646	0.0000	1013 - 1017	GYILR
580.3221	580.3221	0.0000	1018 - 1022	VTAYK
3010.3846	3010.3866	-0.0020	1018 - 1043	VTAY...DELK
4094.7379	4094.7422	-0.0043	1044 - 1077	FNNC...YTSR
2807.2318	2807.2310	0.0008	1078 - 1102	NRGY...YEEK
2537.0892	2537.0870	0.0022	1080 - 1102	GYDE...YEEK
640.2822	640.2816	0.0006	1103 - 1107	SYTDR
796.3828	796.3828	0.0000	1103 - 1108	SYTDRR
1316.6012	1316.6003	0.0009	1108 - 1117	RREN...ESNR
1160.4985	1160.4992	-0.0007	1109 - 1117	RENP...ESNR
1004.3982	1004.3981	0.0001	1110 - 1117	ENPCESNR
1600.7768	1600.7773	-0.0005	1118 - 1132	GYGD...YVTK
1269.5765	1269.5765	0.0000	1133 - 1142	ELEY...ETDK
4001.9309	4001.9271	0.0038	1133 - 1166	ELEY...LMEE
2750.3644	2750.3612	0.0032	1143 - 1166	VWIE...LMEE

[1] All imported values were rounded to 4 decimal places.
[2] Only experimental masses that matched calculated masses with the highest scores are listed in the table.
[3] The calculated mass is the exact molecular mass calculated from the matched peptide sequence.
[4] The calculated difference = experimental mass – calculated mass.
[5] Position refers to amino acid residues within the predicted MON 95379-produced Cry1Da_7 sequence as depicted in Figure 27, Panel A.
[6] For peptide matches greater than nine amino acids in length, the first 4 residues and last 4 residues are show separated by three dots (...).

Table 16. Summary of the Tryptic Masses Identified for the *Bt*-Produced Cry1Da_7 Using LC-MS/MS[1]

Experimental Mass[2]	Calculated Mass[3]	Difference[4]	Fragment[5]	Sequence[6]
2262.015	2262.0157	-0.0007	2 - 20	AEIN...SNPK
3201.5143	3201.5182	-0.0039	2 - 28	AEIN...GEER
957.5144	957.5131	0.0013	21 - 28	EIILGEER
763.3872	763.3864	0.0008	88 - 93	IEEFAR
687.3666	687.3664	0.0002	94 - 99	NQAISR
1704.9171	1704.9158	0.0013	94 - 108	NQAI...NLYK
2222.2168	2222.2171	-0.0003	94 - 112	NQAI...VYVR
1035.5602	1035.56	0.0002	100 - 108	LEGL...NLYK
1745.8373	1745.8373	0.0000	113 - 127	AFSD...PALR
2291.0721	2291.064	0.0081	113 - 131	AFSD...EEMR
882.4562	882.4559	0.0003	120 - 127	DPTNPALR
1427.6821	1427.6827	-0.0006	120 - 131	DPTN...EEMR
2063.089	2063.0874	0.0016	132 - 149	IQFN...PLFR
2712.4942	2712.4962	-0.0020	150 - 173	VQNY...SILR
907.44	907.44	0.0000	174 - 181	DVSVFGER
1309.6056	1309.6051	0.0005	182 - 192	WGYD...INNR
2868.3523	2868.3501	0.0022	193 - 216	YSDL...QGLR
1311.6612	1311.6612	0.0000	222 - 231	FLSD...VYNR
1614.8332	1614.8307	0.0025	222 - 233	FLSD...NRFR
1770.932	1770.9318	0.0002	222 - 234	FLSD...RFRR
2379.2964	2379.2951	0.0013	234 - 253	RQLT...YDIR
2223.1949	2223.194	0.0009	235 - 253	QLTI...YDIR
1391.7414	1391.7409	0.0005	254 - 265	TYPI...QLTR
4783.4748	4783.4748	0.0000	254 - 296	TYPI...AIIR
3409.7481	3409.7445	0.0036	266 - 296	EVYL...AIIR
2295.1527	2295.1535	-0.0008	297 - 316	SPHL...SLAR
1492.7235	1492.7211	0.0024	317 - 329	SAYW...NSFR
2450.2467	2450.2455	0.0012	317 - 338	SAYW...NLIR
3123.5982	3123.6003	-0.0021	317 - 344	SAYW...LYGR
975.536	975.5349	0.0011	330 - 338	TGTT...NLIR
691.3659	691.3653	0.0006	339 - 344	SPLYGR
2170.1405	2170.1382	0.0023	345 - 364	EGNT...PIFR
2978.4662	2978.4621	0.0041	365 - 392	TLSY...TISR
3497.7438	3497.7427	0.0011	365 - 396	TLSY...SIYR
3625.8386	3625.8376	0.0010	365 - 397	TLSY...IYRK
2841.3951	2841.3933	0.0018	397 - 423	KSGP...YSHR
2713.3017	2713.2984	0.0033	398 - 423	SGPI...YSHR
1145.5655	1145.5652	0.0003	424 - 432	LCHA...FLER
1655.8571	1655.8566	0.0005	424 - 437	LCHA...SGPR
2996.5252	2996.5217	0.0035	433 - 460	ISGP...SPSR

Experimental Mass[2]	Calculated Mass[3]	Difference[4]	Fragment[5]	Sequence[6]
1273.6562	1273.6568	-0.0006	438 - 448	IAGT...WTHR
2486.2324	2486.2302	0.0022	438 - 460	IAGT...SPSR
1230.5847	1230.584	0.0007	449 - 460	SASP...SPSR
2196.1544	2196.1539	0.0005	449 - 468	SASP...PWVK
983.5805	983.5804	0.0001	461 - 468	ITQIPWVK
2119.2152	2119.2153	-0.0001	461 - 480	ITQI...SVIK
3290.8122	3290.814	-0.0018	461 - 492	ITQI...ILTR
1153.6462	1153.6455	0.0007	469 - 480	AHTL...SVIK
2325.2484	2325.2441	0.0043	469 - 492	AHTL...ILTR
1189.6085	1189.6092	-0.0007	481 - 492	GPGF...ILTR
2248.1292	2248.127	0.0022	481 - 502	GPGF...GTLR
2909.4823	2909.4818	0.0005	481 - 508	GPGF...FTGR
1076.5288	1076.5284	0.0004	493 - 502	NSMG...GTLR
1737.8858	1737.8832	0.0026	493 - 508	NSMG...FTGR
679.3647	679.3653	-0.0006	503 - 508	VTFTGR
1699.905	1699.9046	0.0004	503 - 516	VTFT...YYIR
1038.5506	1038.5498	0.0008	509 - 516	LPQSYYIR
2103.1018	2103.1013	0.0005	509 - 525	LPQS...VANR
779.3924	779.3926	-0.0002	519 - 525	YASVANR
1327.6578	1327.6633	-0.0055	519 - 530	YASV...GTFR
1469.7193	1469.7191	0.0002	531 - 543	YSQP...SFPK
2628.2613	2628.253	0.0083	531 - 554	YSQP...LTSR
1176.5456	1176.5445	0.0011	544 - 554	TMDA...LTSR
2883.4187	2883.4225	-0.0038	544 - 569	TMDA...TFSR
1724.8919	1724.8886	0.0033	555 - 569	SFAH...TFSR
2044.9735	2044.9742	-0.0007	570 - 586	AQEE...YIDR
4169.0169	4169.0157	0.0012	570 - 604	AQEE...DLER
2142.0526	2142.0521	0.0005	587 - 604	IEFI...DLER
1931.0842	1931.084	0.0002	605 - 622	AQKV...LGLK
1603.8943	1603.8934	0.0009	608 - 622	VVNA...LGLK
3185.4193	3185.4169	0.0024	623 - 649	TDVT...LDEK
3341.5189	3341.518	0.0009	623 - 650	TDVT...DEKR
3927.8037	3927.8143	-0.0106	623 - 655	TDVT...LSEK
760.4078	760.4079	-0.0001	650 - 655	RELSEK
831.4701	831.4702	-0.0001	651 - 657	ELSEKVK
774.3987	774.3984	0.0003	661 - 666	RLSDER
1871.9602	1871.9602	0.0000	661 - 675	RLSD...PNFR
1715.8562	1715.8591	-0.0029	662 - 675	LSDE...PNFR
1115.5729	1115.5723	0.0006	667 - 675	NLLQ...PNFR
954.499	954.4995	-0.0005	676 - 683	GINRQPDR

Experimental Mass[2]	Calculated Mass[3]	Difference[4]	Fragment[5]	Sequence[6]
913.4513	913.4518	-0.0005	680 - 686	QPDRGWR
1950.9428	1950.9436	-0.0008	684 - 701	GWRG...DVFK
1551.7398	1551.7417	-0.0019	687 - 701	GSTD...DVFK
4133.909	4133.9092	-0.0002	687 - 722	GSTD...LYQK
2600.1793	2600.1781	0.0012	702 - 722	ENYV...LYQK
831.4704	831.4702	0.0002	723 - 729	IDESKLK
1322.7204	1322.7194	0.0010	723 - 733	IDES...AYTR
750.4387	750.4388	-0.0001	728 - 733	LKAYTR
1069.5683	1069.5668	0.0015	730 - 737	AYTRYQLR
1825.9098	1825.9098	0.0000	738 - 752	GYIE...YLIR
3631.788	3631.7841	0.0039	753 - 785	YNAK...EPNR
3155.5482	3155.5458	0.0024	757 - 785	HEIV...EPNR
5188.3761	5188.3913	-0.0152	757 - 801	HEIV...CSCR
2050.8556	2050.856	-0.0004	786 - 801	CAPH...CSCR
1024.5416	1024.5414	0.0002	836 - 844	IKTQ...GHAR
783.3623	783.3624	-0.0001	838 - 844	TQDGHAR
2111.1649	2111.1626	0.0023	845 - 863	LGNL...ALAR
1592.8784	1592.8774	0.0010	875 - 887	RETL...IVYK
1921.0559	1921.052	0.0039	875 - 890	RETL...KEAK
1436.7766	1436.7762	0.0004	876 - 887	ETLQ...IVYK
1764.9496	1764.9509	-0.0013	876 - 890	ETLQ...KEAK
3388.7085	3388.7038	0.0047	876 - 904	ETLQ...QYDR
1969.9387	1969.9381	0.0006	888 - 904	EAKE...QYDR
1641.7646	1641.7635	0.0011	891 - 904	ESVD...QYDR
3234.563	3234.5615	0.0015	891 - 919	ESVD...AADK
3390.6575	3390.6626	-0.0051	891 - 920	ESVD...ADKR
1610.8088	1610.8086	0.0002	905 - 919	LQAD...AADK
1766.9087	1766.9097	-0.0010	905 - 920	LQAD...ADKR
2159.1381	2159.1382	-0.0001	905 - 923	LQAD...RVHR
2956.5539	2956.5545	-0.0006	924 - 949	IREA...LEER
2687.3712	2687.3694	0.0018	926 - 949	EAYL...LEER
3972.025	3972.0196	0.0054	926 - 960	EAYL...YDAR
1302.6615	1302.6608	0.0007	950 - 960	IFTA...YDAR
1649.7618	1649.762	-0.0002	965 - 978	NGDF...WNVK
1446.6599	1446.66	-0.0001	979 - 990	GHVE...NNHR
3397.666	3397.6651	0.0009	979 - 1007	GHVE...QEVR
1969.016	1969.0156	0.0004	991 - 1007	SVLV...QEVR
1189.6389	1189.639	-0.0001	1008 - 1017	VCPG...YILR
1182.6756	1182.6761	-0.0005	1013 - 1022	GYIL...TAYK
2968.3751	2968.376	-0.0009	1018 - 1043	VTAY...DELK

Experimental Mass[2]	Calculated Mass[3]	Difference[4]	Fragment[5]	Sequence[6]
2406.0655	2406.0645	0.0010	1023 - 1043	EGYG...DELK
4094.7467	4094.7422	0.0045	1044 - 1077	FNNC...YTSR
2807.2285	2807.231	-0.0025	1078 - 1102	NRGY...YEEK
2537.0816	2537.087	-0.0054	1080 - 1102	GYDE...YEEK
3159.3576	3159.3581	-0.0005	1080 - 1107	GYDE...YTDR
796.3828	796.3828	0.0000	1103 - 1108	SYTDRR
1316.6022	1316.6003	0.0019	1108 - 1117	RREN...ESNR
1160.4985	1160.4992	-0.0007	1109 - 1117	RENP...ESNR
2743.267	2743.266	0.0010	1109 - 1132	RENP...YVTK
1004.3996	1004.3981	0.0015	1110 - 1117	ENPCESNR
2587.1674	2587.1649	0.0025	1110 - 1132	ENPC...YVTK
1600.7776	1600.7773	0.0003	1118 - 1132	GYGD...YVTK
2852.3411	2852.3432	-0.0021	1118 - 1142	GYGD...ETDK
1269.5768	1269.5765	0.0003	1133 - 1142	ELEY...ETDK
4001.9295	4001.9271	0.0024	1133 - 1166	ELEY...LMEE
2750.3631	2750.3612	0.0019	1143 - 1166	VWIE...LMEE

[1] All imported values were rounded to 4 decimal places.
[2] Only experimental masses that matched calculated masses with the highest scores are listed in table.
[3] The calculated mass is the exact molecular mass calculated from the matched peptide sequence.
[4] The calculated difference = experimental mass – calculated mass.
[5] Position refers to amino acid residues within the predicted *Bt*-produced Cry1Da_7 sequence as depicted in Figure 27, Panel B.
[6] For peptide matches greater than nine amino acids in length the first 4 residues and last 4 residues are shown separated by dots (…).

(A)

```
   1 MAEINNQNQC VPYNCLSNPK EIILGEERLE TGNTVADISL GLINFLYSNF
  51 VPGGGFIVGL LELIWGFIGP SQWDIFLAQI EQLISQRIEE FARNQAISRL
 101 EGLSNLYKVY VRAFSDWEKD PTNPALREEM RIQFNDMNSA LITAIPLFRV
 151 QNYEVALLSV YVQAANLHLS ILRDVSVFGE RWGYDTATIN NRYSDLTSLI
 201 HVYTNHCVDT YNQGLRRLEG RFLSDWIVYN RFRRQLTISV LDIVAFFPNY
 251 DIRTYPIQTA TQLTREVYLD LPFINENLSP AAVYPTFSAA ESAIIRSPHL
 301 VDFLNSFTIY TDSLARSAYW GGHLVNSFRT GTTTNLIRSP LYGREGNTER
 351 PVTITASPSV PIFRTLSYPT GLDNSNPVAG IEGVEFQNTI SRSIYRKSGP
 401 IDSFSELPPQ DASVSPAIGY SHRLCHATFL ERISGPRIAG TVFSWTHRSA
 451 SPTNEVSPSR ITQIPWVKAH TLASGASVIK GPGFTGGDIL TRNSMGELGT
 501 LRVTFTGRLP QSYYIRFRYA SVANRSGTFR YSQPPSYGIS FPKTMDAGEP
 551 LTSRSFAHTT LFTPITFSRA QEEFDLYIQS GVYIDRIEFI PVTATFEAEY
 601 DLERAQKVVN ALFTSTNQLG LKTDVTDYHI DQVSNLVACL SDEFCLDEKR
 651 ELSEKVKHAK RLSDERNLLQ DPNFRGINRQ PDRGWRGSTD ITIQGGDDVF
 701 KENYVTLPGT FDECYPTYLY QKIDESKLKA YTRYQLRGYI EDSQDLEIYL
 751 IRYNAKHEIV NVPGTGSLWP LSVENQIGPC GEPNRCAPHL EWNPDLHCSC
 801 RDGEKCAHHS HHFSLDIDVG CTDLNEDLGV WVIFKIKTQD GHARLGNLEF
 851 LEEKPLLGEA LARVKRAEKK WRDKRETLQL ETTIVYKEAK ESVDALFVNS
 901 QYDRLQADTN IAMIHAADKR VHRIREAYLP ELSVIPGVNA AIFEELEERI
 951 FTAFSLYDAR NIIKNGDFNN GLLCWNVKGH VEVEEQNNHR SVLVIPEWEA
1001 EVSQEVRVCP GRGYILRVTA YKEGYGEGCV TIHEIENNTD ELKFNNCVEE
1051 EVYPNNTVTC INYTATQEEY EGTYTSRNRG YDEAYGNNPS VPADYASVYE
1101 EKSYTDRRRE NPCESNRGYG DYTPLPAGYV TKELEYFPET DKVWIEIGET
1151 EGTFIVDSVE LLLMEE
```

(B)

```
   1 MAEINNQNQC VPYNCLSNPK EIILGEERLE TGNTVADISL GLINFLYSNF
  51 VPGGGFIVGL LELIWGFIGP SQWDIFLAQI EQLISQRIEE FARNQAISRL
 101 EGLSNLYKVY VRAFSDWEKD PTNPALREEM RIQFNDMNSA LITAIPLFRV
 151 QNYEVALLSV YVQAANLHLS ILRDVSVFGE RWGYDTATIN NRYSDLTSLI
 201 HVYTNHCVDT YNQGLRRLEG RFLSDWIVYN RFRRQLTISV LDIVAFFPNY
 251 DIRTYPIQTA TQLTREVYLD LPFINENLSP AAVYPTFSAA ESAIIRSPHL
 301 VDFLNSFTIY TDSLARSAYW GGHLVNSFRT GTTTNLIRSP LYGREGNTER
 351 PVTITASPSV PIFRTLSYPT GLDNSNPVAG IEGVEFQNTI SRSIYRKSGP
 401 IDSFSELPPQ DASVSPAIGY SHRLCHATFL ERISGPRIAG TVFSWTHRSA
 451 SPTNEVSPSR ITQIPWVKAH TLASGASVIK GPGFTGGDIL TRNSMGELGT
 501 LRVTFTGRLP QSYYIRFRYA SVANRSGTFR YSQPPSYGIS FPKTMDAGEP
 551 LTSRSFAHTT LFTPITFSRA QEEFDLYIQS GVYIDRIEFI PVTATFEAEY
 601 DLERAQKVVN ALFTSTNQLG LKTDVTDYHI DQVSNLVACL SDEFCLDEKR
 651 ELSEKVKHAK RLSDERNLLQ DPNFRGINRQ PDRGWRGSTD ITIQGGDDVF
 701 KENYVTLPGT FDECYPTYLY QKIDESKLKA YTRYQLRGYI EDSQDLEIYL
 751 IRYNAKHEIV NVPGTGSLWP LSVENQIGPC GEPNRCAPHL EWNPDLHCSC
 801 RDGEKCAHHS HHFSLDIDVG CTDLNEDLGV WVIFKIKTQD GHARLGNLEF
 851 LEEKPLLGEA LARVKRAEKK WRDKRETLQL ETTIVYKEAK ESVDALFVNS
 901 QYDRLQADTN IAMIHAADKR VHRIREAYLP ELSVIPGVNA AIFEELEERI
 951 FTAFSLYDAR NIIKNGDFNN GLLCWNVKGH VEVEEQNNHR SVLVIPEWEA
1001 EVSQEVRVCP GRGYILRVTA YKEGYGEGCV TIHEIENNTD ELKFNNCVEE
1051 EVYPNNTVTC INYTATQEEY EGTYTSRNRG YDEAYGNNPS VPADYASVYE
1101 EKSYTDRRRE NPCESNRGYG DYTPLPAGYV TKELEYFPET DKVWIEIGET
1151 EGTFIVDSVE LLLMEE
```

Figure 27. Peptide Map of the MON 95379-Produced Cry1Da_7 and *Bt*-Produced Cry1Da_7 Proteins

(A). The amino acid sequence of the MON 95379-produced Cry1Da_7 protein was deduced from the *cry1Da_7* gene present in MON 95379. Boxed regions correspond to peptides that were identified from the MON 95379-produced Cry1Da_7 protein sample using LC-MS/MS. In total, 89% coverage (1049 out of 1166 amino acids) of the expected protein sequence was covered by the identified peptides. Gray highlighted regions correspond to the receptor binding domain.

(B). The amino acid sequence of the *Bt*-produced Cry1Da_7 protein was deduced from the *cry1Da_7* gene that is contained on the expression plasmid pMON417133. Boxed regions correspond to peptides that were identified from the *Bt*-produced Cry1Da_7 protein sample using LC-MS/MS. In total, 89% coverage (1049 out of 1166 amino acids) of the expected protein sequence was covered by the identified peptides. Gray highlighted regions correspond to the receptor binding domain.

B.1(a)(ii)(iii) Results of western blot analysis of the Cry1Da_7 protein isolated from the grain of MON 95379 and immunoreactivity comparison to *Bt*-produced Cry1Da_7 protein

Western blot analysis was conducted using goat anti-Cry1Da_7 polyclonal antibody as additional means to confirm the identity of the Cry1Da_7 protein isolated from the grain of MON 95379 and to assess the equivalence of the immunoreactivity of the MON 95379-produced and *Bt*-produced Cry1Da_7 proteins.

The results showed that immunoreactive bands with the same electrophoretic mobility were present in all lanes loaded with the MON 95379-produced and *Bt*-produced Cry1Da_7 proteins (Figure 28). For each amount loaded, comparable signal intensity was observed between the MON 95379-produced and *Bt*-produced Cry1Da_7 protein bands. As expected, the signal intensity increased with increasing load amounts of the MON 95379-produced and *Bt*-produced Cry1Da_7 proteins, thus, supporting identification of MON 95379-produced Cry1Da_7 protein.

To compare the immunoreactivity of the MON 95379-produced and *Bt*-produced Cry1Da_7 proteins, densitometric analysis was conducted on the bands that migrated at the expected apparent MW for Cry1Da_7 proteins (~ 130 kDa). The signal intensity (reported in OD) of the band of interest in lanes loaded with MON 95379-produced and *Bt*-produced Cry1Da_7 proteins was measured (Table 17). Because the mean signal intensity of the MON 95379-produced Cry1Da_7 protein was within 35% of the mean signal intensity of the *Bt*-produced Cry1Da_7 protein, the MON 95379-produced Cry1Da_7 and *Bt*-produced Cry1Da_7 proteins were determined to have equivalent immunoreactivity.

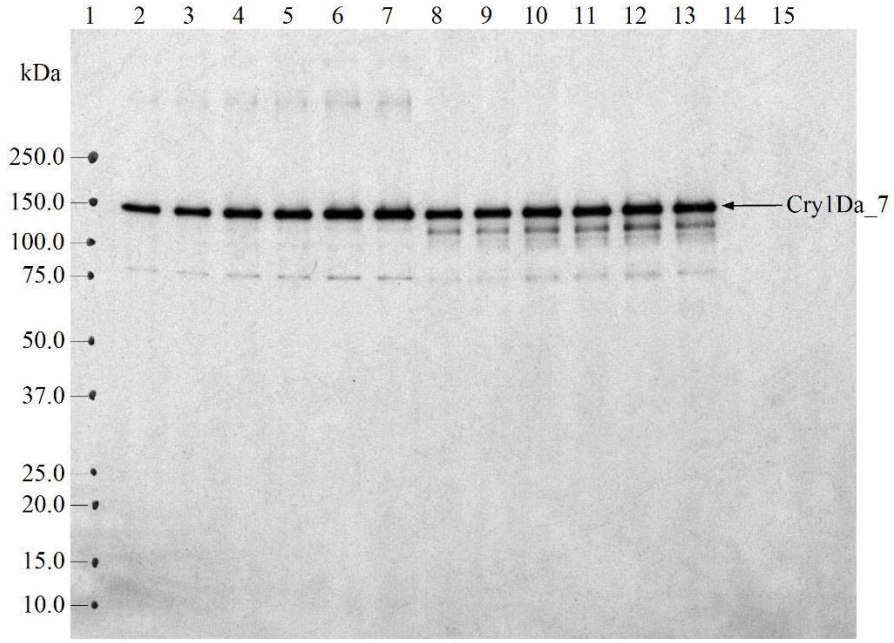

Figure 28. Western Blot Analysis and Immunoreactivity of MON 95379-Produced and *Bt*-Produced Cry1Da_7 Proteins

Aliquots of the MON 95379-produced and *Bt*-produced Cry1Da_7 proteins were subjected to SDS-PAGE and electrotransferred to a nitrocellulose membrane. Proteins were detected using goat anti-Cry1Da_7 polyclonal antibodies as the primary antibodies. Immunoreactive bands were visualized using HRP-conjugated secondary antibodies and an ECL system. The 3-minute exposure is shown. The approximate MW (kDa) of the standards are shown on the left. Lane designations are as follows:

Lane	Sample	Amount (ng)
1	Precision Plus Protein™ Standards	-
2	*Bt*-produced Cry1Da_7	10
3	*Bt*-produced Cry1Da_7	10
4	*Bt*-produced Cry1Da_7	15
5	*Bt*-produced Cry1Da_7	15
6	*Bt*-produced Cry1Da_7	20
7	*Bt*-produced Cry1Da_7	20
8	MON 95379-produced Cry1Da_7	10
9	MON 95379-produced Cry1Da_7	10
10	MON 95379-produced Cry1Da_7	15
11	MON 95379-produced Cry1Da_7	15
12	MON 95379-produced Cry1Da_7	20
13	MON 95379-produced Cry1Da_7	20
14	Blank	-
15	Blank	-

Table 17. Immunoreactivity of the MON 95379-Produced and *Bt*-Produced Cry1Da_7 Proteins

Mean Signal Intensity from MON 95379-Produced Cry1Da_7 [1] (OD)	Mean Signal Intensity from *Bt*-Produced Cry1Da_7 [1] (OD)	Acceptance Limits[2] (OD)
1260.28	1175.99	764.39 – 1587.59

[1] Each value represents the mean of six values (n = 6).

[2] The acceptance limits are for the MON 95379-produced Cry1Da_7 protein and are based on the interval between -35% (1175.99 x 0.65 = 764.39) and +35 % (1175.99 x 1.35 = 1587.59) of the mean of the *Bt*-produced Cry1Da_7 signal intensity across all loads.

B.1(a)(ii)(iv) Results of the Cry1Da_7 protein molecular weight and purity analysis

For apparent MW and purity determination, the MON 95379-produced Cry1Da_7 and the *Bt*-produced Cry1Da_7 proteins were subjected to SDS-PAGE. Following electrophoresis, the gel was stained with Brilliant Blue G-Colloidal stain and analyzed by densitometry. The MON 95379-produced Cry1Da_7 protein (Figure 29, lanes 3-8) migrated to the same position on the gel as the *Bt*-produced Cry1Da_7 protein (Figure 29, lane 2) and the apparent MW was calculated to be 132.1 kDa (Table 18). Because the experimentally determined apparent MW of the MON 95379-produced Cry1Da_7 protein was within the acceptance limits for equivalence (Table 19), the MON 95379-produced Cry1Da_7 and *Bt*-produced Cry1Da_7 proteins were determined to have equivalent apparent molecular weights.

The purity of the MON 95379-produced Cry1Da_7 protein was calculated based on the six lanes loaded on the gel (Figure 29, lanes 3-8). The average purity was determined to be 52% (Table 18).

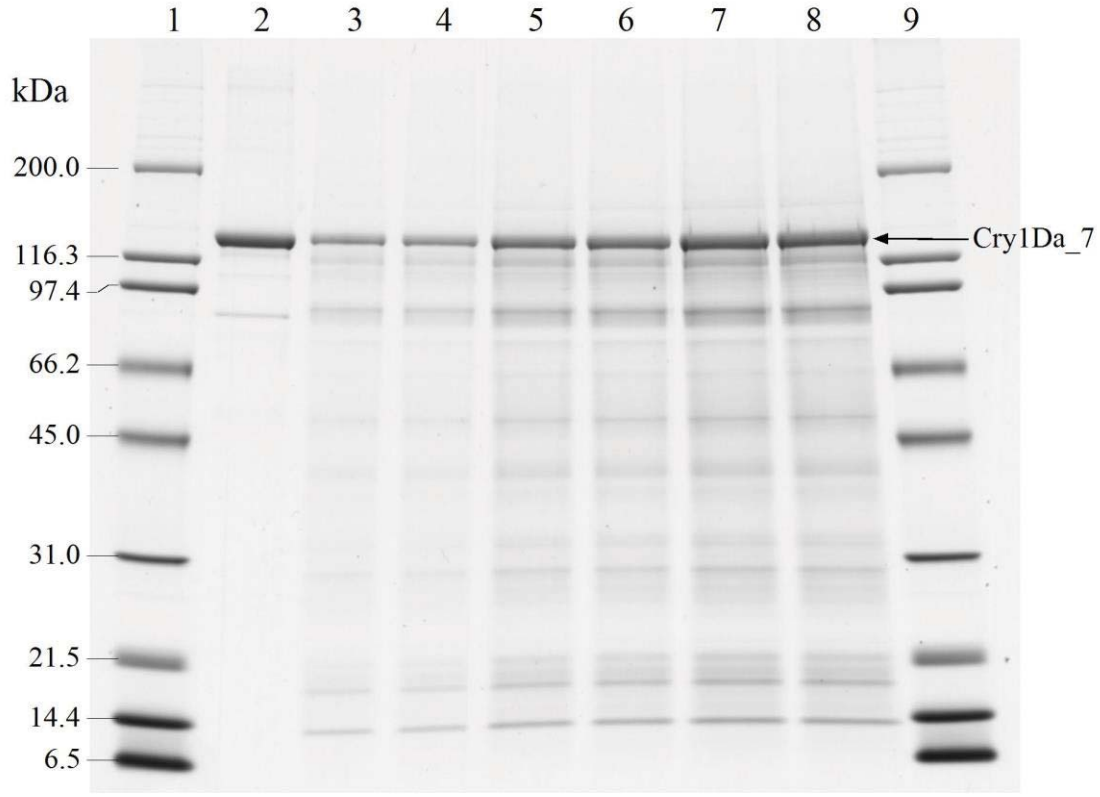

Figure 29. Purity and Apparent Molecular Weight Analysis of the MON 95379-Produced Cry1Da_7 Protein

Aliquots of the MON 95379-produced and the *Bt*-produced Cry1Da_7 proteins were subjected to SDS-PAGE and the gel was stained with Brilliant Blue G-Colloidal stain. The MWs (kDa) are shown on the left and correspond to the standards loaded in lanes 1 and 9. Lane 10 was cropped from the image. The intact Cry1Da_7 protein is indicated with an arrow in the image. Lane designations are as follows:

Lane	Sample	Amount (µg)
1	Broad Range MW Standard	5.0
2	*Bt*-produced Cry1Da_7	1.0
3	MON 95379-produced Cry1Da_7	1.0
4	MON 95379-produced Cry1Da_7	1.0
5	MON 95379-produced Cry1Da_7	2.0
6	MON 95379-produced Cry1Da_7	2.0
7	MON 95379-produced Cry1Da_7	3.0
8	MON 95379-produced Cry1Da_7	3.0
9	Broad Range MW Standard	5.0
10	Blank	

Table 18. Apparent Molecular Weight and Purity Analysis of the MON 95379-Produced Cry1Da_7 Protein

	Apparent MW[1] (kDa)	Purity[2] (%)
Average (n=6)	132.1	52

[1]Final MW was rounded to one decimal place.
[2]Average % purity was rounded to the nearest whole number.

Table 19. Apparent Molecular Weight Comparison Between the MON 95379-Produced Cry1Da_7 and *Bt*-Produced Cry1Da_7 Proteins

Apparent MW of MON 95379-Produced Cry1Da_7 Protein (kDa)	Apparent MW of *Bt*-Produced Cry1Da_7 Protein[1] (kDa)	Acceptance Limits[2] (kDa)
132.1	126.5	119.9 – 133.1

[1] As reported on the COA of the *Bt*-produced Cry1Da_7 protein (lot 7799).
[2]Data obtained for the *Bt*-produced Cry1Da_7 protein were used to generate the prediction interval. Values in this column represent a 95% prediction interval developed from eight individual assays with *Bt*-produced Cry1Da_7 protein (Appendix 7).

B.1(a)(ii)(v) Cry1Da_7 glycosylation analysis

Some eukaryotic proteins are post-translationally modified by the addition of carbohydrate moieties (Rademacher *et al.*, 1988). To test whether the Cry1Da_7 protein was glycosylated when expressed in the maize grain of MON 95379, the MON 95379-produced Cry1Da_7 protein was analyzed using an ECL™ glycoprotein detection method. Transferrin, a glycosylated protein, was used as a positive control in the assay. To assess equivalence of the MON 95379-produced and *Bt*-produced Cry1Da_7 proteins, the *Bt*-produced Cry1Da_7 protein was also analyzed.

A clear glycosylation signal was observed at the expected molecular weight (~80 kDa) in the lanes containing the positive control (transferrin) and the band intensity increased with increasing concentration (Figure 30A). In contrast, no glycosylation signal was observed in the lanes containing the *Bt*-produced Cry1Da_7 protein or MON 95379-produced Cry1Da_7 protein (Figure 30A).

To confirm that MON 95379-produced Cry1Da_7 and *Bt*-produced Cry1Da_7 proteins were appropriately loaded for glycosylation analysis, a second membrane with identical loadings and transfer time was stained with Coomassie Blue R250 for protein detection. Both the MON 95379-produced and *Bt*-produced Cry1Da_7 proteins were detected (Figure 30B). These data indicate that the glycosylation status of MON 95379-produced Cry1Da_7 protein is equivalent to that of the *Bt*-produced Cry1Da_7 protein and that neither is glycosylated.

A. B.

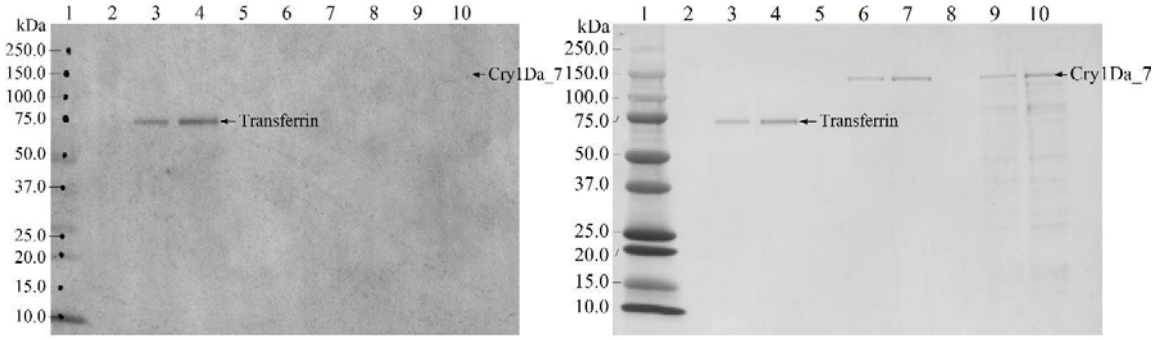

Figure 30. Glycosylation Analysis of the MON 95379-Produced and *Bt*-Produced Cry1Da_7 Proteins

Aliquots of the transferrin (positive control), *Bt*-produced Cry1Da_7 and MON 95379-produced Cry1Da_7 proteins were subjected to SDS-PAGE and electrotransferred to a PVDF membrane. The MWs (kDa) correspond to the Precision Plus Protein™ Standards. The arrows show the expected migration of the MON 95379-produced and *Bt*-produced Cry1Da_7 proteins and transferrin. (A) Where present, the labeled carbohydrate moieties were detected by using ECL reagents and exposure to Hyperfilm™. The 4-minute exposure is shown. (B) An equivalent blot was stained with Coomassie Blue R250 to confirm the presence of proteins. Lane designations are as follows:

Lane	Sample	Amount (ng)
1	Precision Plus Protein™ Standards	-
2	Blank	-
3	Transferrin (positive control)	100
4	Transferrin (positive control)	200
5	Blank	-
6	*Bt*-produced Cry1Da_7	100
7	*Bt*-produced Cry1Da_7	200
8	Blank	-
9	MON 95379-produced Cry1Da_7	100
10	MON 95379-produced Cry1Da_7	200

B.1(a)(ii)(vi) Cry1Da_7 functional activity

The MON 95379-produced Cry1Da_7 and *Bt*-produced Cry1Da_7 proteins were considered to have equivalent functional activity if the activities of both proteins (measured by EC_{50} values) were within the acceptance limits of 0.076 to 0.293 µg of Cry1Da_7 protein/mL diet, which is the prediction interval calculated from a data set of *Bt*-produced Cry1Da_7 protein activity.

The experimentally determined functional activity for the MON 95379-produced and *Bt*-produced Cry1Da_7 proteins are presented in Table 20. The functional activities of MON 95379-produced and *Bt*-produced Cry1Da_7 proteins were 0.17 and 0.12 µg of Cry1Da_7 protein/mL diet, respectively. Because the functional activities of MON 95379-produced and *Bt*-produced Cry1Da_7 proteins fall within the preset acceptance limits (Table 20), the MON 95379-produced Cry1Da_7 protein was considered to have equivalent functional activity to that of the *Bt*-produced Cry1Da_7 protein.

Table 20. Functional Activity of MON 95379-Produced and *Bt*-Produced Cry1Da_7 Proteins

Replicates	MON 95379-Produced Cry1Da_7 EC_{50} [1] (µg protein/mL diet)	*Bt*-Produced Cry1Da_7 EC_{50} [1] (µg protein/mL diet)	EC_{50} Acceptance Limits[2] (µg protein/mL diet)
1	0.20	0.11	0.076 – 0.293
2	0.14	0.076	
3	0.17	0.16	
Mean	0.17	0.12	-

[1] Value refers to mean calculated based on three independent assays (n=3).
[2] Data obtained for the *Bt*-produced Cry1Da_7 proteins were used to generate a prediction interval for setting the acceptance limits for EC_{50} values of 3 future independent assays. Values in this column represent a 95% prediction interval developed from 24 individual bioassays with *Bt*-produced Cry1Da_7 protein (Appendix 7).

B.1(a)(ii)(vii) MON 95379 Cry1Da_7 protein identity and equivalence conclusion

The MON 95379-produced Cry1Da_7 protein purified from MON 95379 grain was characterized, and a comparison of the physicochemical and functional properties between the MON 95379-produced and the *Bt*-produced Cry1Da_7 proteins was conducted following a panel of analytical tests: 1) N-terminal sequence analysis established the same identity for the MON 95379-produced and the *Bt*-produced Cry1Da_7 proteins; 2) Nano LC-MS/MS analysis yielded peptide masses consistent with the expected peptide masses from the theoretical trypsin digest of the *cry1Da_7* gene product present in MON 95379; 3) the MON 95379-produced and the *Bt*-produced Cry1Da_7 proteins were both detected on a western blot probed with antibodies specific for Cry1Da_7 protein and the immunoreactive properties of both proteins was shown to be equivalent; 4) the electrophoretic mobility and apparent molecular weight of the MON 95379-produced and the *Bt*-produced Cry1Da_7 proteins were shown to be equivalent; 5) the glycosylation status of MON 95379-produced and the *Bt*-produced Cry1Da_7 proteins was determined to be equivalent; and 6)

the functional activity of the MON 95379-produced and the *Bt*-produced Cry1Da_7 was demonstrated to be equivalent. These results demonstrate that the MON 95379-produced and the *Bt*-produced Cry1Da_7 protein are equivalent.

The ability of the Cry1Da_7 to bind to its target receptor is dependent on the confirmation of the Cry1Da_7 receptor binding domain. Protein structure, or confirmation, is determined by the specific sequence of amino acids that comprise the different structural and functional elements. It can inferred that once properly folded, proteins that possess equivalent amino acid sequences would have equivalent functional activity or receptor binding. The MON 95379- and *Bt*-produced Cry1Da_7 proteins possess equivalent amino sequences, and thereby equivalent receptor binding domains, as evidenced by the very high amino acid sequence similarity seen by mass fingerprint analysis where >90% coverage was observed. The equivalency of the protein sequences was also confirmed indirectly through sequencing the of genes of the expressed MON 95379- and *Bt*-produced Cry1Da_7 proteins. Finally, the equivalent functional activity of the protein isolated from both sources indicates that the confirmation of the receptor binding domains in both proteins are equivalent.

Taken together, the equivalency data provided in support of MON 95379 Cry1Da_7 confirms that the *Bt*-produced Cry1Da_7 protein is appropriate surrogate for use in the evaluation of the safety of the MON 95379-produced Cry1Da_7 protein.

For details, please also refer to Appendix 7 ([redacted] 2020 (MSL0030547)).

B.1(a)(iii) Expression levels of Cry1B.868 and Cry1Da_7 proteins in MON 95379

The ELISA protein expression data below shows that Cry1B.868 and Cry1Da_7 proteins are expressed across multiple tissue types over several growth stages.

Tissues of MON 95379 were collected from four replicate plots planted in a randomized complete block design during the 2018 growing season from five field sites in the United States: Boone County, Iowa (IAOG), Jefferson County, Iowa (IARL), Clinton County, Illinois (ILHY), York County, Nebraska (NEYO), and Miami County, Ohio (OHTR). The field sites were representative of maize-producing regions suitable for commercial production. Leaf, root, pollen, forage and grain tissue samples were collected from each replicated plot at all field sites.

For details, please refer to Appendix 8 ([redacted] 2020 (TRR0000556)).

B.1(a)(iii)(i) Expression levels of Cry1B.868 protein

Cry1B.868 protein levels were determined in leaf, root, pollen, forage and grain tissues. The results obtained from the ELISA are summarized in Table 21. The expression of Cry1B.868 in MON 95379 maize was determined and reported on a dry weight basis. The mean Cry1B.868 protein levels in MON 95379 across all sites was highest in leaf at 630 µg/g dw and lowest in grain at 26 µg/g dw. The mean level in the grain was 26 µg/g dw.

Table 21. Summary of Cry1B.868 Protein Levels in Maize Tissues Collected from MON 95379 Produced in United States Field Trials in 2018

Tissue Type	Development Stage[1]	Mean (SE) Range (µg/g dw)[2]	LOQ/LOD (µg/g dw)[3]
Leaf	V2-V4	630 (22) 310 - 760	0.625/0.348
Root	V2-V4	110 (8.2) 67 - 210	0.625/0.254
Pollen	R1	91 (2.1) 73 - 110	0.625/0.323
Forage	R5	110 (8.2) 50 - 170	0.625/0.455
Grain	R6	26 (3.5) 7.8 - 77	0.625/0.420

[1] The crop development stage at which each tissue was collected.
[2] Protein levels are expressed as the arithmetic mean and standard error (SE) as microgram (µg) of protein per gram (g) of tissue on a dry weight (dw) basis. The means, SE, and ranges (minimum and maximum values) were calculated for each tissue across all sites (n = 20).
[3] LOQ = limit of quantitation, LOD = limit of detection.

B.1(a)(iii)(ii) Expression levels of Cry1Da_7 protein

Cry1Da_7 protein levels were determined in, leaf, root, pollen, forage and grain tissues. The results obtained from the ELISA are summarized in Table 22. The expression of Cry1Da_7 in MON 95379 maize was determined and reported on a dry weight basis. The mean Cry1Da_7 protein levels in MON 95379 across all sites was highest in leaf at 92 µg/g dw and lowest in pollen at less than the limit of quantification (LOQ) µg/g dw. The mean level in grain was 0.25 µg/g dw.

Table 22. Summary of Cry1Da_7 Protein Levels in Maize Tissues Collected from MON 95379 Produced in United States Field Trials in 2018

Tissue Type	Development Stage[1]	Mean (SE) Range (µg/g dw)[2]	LOD/LOQ (µg/g dw)[3]
Leaf	V2-V4	92 (5.2) 56 - 140	0.125/0.061
Root	V2-V4	43 (3.1) 26 - 72	0.125/0.065
Pollen	R1	<LOQ (NA) NA – NA[4]	0.125/0.065
Forage	R5	26 (2.1) 13 - 50	0.125/0.078
Grain	R6	0.25 (0.032) 0.13 - 0.64	0.125/0.037

[1] The crop development stage at which each tissue was collected.
[2] Protein levels are expressed as the arithmetic mean and standard error (SE) as microgram (µg) of protein per gram (g) of tissue on a dry weight (dw) basis. The means, SE, and ranges (minimum and maximum values) were calculated for each tissue across all sites (n = 20).
[3] LOQ = limit of quantitation, LOD = limit of detection.
[4] NA= Not applicable.

B.1(b) Information about prior history of human consumption of the new substances, if any, or their similarity to substances previously consume in food.

Refer to Section A.2(a)(i).

B.1(c) Information on whether any new protein has undergone any unexpected post-translational modification in the new host

Refer to Section B.1(a)(i)(v) and Section B.1(a)(ii)(v).

B.1(d) Where any ORFs have been identified, bioinformatics analysis to indicate the potential for allergenicty and toxicity of the ORFs

Refer to Section A.3(c)(v).

B.2 New Proteins

B.2(a) Information on the potential toxicity of any new proteins, including:

B.2(a)(i) A bioinformatic comparison of the amino acid sequence of each of the new proteins to know protein toxins and anti-nutrients (e.g. protease inhibitors, lectins)

Potential structural similarities shared between the MON 95379 Cry1B.868 and Cry1Da_7 proteins with sequences in a protein database were evaluated using the FASTA sequence alignment tool. The FASTA program directly compares amino acid sequences (*i.e.*, primary, linear protein structure) and the alignment data may be used to infer shared higher order structural similarities between two sequences (*i.e.*, secondary and tertiary protein structures). Proteins that share a high degree of similarity throughout the entire sequence are often homologous. Homologous proteins often have common secondary structures, common three-dimensional configuration, and, consequently, may share similar functions (Caetano-Anollés *et al.*, 2009; Illergård *et al.*, 2009).

FASTA bioinformatic alignment searches using the MON 95379 Cry1B.868 amino acid sequence and Cry1Da_7 amino acid sequence were performed with the toxin database to identify possible homology with proteins that may be harmful to human and animal health. Periodically, the databases used to evaluate proteins are updated. The toxin database, TOX_2020, is a subset of sequences derived from the Swiss-Prot database (found at https://www.uniprot.org) that was selected using a keyword search and filtered to remove likely non-toxin proteins. The TOX_2020 database contains 7,728 sequences and has been curated to remove *Bt* insecticidal Cry proteins. The results of the bioinformatic analyses demonstrated that no structurally relevant similarity exists between the Cry1B.868 and Cry1Da_7 proteins and any sequence in the TOX_2020 database.

Using MON 95379 Cry1B.868 and Cry1Da_7 as the query sequences, no alignment with an *E*-score of ≤1e-5 was observed using the TOX_2020 database to run a FASTA search.

For details, please refer to Appendix 9 ([redacted], 2020 (TRR0000118)).

B.2(a)(ii) Information on the stability of the proteins to proteolysis in appropriate gastrointestinal model systems

B.2(a)(ii)(i) Digestive fate of the Cry1B.868 protein

Degradation of the MON 95379 Cry1B.868 Protein by Pepsin

Degradation of the *Bt*-produced Cry1B.868 protein by pepsin was evaluated over time by analyzing digestion mixtures incubated for targeted time intervals following a standardized protocol validated in an international, multi-laboratory ring study (Thomas *et al.*, 2004) collected at targeted incubation time points. The susceptibility of the Cry1B.868 protein to pepsin degradation was assessed by visual analysis of a Brilliant Blue G Colloidal stained SDS-PAGE gel and by visual analysis of a western blot probed with an polyclonal anti-Cry1B.868 antibody. Both visualization methods were run concurrently with separate SDS-PAGE and western blot analyses to estimate the limit of detection (LOD) of the Cry1B.868 protein for each method.

For SDS-PAGE analysis of the digestibility of the Cry1B.868 protein in pepsin, the gel was loaded with 1 µg of total test protein (based on pre-digestion protein concentrations) for each of the digestion samples (Figure 31, Panel A). The SDS-PAGE gel for the digestibility assessment was run concurrently with a separate SDS-PAGE gel to estimate the LOD of the

Cry1B.868 protein (Figure 31, Panel B). The LOD of intact Cry1B.868 protein was approximately 1.6 ng (Figure 31, Panel B, lane 9). Visual examination of SDS-PAGE data showed that the intact Cry1B.868 protein was digested within 0.5 min of incubation in pepsin (Figure 31, Panel A, lane 5). Therefore, based on the LOD, more than 99.8% (100% - 0.2% = 99.8%) of the intact Cry1B.868 protein was digested within 0.5 -min of incubation in pepsin. Transiently-stable peptide fragments at ~4-kDa were observed throughout the course of the digestion.

No change in the Cry1B.868 protein band intensity was observed in the absence of pepsin in the 0 min No Pepsin Control and 60 min No Pepsin Control (Figure 31, Panel A, lanes 3 and 12). This indicates that the degradation of the Cry1B.868 protein was due to the proteolytic activity of pepsin and not due to instability of the protein while incubated in 2 mg/ml NaCl, 10 mM HCl, pH ~1.2 for 60 min. The 0 min No Test Protein Control and 60 min No Test Protein Control (Figure 31, Panel A, lanes 2 and 13) demonstrated that the pepsin is stable throughout the experimental phase.

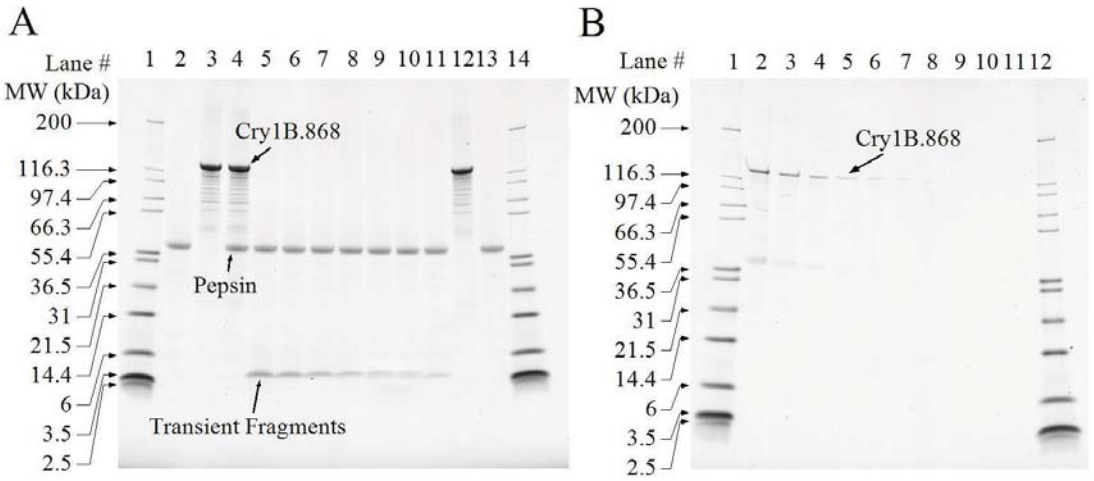

Figure 31. SDS-PAGE Analysis of the Degradation of Cry1B.868 Protein by Pepsin

Colloidal Brilliant Blue G stained SDS-PAGE gels were used to assess the degradation of Cry1B.868 protein by pepsin. Molecular weights (kDa) are shown on the left of each gel and correspond to the markers loaded. In each gel, the Cry1B.868 protein migrated to approximately 129.6 kDa and pepsin to approximately 38 kDa. Empty lanes and molecular weight markers that were not visible on the film were cropped from the images.

A: Cry1B.868 protein degradation in the presence of pepsin. Based on pre-reaction protein concentrations, 1 µg of test protein was loaded in each lane containing Cry1B.868 protein.

B: LOD determination. Indicated amounts of the test protein from the Pepsin Treated T0 sample were loaded to estimate the LOD of the Cry1B.868 protein.

A

Lane	Sample	Incubation Time (min)
1	Mark12 MWM	-
2	0 min No Test Protein Control	0
3	0 min No Pepsin Control	0
4	Pepsin Treated T0	0
5	Pepsin Treated T1	0.5
6	Pepsin Treated T2	2
7	Pepsin Treated T3	5
8	Pepsin Treated T4	10
9	Pepsin Treated T5	20
10	Pepsin Treated T6	30
11	Pepsin Treated T7	60
12	60 min No Pepsin Control	60
13	60 min No Test Protein Control	60
14	Mark12 MWM	-
15	Empty	-

B

Lane	Sample	Amount (ng)
1	Mark12 MWM	-
2	Pepsin Treated T0	200
3	Pepsin Treated T0	100
4	Pepsin Treated T0	50
5	Pepsin Treated T0	25
6	Pepsin Treated T0	12.5
7	Pepsin Treated T0	6.25
8	Pepsin Treated T0	3.1
9	Pepsin Treated T0	1.6
10	Pepsin Treated T0	0.8
11	Pepsin Treated T0	0.4
12	Mark12 MWM	-
13	Empty	-
14	Empty	-
15	Empty	-

For western blot analysis of Cry1B.868 pepsin susceptibility, the Cry1B.868 protein was loaded with approximately 40 ng per lane of total protein (based on pre-reaction total protein concentrations) for each reaction time point examined. The western blot used to assess Cry1B.868 protein degradation (Figure 32, Panel A) was run concurrently with the western blot used to estimate the LOD (Figure 32, Panel B). The LOD of the Cry1B.868 protein was approximately 0.63 ng (Figure 32, Panel B, lane 10).

Western blot analysis demonstrated that the intact Cry1B.868 protein was degraded below the LOD within 0.5 min of incubation in the presence of pepsin (Figure 32, Panel A, lane 6). Based on the western blot LOD for the Cry1B.868 protein, more than 98.4% (100% - 1.6% = 98.4%) of the intact Cry1B.868 protein was degraded within 0.5 min. No peptide fragments were detected at the 0.5 min and beyond time points in the western blot analysis.

No change in the intact Cry1B.868 protein band (~129.6 kDa) intensity was observed in the absence of pepsin in the 0 min No Pepsin Control and 60 min No Pepsin Control (Figure 32, Panel A, lanes 4 and 13) on western blot. This indicates that the degradation of the Cry1B.868 protein was due to the proteolytic activity of pepsin and not due to instability of the protein while incubated in 2 mg/ml NaCl, 10 mM HCl, pH ~1.2 for 60 min. The transiently-stable fragments at ~4 kDa that were observed by SDS-PAGE were not recognized by the antibody used in this western blot.

No immunoreactive bands were observed in 0 min No Protein Control and 60 min No Protein Control (Figure 32, Panel A, lanes 3 and 14). This result indicates that there was no non-specific interaction between the pepsin solution and the Cry1B.868-specific antibody under these experimental conditions.

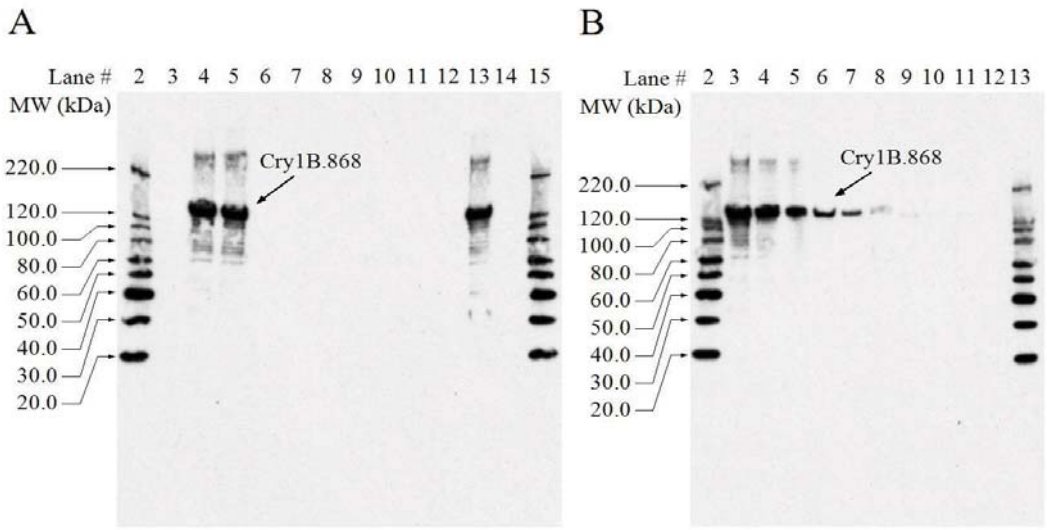

Figure 32. Western Blot Analysis of the Degradation of Cry1B.868 Protein by Pepsin

Western blots probed with an anti-Cry1B.868 antibody were used to assess the degradation of Cry1B.868 by pepsin. Molecular weights (kDa) are shown on the left of each gel and correspond to the MagicMark™ molecular weight marker. Empty lanes and molecular weight markers that were not visible on the film were cropped from the images. A 1.5 min-exposure is shown.
A: Cry1B.868 protein degradation by pepsin. Based on pre-reaction protein concentrations, 40 ng of test protein was loaded in each lane containing Cry1B.868 protein.
B: LOD determination. Indicated amounts of the test protein from the Pepsin Treated T0 sample were loaded to estimate the LOD of the Cry1B.868 protein.

A

Lane	Sample	Incubation Time (min)
1	Precision Plus MWM	-
2	MagicMark MWM	-
3	0 min No Test Protein Control	0
4	0 min No Pepsin Control	0
5	Pepsin Treated T0	0
6	Pepsin Treated T1	0.5
7	Pepsin Treated T2	2
8	Pepsin Treated T3	5
9	Pepsin Treated T4	10
10	Pepsin Treated T5	20
11	Pepsin Treated T6	30
12	Pepsin Treated T7	60
13	60 min No Pepsin Control	60
14	60 min No Test Protein Control	60
15	MagicMark MWM	-

B

Lane	Sample	Amount (ng)
1	Precision Plus MWM	-
2	MagicMark MWM	-
3	Pepsin Treated T0	40
4	Pepsin Treated T0	20
5	Pepsin Treated T0	10
6	Pepsin Treated T0	5
7	Pepsin Treated T0	2.5
8	Pepsin Treated T0	1.25
9	Pepsin Treated T0	0.63
10	Pepsin Treated T0	0.31
11	Pepsin Treated T0	0.16
12	Pepsin Treated T0	0.08
13	MagicMark MWM	-
14	Precision Plus MWM	-
15	Empty	-

Degradation of the MON 95379 Cry1B.868 by Pancreatin

The degradation of Cry1B.868 protein by pancreatin was assessed by western blot analysis (Figure 33). The total loading of the Cry1B.868 test protein for each timepoint examined was approximately 40 ng per lane (based on pre-reaction total protein concentrations). The western blot used to assess the Cry1B.868 protein degradation (Figure 33, Panel A) was run concurrently with the western blot used to estimate the LOD Figure 33, Panel B) of the Cry1B.868 protein. The LOD of the Cry1B.868 protein was observed at approximately the 0.16 ng protein loading (Figure 33, Panel A, lane 11). Based on the LOD for the Cry1B.868 protein, more than 99.6% (100% - 0.4% = 99.6%) of the intact Cry1B.868 protein was degraded within 5 min. Bands of ~60 kDa corresponding to fragments of Cry1B.868 were present over the course of the assessment (Figure 33, Panel A, lanes 5-12). The Cry1B.868 demonstrated typical characteristics that are present in many other Cry proteins, such as Cry1A.105 (Wang *et al.*, 2018) and Cry2Ab2 in MON 87751 soybean (A1110).

No obvious change in the intact Cry1B.868 (~129.6 kDa) band intensity was observed in the absence of pancreatin in the 0 min No Pancreatin Control and 24 hour No Pancreatin Control (Figure 33, Panel A, lanes 3 and 13). This indicates that the degradation of all immunoreactive forms of the Cry1B.868 protein was due to the proteolytic activity of pancreatin and not due to instability of the protein when incubated in 50 mM KH_2PO_4, pH 7.5 over the course of the experiment.

No immunoreactive bands were observed in the 0 min No Test Protein Control and 24 hour No Test Protein Contro (Figure 33, Panel A, lanes 2 and 14), demonstrating the absence of non-specific antibody interactions with the pancreatin solution.

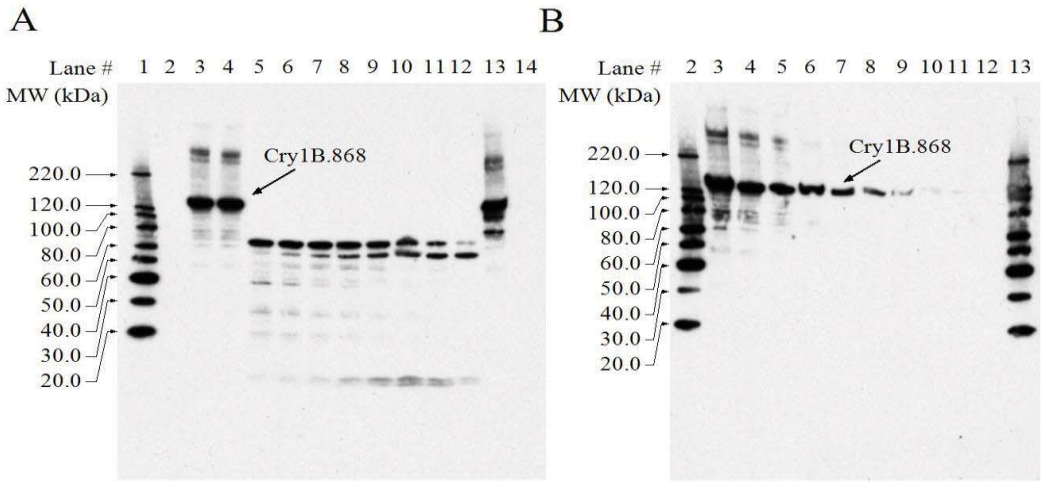

Figure 33. Western Blot Analysis of the Degradation of Cry1B.868 Protein by Pancreatin

Western blots probed with an anti-Cry1B.868 antibody were used to assess the degradation of Cry1B.868 by pancreatin. Molecular weights (kDa) are shown on the left of each gel and correspond to the MagicMark™ molecular weight marker. Empty lanes and molecular weight markers that were not visible on the film were cropped from the images. A 1.0 min-exposure is shown.
A: Cry1B.868 protein degradation by pancreatin. Based on pre-reaction protein concentrations, 40 ng of test protein was loaded in each lane containing Cry1B.868 protein.
B: LOD determination. Indicated amounts of the test protein from the Pancreatin Treated T0 sample were loaded to estimate the LOD of the Cry1B.868 protein.

A

Lane	Sample	Incubation Time
1	MagicMark MWM	-
2	0 min No Test Protein Control	0
3	0 min No Pancreatin Control	0
4	Pancreatin Treated T0	0
5	Pancreatin Treated T1	5 min
6	Pancreatin Treated T2	15 min
7	Pancreatin Treated T3	30 min
8	Pancreatin Treated T4	1 h
9	Pancreatin Treated T5	2 h
10	Pancreatin Treated T6	4 h
11	Pancreatin Treated T7	8 h
12	Pancreatin Treated T8	24 h
13	24 h No Pancreatin Control	24 h
14	24 h No Test Protein Control	24 h
15	Precision Plus MWM	-

B

Lane	Sample	Amount (ng)
1	Precision Plus MWM	-
2	MagicMark MWM	-
3	Pancreatin Treated T0	40
4	Pancreatin Treated T0	20
5	Pancreatin Treated T0	10
6	Pancreatin Treated T0	5
7	Pancreatin Treated T0	2.5
8	Pancreatin Treated T0	1.25
9	Pancreatin Treated T0	0.63
10	Pancreatin Treated T0	0.31
11	Pancreatin Treated T0	0.16
12	Pancreatin Treated T0	0.08
13	MagicMark MWM	-
14	Precision Plus MWM	-
15	Empty	-

Degradation of Cry1B.868 Protein by Pepsin Followed by Pancreatin

To better understand the fate of the transiently-stable peptide fragments at ~4-kDa that were observed in the reaction mixtures throughout the course of the pepsin digestion of Cry1B.868, sequential digestibility of the Cry1B.868 protein was conducted. This sequential digestibility was assessed both by visual analysis of a Colloidal Brilliant Blue G stained SDS-PAGE gel, and visual analysis of a western blot probed with an anti-Cry1B.868-polyclonal antibody.

For the sequential degradation assay, the Cry1B.868 protein was incubated with pepsin for 2 min, followed by incubation with pancreatin. For the Colloidal Brilliant Blue G stained SDS-PAGE assessment, the gel was loaded with 1 µg of Cry1B.868 protein (based on pre-digestion protein concentrations) for each of the digestion samples. Examination of SDS-PAGE data showed that the intact Cry1B.868 protein was digested within 2 min of incubation in pepsin (Figure 34, Panel A, lane 3) and the small transient fragments at ~4 kDa was completely digested within 0.5 min of pancreatin exposure (Figure 34, Panel A, lane 7).

No change in the transient fragment band (~4 kDa) intensities was observed in the absence of pancreatin in the SEQ 0 min No Pancreatin Control and SEQ 2 hour No Pancreatin Control (Figure 34, Panel A, lanes 5 and 14). This indicates that the digestion of the transient fragments (~4 kDa) was due to the proteolytic activity of pancreatin and not due to instability of the fragment when incubated in 50 mM KH_2PO_4 at pH 7.5 over the course of the experiment.

The SEQ 0 min No Test Protein Control and SEQ 2 hour No Test Protein Control (Figure 34, Panel A, lanes 4 and 15) demonstrated the integrity of the pancreatin over the course of the experiment. The intensity of some pancreatin bands decreased during the course of the experiment, most likely due to auto-digestion. This is not expected to adversely impact the pancreatin degradation results, as the transiently stable fragments (~4 kDa) were digested within 0.5 min of exposure to pancreatin.

The sequential digestion of the Cry1B.868 protein was also assessed by western blot (Figure 34, Panel B), with 40 ng of the test protein (based on total protein pre-digestion concentrations) loaded per lane. No bands were detected in the 2 min Pepsin Treated sample (Figure 34, Panel B, lane 3).

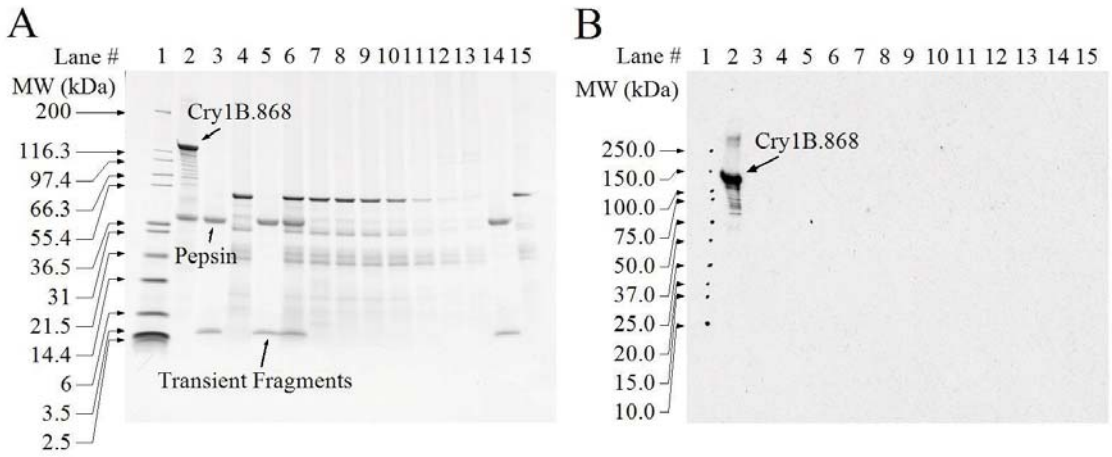

Figure 34. SDS-PAGE and Western Blot Analysis of the Degradation of Cry1B.868 Protein by Sequential Digestion

SDS-PAGE and western blot analysis were used to assess the degradation of Cry1B.868 in sequential digestion. Molecular weights (kDa) are shown on the left of each gel and correspond to the markers loaded.

A: Colloidal Brilliant Blue G stained SDS-PAGE gel analysis of Cry1B.868 in sequential digestion. Based on pre-digestion protein concentrations, 1 µg of test protein was loaded in each lane containing Cry1B.868 protein.

B: Western blot analysis of Cry1B.868 in sequential digestion. Based on pre-digestion protein concentrations, 40 ng of test protein was loaded in each lane containing Cry1B.868 protein. A 1.0 min-exposure is shown.

A

Lane	Sample	Incubation Time
1	Mark12 MWM	-
	Pepsin Degradation	
2	0 min Pepsin Treated	0 min
3	2 min Pepsin Treated	2 min
	Pancreatin Degradation	
4	SEQ 0 min No Test Protein Control	0 min
5	SEQ 0 min No Pancreatin Control	0 min
6	SEQ T0	0 min
7	SEQ T1	0.5 min
8	SEQ T2	2 min
9	SEQ T3	5 min
10	SEQ T4	10 min
11	SEQ T5	30 min
12	SEQ T6	1 h
13	SEQ T7	2 h
14	SEQ 2 h No Pancreatin Control	2 h
15	SEQ 2 h No Test Protein Control	2 h

B

Lane	Sample	Incubation Time
1	Precision Plus MWM	-
	Pepsin Degradation	
2	0 min Pepsin Treated	0 min
3	2 min Pepsin Treated	2 min
	Pancreatin Degradation	
4	SEQ 0 min No Test Protein Control	0 min
5	SEQ 0 min No Pancreatin Control	0 min
6	SEQ T0	0 min
7	SEQ T1	0.5 min
8	SEQ T2	2 min
9	SEQ T3	5 min
10	SEQ T4	10 min
11	SEQ T5	30 min
12	SEQ T6	1 h
13	SEQ T7	2 h
14	SEQ 2 h No Pancreatin Control	2 h
15	SEQ 2 h No Test Protein Control	2 h

Digestive Fate of the Cry1B.868 Protein Conclusions

The ability of Cry1B.868 protein to be degraded by pepsin and by pancreatin was evaluated in this study. The results showed that at least 99.8% of the intact Cry1B.868 protein was degraded by pepsin within 0.5 min when analyzed by SDS-PAGE and 98.4% of the intact Cry1B.868 was degraded by pepsin within 0.5 min when analyzed by western blot using a Cry1B.868-specific antibody. SDS-PAGE analysis showed that transient peptide fragments at ~4 kDa were observed throughout the course of the pepsin digestion. At least 99.6% of the intact Cry1B.868 protein was degraded by pancreatin within 5 min when analyzed by western blot. These results show that the full-length Cry1B.868 is rapidly degraded by pepsin and pancreatin. The transient fragments at ~4 kDa were rapidly degraded by sequential digestion. Rapid degradation of the intact Cry1B.868 protein by pepsin or pancreatin alone and complete degradation by pepsin followed by pancreatin indicates that the Cry1B.868 protein is highly unlikely to pose any safety concern to human or animal health.

For details, please refer to Appendix 10 ([redacted], 2020 (TRR0000667)).

B.2(a)(ii)(ii) Digestive fate of the Cry1Da_7 protein

Degradation of Cry1Da_7 Protein in the Presence of Pepsin

Degradation of the *Bt*-produced Cry1Da_7 protein by pepsin was evaluated over time by analyzing digestion mixtures incubated for targeted time intervals following a standardized protocol validated in an international, multi-laboratory ring study (Thomas *et al.*, 2004) collected at targeted incubation time points. The susceptibility of Cry1Da_7 protein to pepsin degradation was assessed by visual analysis of a Brilliant Blue G Colloidal stained SDS-PAGE gel and by visual analysis of a western blot probed with an anti-Cry1Da_7 polyclonal antibody. Both visualization methods were run concurrently with separate SDS-PAGE and western blot analyses to estimate the limit of detection (LOD) of the Cry1Da_7 protein for each method.

For SDS-PAGE analysis of the digestibility of the Cry1Da_7 protein in pepsin, the gel was loaded with 1 µg of total test protein (based on pre-digestion protein concentrations) for each of the digestion samples (Figure 35, Panel A). The SDS-PAGE gel for the digestibility assessment was run concurrently with a separate SDS-PAGE gel to estimate the LOD of the Cry1Da_7 protein (Figure 35, Panel B). The LOD of intact Cry1Da_7 protein was approximately 6.3 ng (Figure 35, Panel B, lane 8). Visual examination of SDS-PAGE data showed that the intact Cry1Da_7 protein was digested within 0.5 min of incubation in pepsin (Figure 35, Panel A, lane 5). Therefore, based on the LOD, more than 99.4% (100% - 0.6% = 99.4%) of the intact Cry1Da_7 protein was digested within 0.5 min of incubation in pepsin. Transiently-stable peptide fragments at ~4-kDa were observed throughout the course of the digestion.

No change in the Cry1Da_7 protein band intensity was observed in the absence of pepsin in the 0 min No Pepsin Control and 60 min No Pepsin Control (Figure 35, Panel A, lanes 3 and 12). This indicates that the degradation of the Cry1Da_7 protein was due to the proteolytic activity of pepsin and not due to instability of the protein while incubated in 10 mM HCl, 2 mg/ml NaCl, pH ~1.2 for 60 min. The 0 min No Test Protein Control and 60 min No Test Protein Control (Figure 35, Panel A, lanes 2 and 13) demonstrated that the pepsin is stable throughout the experimental phase.

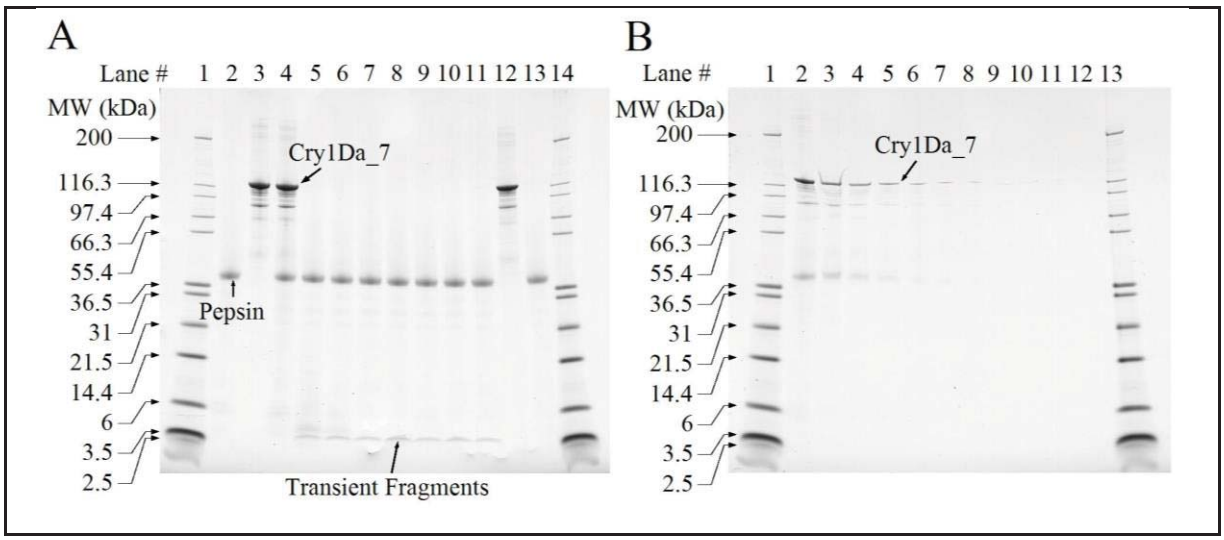

Figure 35. SDS-PAGE Analysis of the Degradation of Cry1Da_7 Protein by Pepsin

Colloidal Brilliant Blue G stained SDS-PAGE gels were used to assess the degradation of Cry1Da_7 protein by pepsin. Molecular weights (kDa) are shown on the left of each gel and correspond to the markers loaded. In each gel, the Cry1Da_7 protein migrated to approximately 126.5 kDa and pepsin to approximately 38 kDa. Empty lanes and molecular weight markers that were not visible on the film were cropped from the images.

A: Cry1Da_7 protein degradation in the presence of pepsin. Based on pre-reaction protein concentrations, 1 µg of test protein was loaded in each lane containing Cry1Da_7 protein.

B: LOD determination. Indicated amounts of the test protein from the Pepsin Treated T0 sample were loaded to estimate the LOD of the Cry1Da_7 protein.

A

Lane	Sample	Incubation Time (min)
1	Mark12 MWM	-
2	0 min No Test Protein Control	0
3	0 min No Pepsin Control	0
4	Pepsin Treated T0	0
5	Pepsin Treated T1	0.5
6	Pepsin Treated T2	2
7	Pepsin Treated T3	5
8	Pepsin Treated T4	10
9	Pepsin Treated T5	20
10	Pepsin Treated T6	30
11	Pepsin Treated T7	60
12	60 min No Pepsin Control	60
13	60 min No Test Protein Control	60
14	Mark12 MWM	-
15	Empty	-

B

Lane	Sample	Amount (ng)
1	Mark12 MWM	-
2	Pepsin Treated T0	400
3	Pepsin Treated T0	200
4	Pepsin Treated T0	100
5	Pepsin Treated T0	50
6	Pepsin Treated T0	25
7	Pepsin Treated T0	12.5
8	Pepsin Treated T0	6.3
9	Pepsin Treated T0	3.1
10	Pepsin Treated T0	1.6
11	Pepsin Treated T0	0.8
12	Pepsin Treated T0	0.4
13	Mark12 MWM	-
14	Empty	-
15	Empty	-

For western blot analysis of Cry1Da_7 pepsin susceptibility, the Cry1Da_7 protein was loaded with approximately 40 ng per lane of total protein (based on pre-reaction total protein concentrations) for each reaction time point examined. The western blot used to assess Cry1Da_7 protein degradation (Figure 36, Panel A) was run concurrently with the western blot used to estimate the LOD (Figure 36, Panel B). The LOD of the Cry1Da_7 protein was approximately 1.25 ng (Figure 36, Panel B, lane 7). Western blot analysis demonstrated that the intact Cry1Da_7 protein was degraded below the LOD within 0.5 min of incubation in the presence of pepsin (Figure 36, Panel A, lane 6). Based on the western blot LOD for the Cry1Da_7 protein, more than 96.9% (100% - 3.1% = 96.9%) of the intact Cry1Da_7 protein was degraded within 0.5 min. No peptide fragments were detected at the 0.5 min and beyond time points in the western blot analysis.

No change in the Cry1Da_7 protein band intensity was observed in the absence of pepsin in the 0 min No Pepsin Control and 60 min No Pepsin Control (Figure 36, Panel A, lanes 4 and 13). This indicates that the degradation of the Cry1Da_7 protein was due to the proteolytic activity of pepsin and not due to instability of the protein while incubated in 2 mg/ml NaCl, 10 mM HCl, pH ~1.2 for 60 min. The transiently-stable fragments at ~4 kDa that were observed by SDS-PAGE were not recognized by the antibody used in this western blot.

No immunoreactive bands were observed in 0 min No Protein Control and 60 min No Protein Control (Figure 36, Panel A, lanes 3 and 14). This result indicates that there was no non-specific interaction between the pepsin solution and the Cry1Da_7-specific antibody under these experimental conditions.

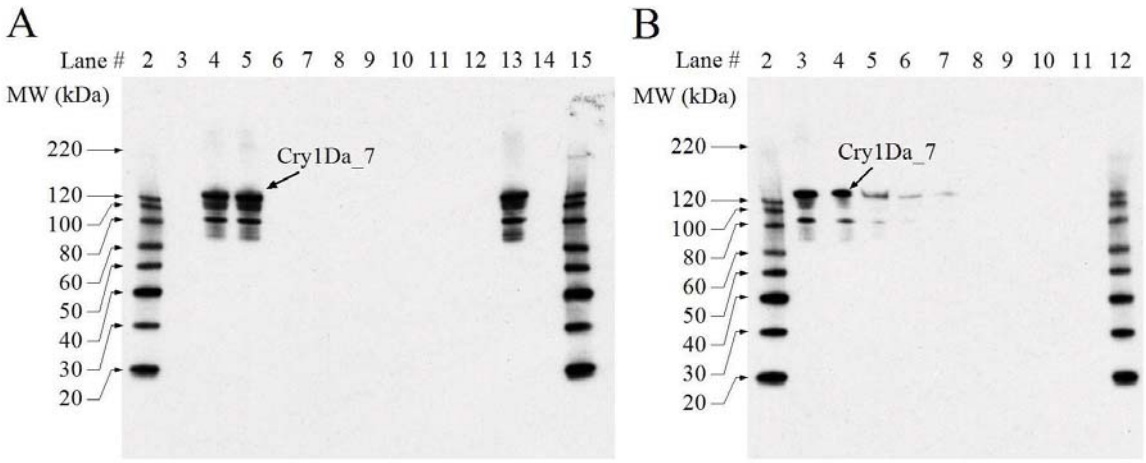

Figure 36. Western Blot Analysis of the Degradation of Cry1Da_7 Protein by Pepsin

Western blots probed with an anti-Cry1Da_7 antibody were used to assess the degradation of Cry1Da_7 by pepsin. Molecular weights (kDa) are shown on the left of each gel and correspond to the MagicMark™ molecular weight marker. Empty lanes and molecular weight markers that were not visible on the film were cropped from the images. A 1.5 min exposure is shown.
A: Cry1Da_7 protein degradation by pepsin. Based on pre-reaction protein concentrations, 40 ng of test protein was loaded in each lane containing Cry1Da_7 protein.
B: LOD determination. Indicated amounts of the test protein from the Pepsin Treated T0 sample were loaded to estimate the LOD of the Cry1Da_7 protein.

A

Lane	Sample	Incubation Time (min)
1	Precision Plus MWM	-
2	MagicMark MWM	-
3	0 min No Test Protein Control	0
4	0 min No Pepsin Control	0
5	Pepsin Treated T0	0
6	Pepsin Treated T1	0.5
7	Pepsin Treated T2	2
8	Pepsin Treated T3	5
9	Pepsin Treated T4	10
10	Pepsin Treated T5	20
11	Pepsin Treated T6	30
12	Pepsin Treated T7	60
13	60 min No Pepsin Control	60
14	60 min No Test Protein Control	60
15	MagicMark MWM	-

B

Lane	Sample	Amount (ng)
1	Precision Plus MWM	-
2	MagicMark MWM	-
3	Pepsin Treated T0	20
4	Pepsin Treated T0	10
5	Pepsin Treated T0	5
6	Pepsin Treated T0	2.5
7	Pepsin Treated T0	1.25
8	Pepsin Treated T0	0.63
9	Pepsin Treated T0	0.31
10	Pepsin Treated T0	0.16
11	Pepsin Treated T0	0.08
12	MagicMark MWM	-
13	Precision Plus MWM	-
14	Empty	-
15	Empty	-

Degradation of Cry1Da_7 Protein in the Presence of Pancreatin

The degradation of the Cry1Da_7 protein by pancreatin was assessed by western blot analysis (Figure 37). The total loading of the Cry1Da_7 test protein for each timepoint examined was approximately 40 ng per lane (based on pre-reaction total protein concentrations). The western blot used to assess the Cry1Da_7 protein degradation (Figure 37, Panel A) was run concurrently with the western blot used to estimate the LOD (Figure 37, Panel B) of the Cry1Da_7 protein. The LOD of the Cry1Da_7 protein was observed at approximately the 1.25 ng protein loading (Figure 37, Panel A, lane 7). Based on the LOD for the Cry1Da_7 protein, more than 96.9% (100% - 3.1% = 96.9%) of the intact Cry1B.868 protein was degraded within 5 min. A band of ~60 kDa corresponding to a fragment of Cry1Da_7 was present over the course of the assessment (Figure 37, Panel A, lanes 5-12). The Cry1Da_7 demonstrated typical characteristics that are present in many other Cry proteins, such as Cry1A.105 (Wang *et al.*, 2018) and Cry2Ab2 in MON 87751 soybean (A1110).

No obvious change in the intact Cry1Da_7 (~126.5 kDa) band intensity was observed in the absence of pancreatin in the 0 min No Pancreatin Control and 24 hour No Pancreatin Control (Figure 37, Panel A, lanes 3 and 13). This indicates that the degradation of all immunoreactive forms of the Cry1Da_7 protein was due to the proteolytic activity of pancreatin and not due to instability of the protein when incubated in 50 mM KH_2PO_4, pH 7.5 over the course of the experiment.

No immunoreactive bands were observed in the 0 min No Test Protein Control and 24 hour No Test Protein Control (Figure 37, Panel A, lanes 2 and 14), demonstrating the absence of non-specific antibody interactions with the pancreatin solution.

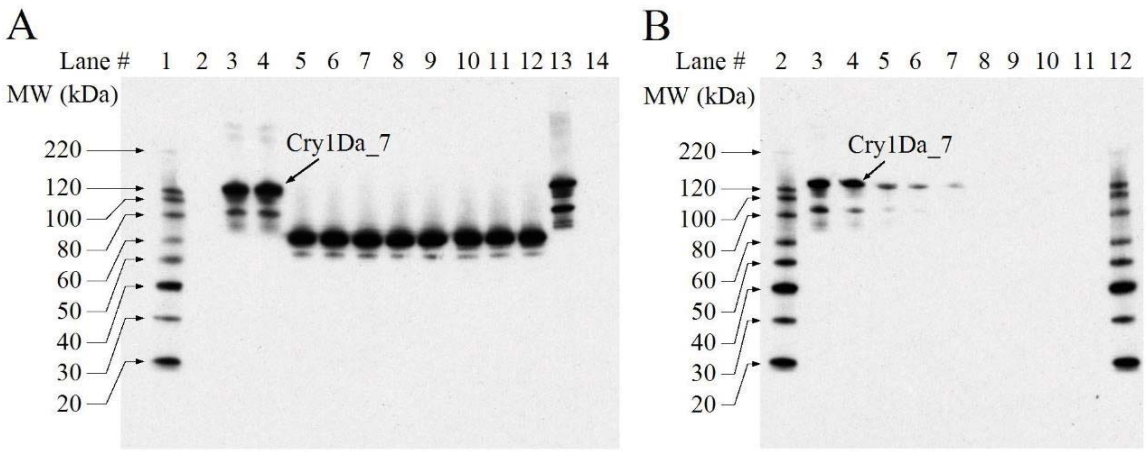

Figure 37. Western Blot Analysis of the Degradation of Cry1Da_7 Protein by Pancreatin

Western blots probed with an anti-Cry1Da_7 antibody were used to assess the degradation of Cry1Da_7 by pancreatin. Molecular weights (kDa) are shown on the left of each gel and correspond to the MagicMark™ molecular weight marker. Empty lanes and molecular weight markers that were not visible on the film were cropped from the images. A 1.5 min exposure is shown.
A: Cry1Da_7 protein degradation by pancreatin. Based on pre-reaction protein concentrations, 40 ng of test protein was loaded in each lane containing Cry1Da_7 protein.
B: LOD determination. Indicated amounts of the test protein from the Pancreatin Treated T0 sample were loaded to estimate the LOD of the Cry1Da_7 protein.

A

Lane	Sample	Incubation Time
1	MagicMark MWM	-
2	0 min No Test Protein Control	0
3	0 min No Pancreatin Control	0
4	Pancreatin Treated T0	0
5	Pancreatin Treated T1	5 min
6	Pancreatin Treated T2	15 min
7	Pancreatin Treated T3	30 min
8	Pancreatin Treated T4	1 h
9	Pancreatin Treated T5	2 h
10	Pancreatin Treated T6	4 h
11	Pancreatin Treated T7	8 h
12	Pancreatin Treated T8	24 h
13	24 h No Pancreatin Control	24 h
14	24 h No Test Protein Control	24 h
15	Precision Plus MWM	-

B

Lane	Sample	Amount (ng)
1	Precision Plus MWM	-
2	MagicMark MWM	-
3	Pancreatin Treated T0	20
4	Pancreatin Treated T0	10
5	Pancreatin Treated T0	5
6	Pancreatin Treated T0	2.5
7	Pancreatin Treated T0	1.25
8	Pancreatin Treated T0	0.63
9	Pancreatin Treated T0	0.31
10	Pancreatin Treated T0	0.16
11	Pancreatin Treated T0	0.08
12	MagicMark MWM	-
13	Precision Plus MWM	-
14	Empty	-
15	Empty	-

Degradation of Cry1Da_7 Protein by Pepsin Followed by Pancreatin

To better understand the fate of the transiently-stable peptide fragments at ~4-kDa that were observed in the reaction mixtures throughout the course of the pepsin digestion of Cry1Da_7, sequential digestibility of the Cry1Da_7 protein was conducted. This sequential digestibility was assessed both by visual analysis of a Colloidal Brilliant Blue G stained SDS-PAGE gel, and visual analysis of a western blot probed with an anti- Cry1Da_7-polyclonal antibody.

For the sequential degradation assay, the Cry1Da_7 protein was incubated with pepsin for 2 min, followed by incubation with pancreatin. For the Colloidal Brilliant Blue G stained SDS-PAGE assessment, the gel was loaded with 1 µg of Cry1Da_7 protein (based on pre-digestion protein concentrations) for each of the digestion samples. Examination of SDS-PAGE data showed that the intact Cry1Da_7 protein was digested within 2 min of incubation in pepsin (Figure 38, Panel A, lane 3) and the small transient fragments at ~4 kDa was completely digested within 0.5 min of pancreatin exposure (Figure 38, Panel A, lane 7).

No change in the fragment band intensities was observed in the absence of pancreatin in the SEQ 0 min No Pancreatin Control and SEQ 2 hour No Pancreatin Control (Figure 38, Panel A, lanes 5 and 14). This indicates that the digestion of the fragments was due to the proteolytic activity of pancreatin and not due to instability of the fragment when incubated in in 50 mM KH_2PO_4 at pH 7.5 over the course of the experiment.

The SEQ 0 min No Test Protein Control and SEQ 2 hour No Test Protein Control (Figure 38, Panel A, lanes 4 and 15) demonstrated the integrity of the pancreatin over the course of the experiment. The intensity of some pancreatin bands decreased somewhat during the course of the experiment, most likely due to auto-digestion. This is not expected to adversely impact the pancreatin degradation results, as the transiently stable fragments were digested within 0.5 min of exposure to pancreatin.

The sequential digestion of the Cry1Da_7 protein was also assessed by western blot (Figure 38, Panel B), with 40 ng of the test protein (based on total protein pre-digestion concentrations) loaded per lane. No bands were detected in the 2 min Pepsin Treated sample (Figure 38, Panel B, lane 3).

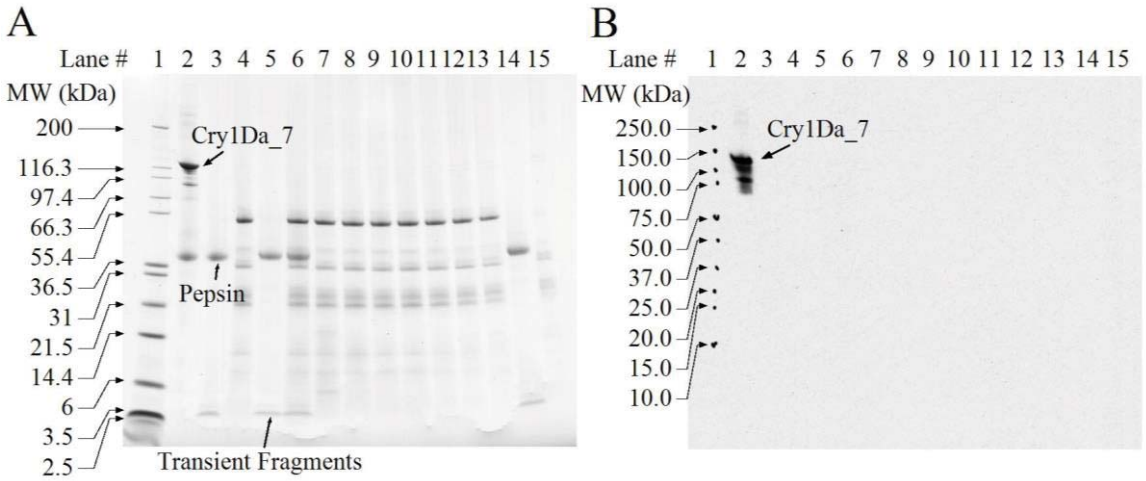

Figure 38. SDS-PAGE and Western Blot Analysis of the Degradation of Cry1Da_7 Protein by Sequential Digestion

SDS-PAGE and western blot analysis were used to assess the degradation of Cry1Da_7 in sequential digestion. Molecular weights (kDa) are shown on the left of each gel and correspond to the markers loaded.

A: Colloidal Brilliant Blue G stained SDS-PAGE gel analysis of Cry1Da_7 in sequential digestion. Based on pre-digestion protein concentrations, 1 µg of test protein was loaded in each lane containing Cry1Da_7 protein.

B: Western blot analysis of Cry1Da_7 in sequential digestion. Based on pre-digestion protein concentrations, 40 ng of test protein was loaded in each lane containing Cry1Da_7 protein. A 1.0 min exposure is shown.

A

Lane	Sample	Incubation Time
1	Mark12 MWM	-
	Pepsin Degradation	
2	0 min Pepsin Treated	0 min
3	2 min Pepsin Treated	2 min
	Pancreatin Degradation	
4	SEQ 0 min No Test Protein Control	0 min
5	SEQ 0 min No Pancreatin Control	0 min
6	SEQ T0	0 min
7	SEQ T1	0.5 min
8	SEQ T2	2 min
9	SEQ T3	5 min
10	SEQ T4	10 min
11	SEQ T5	30 min
12	SEQ T6	1 h
13	SEQ T7	2 h
14	SEQ 2 h No Pancreatin Control	2 h
15	SEQ 2 h No Test Protein Control	2 h

B

Lane	Sample	Incubation Time
1	Precision Plus MWM	-
	Pepsin Degradation	
2	0 min Pepsin Treated	0 min
3	2 min Pepsin Treated	2 min
	Pancreatin Degradation	
4	SEQ 0 min No Test Protein Control	0 min
5	SEQ 0 min No Pancreatin Control	0 min
6	SEQ T0	0 min
7	SEQ T1	0.5 min
8	SEQ T2	2 min
9	SEQ T3	5 min
10	SEQ T4	10 min
11	SEQ T5	30 min
12	SEQ T6	1 h
13	SEQ T7	2 h
14	SEQ 2 h No Pancreatin Control	2 h
15	SEQ 2 h No Test Protein Control	2 h

Digestive Fate of the Cry1Da_7 Protein Conclusions

The ability of Cry1Da_7 protein to be degraded by pepsin and by pancreatin was evaluated in this study. The results showed that at least 99.4% of the intact Cry1Da_7 protein was degraded by pepsin within 0.5 min when analyzed by SDS-PAGE and 96.9% of the intact Cry1Da_7 was degraded by pepsin within 0.5 min when analyzed by western blot using a Cry1Da_7-specific antibody. SDS-PAGE analysis showed that transient peptide fragments at ~4 kDa were observed throughout the course of the pepsin digestion. At least 96.9% of the intact Cry1Da_7 protein was degraded by pancreatin within 5 min when analyzed by western blot. These results show that the full-length Cry1Da_7 is rapidly degraded by pepsin and pancreatin. The transient fragments at ~4 kDa were rapidly degraded by sequential digestion. Rapid degradation of the intact Cry1Da_7 protein by pepsin alone and pancreatin alone and complete degradation by pepsin followed by pancreatin indicates that the Cry1Da_7 protein is highly unlikely to pose any safety concern to human or animal health.

For details, please refer to Appendix 11 ([redacted] 2019 (MSL0030568)).

B.2(a)(iii) An animal toxicity study if the bioinformatic comparison and biochemical studies indicate either a relationship with known protein toxins/anti-nutrients or resistance to proteolysis

Not relevant for this product.

B.2(b) Information on the potential allergenicity of any new proteins, including:

B.2(b)(i) Source of the new proteins

The coding sequences for the Cry1B.868 and Cry1Da_7 proteins are derived from the bacterium *Bacillus thuringiensis*:

Kingdom: Bacteria

Phylum: Firmicutes

Class: Bacilli

Order: Bacillales

Family: Bacillaceae

Genus: *Bacillus*

B.2(b)(ii) A bioinformatics comparison of the amino acid sequence to known allergens

Structural similarity of the Cry1B.868 to known allergens

The extent of sequence similarities between the Cry1B.868 protein sequence and known allergens, gliadins, and glutenins was assessed using the FASTA sequence alignment tool along with an eight-amino acid sliding window search (Codex Alimentarius, 2009; Thomas *et al.*, 2005). The methods used are summarized below and detailed in Appendix 9. The data generated from these analyses confirm that the Cry1B.868 protein does not share amino acid sequence similarities with known allergens, gliadins, or glutenins.

The FASTA program directly compares amino acid sequences (i.e., primary, linear protein structure). This alignment data may be used to infer shared higher order structural similarities between two sequences (i.e., secondary and tertiary protein structures). Proteins that share a high degree of similarity throughout the entire sequence are often homologous.

By definition, homologous proteins have common secondary structures, and three-dimensional configuration, and, consequently, may share similar functions. Periodically, the databases used to evaluate proteins are updated. Since the most recent reports were completed, the allergen (AD_2020) database has been revised and updated. In order to determine if the Cry1B.868 protein shares significant sequence similarity to new sequences contained in the updated allergen database, protein sequences were used as a query for a FASTA and Sliding Window search of the AD_2020 database. The allergen, gliadin, and glutenin protein sequence database (AD_2020) was obtained as the "COMprehensive Protein Allergen REsource" (COMPARE) database from the Health and Environmental Sciences Institute (HESI) and was used for the evaluation of sequence similarities shared between the Cry1B.868 protein and all proteins in the database. The AD_2020 database contains 2,248 sequences. When used to align the sequence of the introduced protein to each protein in the database, the FASTA algorithm produces an *E*-score (expectation score) for each alignment. The *E*-score is a statistical measure of the likelihood that the observed similarity score could have occurred by chance in a search. A larger *E*-score indicates a low degree of similarity between the query sequence and the sequence from the database. Typically, alignments between two sequences which have an *E*-score of less than or equal to 1×10-5 are considered to have meaningful homology. Results indicate that the Cry1B.868 protein sequence does not share meaningful similarity with sequences in the allergen database. No alignment met or exceeded the threshold of 35% identity over 80 amino acids recommended by Codex Alimentarius (2009) or had an *E*-score of less than or equal to 1×10^{-5}.

A second bioinformatic tool, an eight-amino acid sliding window search, was used to specifically identify short linear polypeptide matches to known allergens. It is possible that proteins structurally unrelated to allergens, gliadins, and glutenins may contain smaller immunologically meaningful epitopes. An amino acid sequence may have allergenic potential if it has an exact sequence identity of at least eight linearly contiguous amino acids with a potential allergen epitope (Hileman *et al.*, 2002; Metcalfe *et al.*, 1996). Using a sliding window of less than eight amino acids can produce matches containing considerable uncertainty depending on the length of the query sequence (Silvanovich *et al.*, 2006), and is not useful to the allergy assessment process (Thomas *et al.*, 2005). No eight contiguous amino acid identities were detected when the Cry1B.868 protein sequence was compared to the proteins in the AD_2020 sequence database.

The bioinformatic results demonstrated there were no biologically relevant sequence similarities to allergens when the Cry1B.868 protein sequence was used as a query for a FASTA search of the AD_2020 database. Furthermore, no short (eight amino acid) polypeptide matches were shared between the Cry1B.868 protein sequence and proteins in the allergen database. These data show that Cry1B.868 protein sequence lacks both structurally and immunologically relevant similarities to known allergens, gliadins, and glutenins.

For details, please refer to Appendix 9 ([redacted], 2020 (TRR0000118)).

Structural Similarity of Cry1Da_7 Protein to Known Allergens

The extent of sequence similarities between the Cry1Da_7 protein sequence and known allergens, gliadins, and glutenins was assessed using the FASTA sequence alignment tool along with an eight-amino acid sliding window search (Codex Alimentarius, 2009; Thomas *et al.*, 2005). The methods used are summarized in Section B.2(b)(ii) and Appendix 9. The data generated from these analyses confirm that the Cry1Da_7 protein does not share amino acid sequence similarities with known allergens, gliadins, or glutenins.

The bioinformatic results demonstrated there were no biologically relevant sequence similarities to allergens when the Cry1Da_7 protein sequence was used as a query for a FASTA search of the AD_2020 database. Furthermore, no short (eight amino acid) polypeptide matches were shared between the Cry1Da_7 protein sequence and proteins in the allergen database. These data show that Cry1Da_7 protein sequence lacks both structurally and immunologically relevant similarities to known allergens, gliadins, and glutenins.

For details, please refer to Appendix 9 ([redacted], 2020 (TRR0000118)).

B.2(b)(iii) The new protein's structural properties, including, but not limited to, its susceptibility to enzymatic degregation (e.g. proteolysis), heat and/or acid stability

B.2(b)(iii)(i) Heat susceptibility of the MON 95379 Cry1B.868 protein

The effect of heat treatment on the activity of the *Bt*-produced Cry1B.868 protein was evaluated. Heat treated samples and an unheated control sample of Cry1B.868 protein were analyzed: 1) using an insect bioassay to assess the impact of temperature on the functional activity of the Cry1B.868 protein; and 2) using SDS-PAGE to assess the impact of temperature on protein integrity.

Aliquots of Cry1B.868 protein were heated to 25, 37, 55, 75 and 95 ºC for either 15 or 30 minutes, while a separate aliquot of Cry1B.868 protein was maintained on ice for the duration of the heat treatments to serve as a temperature control. The effect of heat treatment on the activity of Cry1B.868 was evaluated using an insect bioassay (Appendix 12). The effect of heat treatment on the integrity of the Cry1B.868 protein was evaluated using SDS-PAGE analysis of the heated and temperature control Cry1B.868 protein samples.

Results of the functional activity assay for Cry1B.868 protein incubated for 15 and 30 minutes are listed in Table 23 and Table 24, respectively. The control sample had an EC_{50} of 0.18 µg Cry1B.868 protein/ml diet, thus demonstrating that protein activity was maintained during incubation on ice. Protein activity was retained when incubated for 15 and 30 minutes at a temperature of 25, 37 and 55ºC. At temperatures of 75ºC and above for either 15 or 30 minutes, the estimated EC_{50} values were >10 µg Cry1B.868 protein/ml diet, which represents a reduction in functional activity > 98% when compared to the control[11].

The results of the SDS-PAGE analysis of the heat-treated samples incubated for 15 and 30 minutes are illustrated in Figure 39 and Figure 40, respectively. The control sample loaded on each gel (Figure 39 and Figure 40, lane 2) showed equivalent band intensity to the 100% reference standard (Figure 39 and Figure 40, lane 8), demonstrating that the Cry1B.868 protein was stable on wet ice during the incubation period. No apparent decrease in band intensity of the ~129.6 kDa Cry1B.868 protein was observed in the test samples when heated at temperatures of 25, 37 and 55°C for 15 or 30 minutes. Smaller molecular weight degradation products and a decrease in the intensity of the main Cry1B.868 band were evident at 75°C with the most prominent loss of band intensity evident at 30 minutes. At 95°C, a significant portion of the Cry1B.868 band intensity was lost with less than 10% remaining after 30 minutes as compared to the 10% reference standard. In addition, increased smaller molecular weight degradation and slight aggregation is observed at 95°C for both 15 and 30 minute heat treatments.

[11] EC_{50} > 10 µg Cry1B.868/ml diet represents a loss of activity: 1 – (0.18 µg Cry1B.868/ml diet / 10 µg Cry1B.868/ml diet) * 100 = 98.2%

These data demonstrate that the Cry1B.868 protein behaves with a predictable tendency toward protein denaturation and loss of functional activity at elevated temperatures. Heat treatment is widely used in the preparation of foods containing components derived from maize grain. Therefore, it is reasonable to conclude that Cry1B.868 protein would not be consumed as an active protein in food products derived from MON 95379 due to standard processing practices that include heat treatment at or above 75ºC for the majority of foods derived from processed maize (Hammond and Jez, 2011).

For details, please refer to Appendix 12 ([redacted] 2020 (MSL0031013)).

Table 23. EC_{50} Values and 95% Confidence Limits (CI) for the Heat-treated Cry1B.868 Protein After 15 Minutes

Temperature	EC_{50} (µg Cry1B.868/ml diet)	95% CI (µg Cry1B.868/ml diet)
Control (wet ice)	0.18	0.15 – 0.21
25 ºC	0.18	0.13 – 0.24
37 ºC	0.085	0.0 – 0.17[1]
55 ºC	0.14	0.078 – 0.21
75 ºC	>10 [2]	N/A
95 ºC	>10 [2]	N/A

[1]Lower limit manually replace with "0" value.
[2]10 µg Cry1B.868/ml diet represents the highest concentration tested.

Table 24. EC_{50} Values and 95% Confidence Limits (CI) for the Heat-treated Cry1B.868 Protein After 30 Minutes

Temperature	EC_{50} (µg Cry1B.868/ml diet)	95% CI (µg Cry1B.868/ml diet)
Control (wet ice)	0.18	0.15 – 0.21
25 ºC	0.09	0.061 – 0.12
37 ºC	0.14	0.072 - 0.21
55 ºC	0.16	0.051 – 0.26
75 ºC	>10 [1]	N/A
95 ºC	>10 [1]	N/A

[1] 10 µg Cry1B.868/ml diet represents the highest concentration tested.

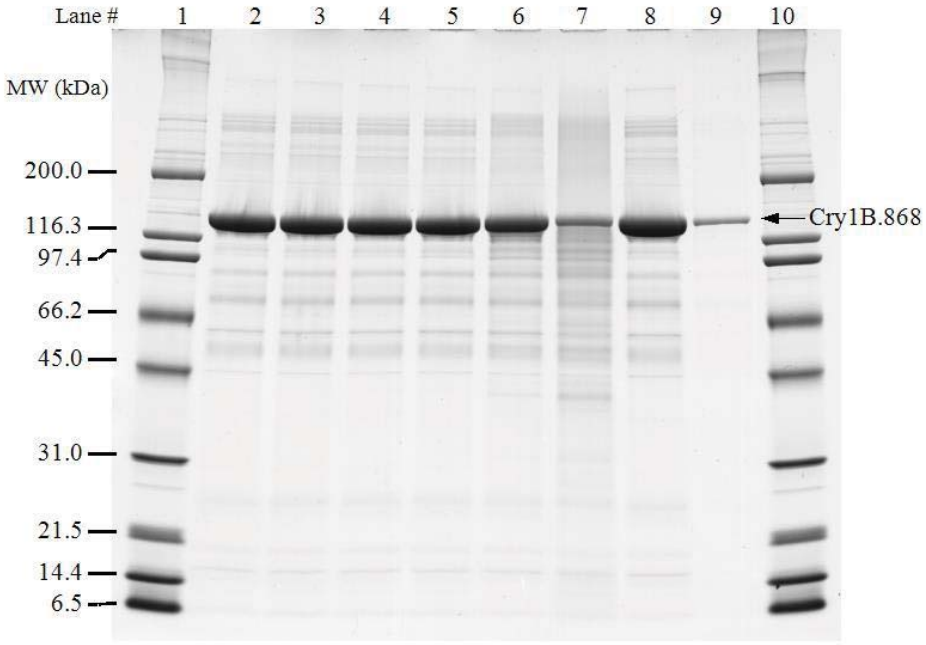

Figure 39. SDS-PAGE of Cry1B.868 Protein Demonstrating the Effect After 15 Minutes at Elevated Temperatures on Protein Structural Stability

Heat-treated samples of Cry1B.868 (3.0 µg total protein) separated on a Tris-glycine 4-20 % polyacrylamide gel under denaturing and reducing conditions. The gel was stained with Brilliant Blue G Colloidal. Approximate molecular weights (kDa) are shown on the left and correspond to molecular weight markers in lanes 1 and 10.

Lane	Description	Total Amount
1	Broad Range Molecular Weight Markers	5.0 µg
2	Cry1B.868 Protein Control	3.0 µg
3	Cry1B.868 Protein 25ºC	3.0 µg
4	Cry1B.868 Protein 37ºC	3.0 µg
5	Cry1B.868 Protein 55ºC	3.0 µg
6	Cry1B.868 Protein 75ºC	3.0 µg
7	Cry1B.868 Protein 95ºC	3.0 µg
8	Cry1B.868 Protein Reference 100% Equivalence	3.0 µg
9	Cry1B.868 Protein Reference 10% Equivalence	0.3 µg
10	Broad Range Molecular Weight Markers	5.0 µg

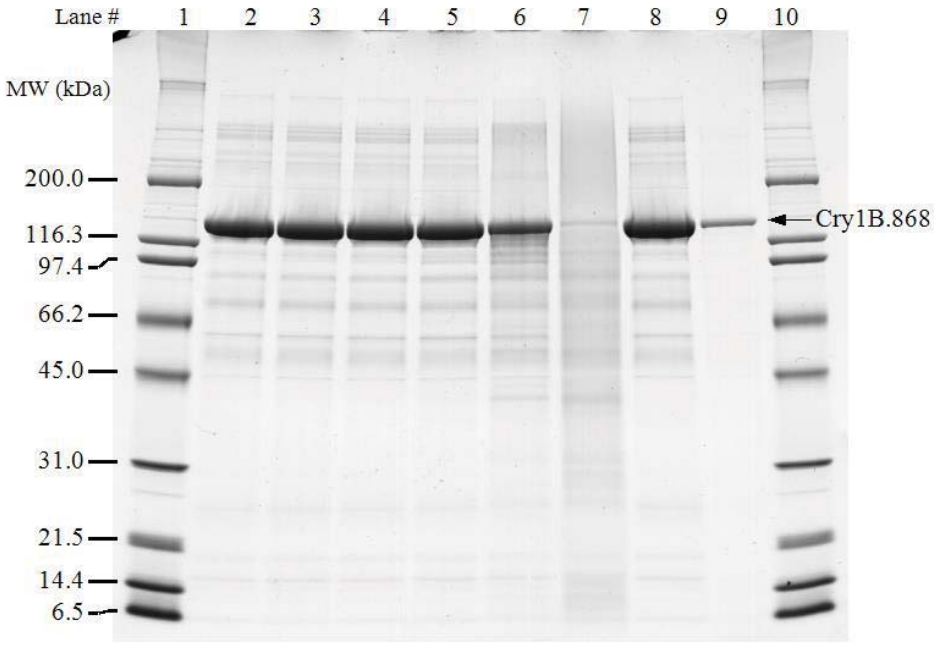

Figure 40. SDS-PAGE of Cry1B.868 Protein Demonstrating the Effect After 30 Minutes at Elevated Temperatures on Protein Structural Stability

Heat-treated samples of Cry1B.868 (3.0 µg total protein) separated on a Tris-glycine 4-20 % polyacrylamide gel under denaturing and reducing conditions. The gel was stained with Brilliant Blue G Colloidal. Approximate molecular weights (kDa) are shown on the left and correspond to molecular weight markers in lanes 1 and 10.

Lane	Description	Total Amount
1	Broad Range Molecular Weight Markers	5.0 µg
2	Cry1B.868 Protein Control	3.0 µg
3	Cry1B.868 Protein 25ºC	3.0 µg
4	Cry1B.868 Protein 37ºC	3.0 µg
5	Cry1B.868 Protein 55ºC	3.0 µg
6	Cry1B.868 Protein 75ºC	3.0 µg
7	Cry1B.868 Protein 95ºC	3.0 µg
8	Cry1B.868 Protein Reference 100% Equivalence	3.0 µg
9	Cry1B.868 Protein Reference 10% Equivalence	0.3 µg
10	Broad Range Molecular Weight Markers	5.0 µg

B.2(b)(iii)(ii) Heat susceptibility of Cry1Da_7 protein

The effect of heat treatment on the activity of the *Bt*-produced Cry1Da_7 protein was evaluated using purified protein. Heat treated samples and an unheated control sample of Cry1Da_7 protein were analyzed: 1) using an insect bioassay to assess the impact of temperature on the functional activity of the Cry1Da_7 protein; and 2) using SDS-PAGE to assess the impact of temperature on protein integrity.

Aliquots of Cry1Da_7 protein were heated to 25, 37, 55, 75 and 95 ºC for either 15 or 30 minutes, while a separate aliquot of Cry1Da_7 protein was maintained on ice for the duration of the heat treatments to serve as a temperature control. The effect of heat treatment on the activity of Cry1Da_7 was evaluated using a insect bioassay (Appendix 13). The effect of heat treatment on the integrity of the Cry1Da_7 protein was evaluated using SDS-PAGE analysis of the heated and temperature control Cry1Da_7 protein samples.

Results of the functional activity assay for Cry1Da_7 protein incubated for 15 and 30 minutes are listed in Table 25 and Table 26, respectively. The control sample had an EC_{50} of 0.16 µg Cry1Da_7 protein/ml diet, thus demonstrating that protein activity was maintained during incubation on ice. Protein activity was retained when incubated for 15 and 30 minutes at a temperature of 25, 37 and 55ºC. Incubation for 15 minutes at 75°C resulted in an estimated EC_{50} of 9.6 µg Cry1Da_7 protein/ml which represents a > 98% reduction in functional activity of the Cry1Da_7 protein when compared to the control[1]. For the 30 minute heat treatment at 75°C and the 15 and 30 minute heat treatments at 95°C, the estimated EC_{50} values were > 10 µg Cry1Da_7 protein/ml diet, which represents a reduction in functional activity of > 98% when compared to the control[2]. These results suggest that temperature has a considerable effect on the activity of Cry1Da_7.

The results of the SDS-PAGE analysis of the heat-treated samples incubated for 15 and 30 minutes are illustrated in Figure 41 and Figure 42, respectively. The control sample loaded on each gel (Figure 41 and Figure 42, lane 2) showed equivalent band intensity to the 100% reference standard (Figure 41 and Figure 42, lane 8), demonstrating that the Cry1Da_7 protein was stable on wet ice during the incubation period. No apparent decrease in band intensity of the ~126.5 kDa Cry1Da_7 protein was observed in the test samples when heated at temperatures of 25, 37 and 55°C for 15 or 30 minutes. A decrease in the intensity of the main Cry1Da_7 band was evident at 75°C with the most prominent loss of band intensity observed at 30 minutes. In addition, degradation and aggregation products were also evident at 75°C for both the 15 and 30 heat treatments. Incubation for 15 minutes at 95°C resulted in a significant loss of the Cry1Da_7 band intensity with less than 10% remaining as compared to the 10% reference standard. Incubation for 30 minutes at 95°C resulted in complete loss of the Cry1Da_7 band. Additionally, both the 15 and 30 minute heat treatments at 95°C exhibited increased smaller molecular weight degradation and higher molecular weight aggregation.

These data demonstrate that the Cry1Da_7 protein remains largely intact but behaves with a predictable tendency toward protein denaturation and loss of functional activity at elevated temperatures. Heat treatment is widely used in the preparation of foods containing components derived from maize grain. Therefore, it is reasonable to conclude that

[1] EC_{50} = 9.6 µg Cry1Da_7/ml diet represents a loss of activity: 1 – (0.16 µg Cry1Da_7/ml diet / 9.6 µg Cry1Da_7/ml diet) * 100 = 98.3%

[2] EC_{50} > 10 µg Cry1Da_7/ml diet represents a loss of activity: 1 – (0.16 µg Cry1Da_7/ml diet / 10 µg Cry1Da_7/ml diet) * 100 = 98.4%

Cry1Da_7 protein would not be consumed as an active protein in food products derived from MON 95379 due to standard processing practices that include heat treatment at or above 75ºC for the majority of foods derived from processed maize (Hammond and Jez, 2011).

For details, please refer to Appendix 13 ([redacted]2020 (TRR0000145)).

Table 25. EC_{50} Values and 95% Confidence Limits (CI) for the Heat Treated Cry1Da_7 Protein After 15 Minutes

Temperature	EC_{50} (µg Cry1Da_7/ml diet)	95% CI (µg Cry1Da_7/ml diet)
0 ºC (control)	0.16	0.14 – 0.18
25 ºC	0.11	0.086 – 0.13
37 ºC	0.16	0.11 – 0.22
55 ºC	0.12	0.097 – 0.14
75 ºC	9.6	0 - 25[1]
95 ºC	>10[2]	N/A

[1]Lower limit manually replaced with "0" value.
[2]10 µg Cry1Da_7/ml diet represents the highest concentration tested.

Table 26. EC_{50} Values and 95% Confidence Limits (CI) for the Heat Treated Cry1Da_7 Protein After 30 Minutes

Temperature	EC_{50} (µg Cry1Da_7/ml diet)	95% CI (µg Cry1Da_7/ml diet)
0 ºC (control)	0.16	0.14 – 0.18
25 ºC	0.12	0.096 – 0.14
37 ºC	0.071	0.044 - 0.098
55 ºC	0.13	0.10 – 0.17
75 ºC	>10[1]	N/A
95 ºC	>10[1]	N/A

[1] 10 µg Cry1Da_7/ml diet represents the highest concentration tested.

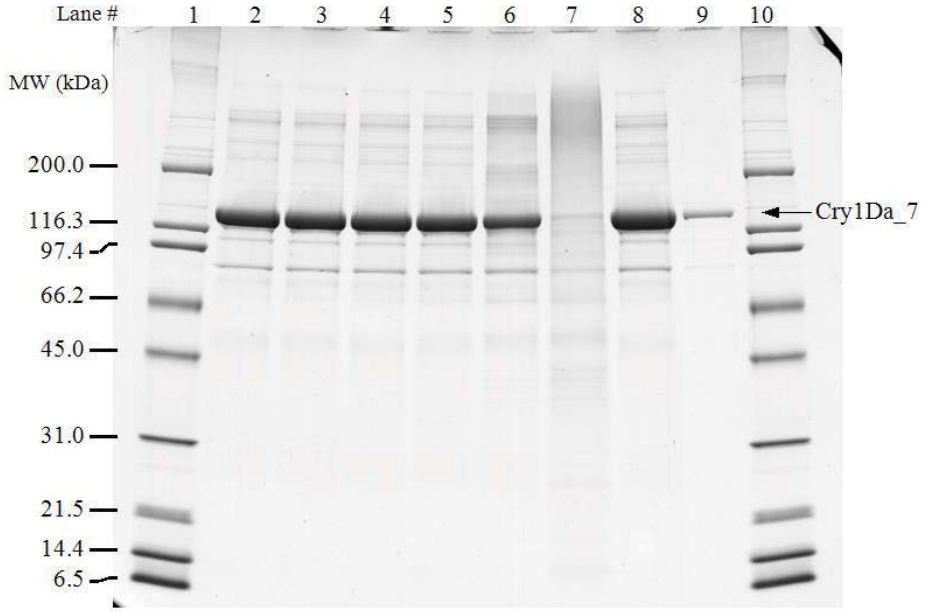

Figure 41. SDS-PAGE of Cry1Da_7 Protein Demonstrating the Effect After 15 Minutes at Elevated Temperatures on Protein Structural Stability

Heat-treated samples of *Bt*-produced Cry1Da_7 (3.0 µg total protein) separated on a Tris-glycine 4-20 % polyacrylamide gel under denaturing and reducing conditions. The gel was stained with Brilliant Blue G Colloidal. Approximate molecular weights (kDa) are shown on the left and correspond to molecular weight markers in lanes 1 and 10.

Lane	Description	Total Amount
1	Broad Range Molecular Weight Markers	5.0 µg
2	Cry1Da_7 Protein Control	3.0 µg
3	Cry1Da_7 Protein 25ºC	3.0 µg
4	Cry1Da_7 Protein 37ºC	3.0 µg
5	Cry1Da_7 Protein 55ºC	3.0 µg
6	Cry1Da_7 Protein 75ºC	3.0 µg
7	Cry1Da_7 Protein 95ºC	3.0 µg
8	Cry1Da_7 Protein Reference 100% Equivalence	3.0 µg
9	Cry1Da_7 Protein Reference 10% Equivalence	0.3 µg
10	Broad Range Molecular Weight Markers	5.0 µg

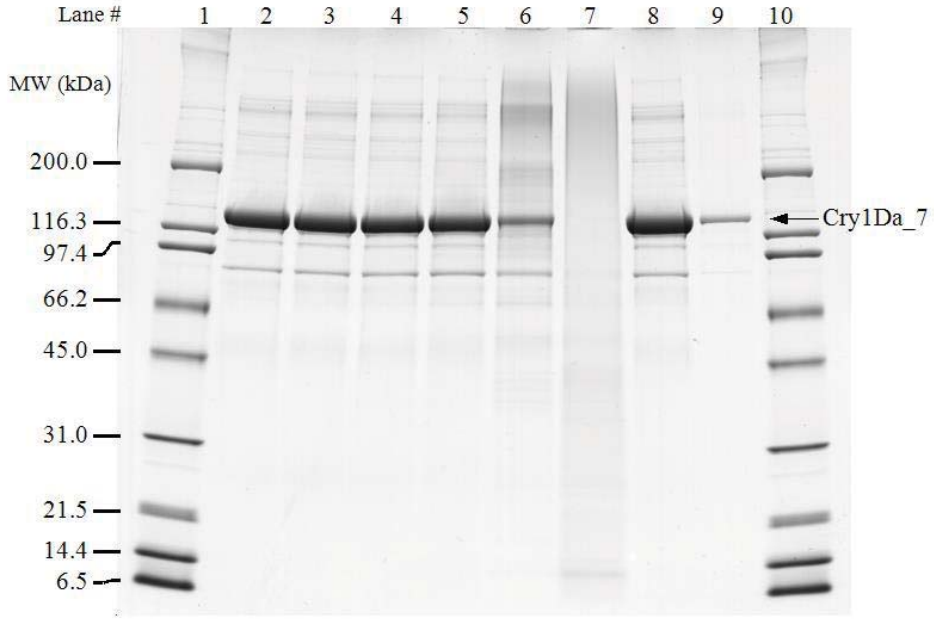

Figure 42. SDS-PAGE of Cry1Da_7 Protein Demonstrating the Effect After 30 Minutes at Elevated Temperatures on Protein Structural Stability

Heat-treated samples of *Bt*-produced Cry1Da_7 (3.0 µg total protein) separated on a Tris-glycine 4-20 % polyacrylamide gel under denaturing and reducing conditions. The gel was stained with Brilliant Blue G Colloidal. Approximate molecular weights (kDa) are shown on the left and correspond to molecular weight markers in lanes 1 and 10.

Lane	Description	Total Amount
1	Broad Range Molecular Weight Markers	5.0 µg
2	Cry1Da_7 Protein Control	3.0 µg
3	Cry1Da_7 Protein 25ºC	3.0 µg
4	Cry1Da_7 Protein 37ºC	3.0 µg
5	Cry1Da_7 Protein 55ºC	3.0 µg
6	Cry1Da_7 Protein 75ºC	3.0 µg
7	Cry1Da_7 Protein 95ºC	3.0 µg
8	Cry1Da_7 Protein Reference 100% Equivalence	3.0 µg
9	Cry1Da_7 Protein Reference 10% Equivalence	0.3 µg
10	Broad Range Molecular Weight Markers	5.0 µg

Degradation and Heat Susceptibility of the MON 95379 Cry1B.868 and Cry1Da_7 Proteins – Conclusions

The susceptibility of a protein to heat or its degradation in the presence of pepsin and pancreatin is a factor in the assessment of its potential toxicity. The degradation of Cry1B.868 and Cry1Da_7 proteins were evaluated by incubation with solutions containing pepsin and pancreatin, and the results show that Cry1B.868 and Cry1Da_7 proteins were readily degraded (Sections B.2(a)(ii)(i) and B.2(a)(ii)(ii), respectively). Exposure to heat during food processing or cooking, and to digestive fluids is likely to have a profound effect on the structure and function of proteins.

The effect of heat treatment on the activity of Cry1B.868 and Cry1Da_7 proteins was evaluated using insect bioassays to assess the impact of temperature on functional activity, and using SDS-PAGE to assess the impact of temperature on protein integrity. The results show that Cry1B.868 protein was completely deactivated by heating at 75ºC or higher for 15 min or more (Section B.2(b)(iii)(i)) and Cry1Da_7 protein was substantially deactivated by heating at 75ºC or above for 15 min or more (Section B.2(b)(iii)(ii)). Therefore, it is anticipated that exposure to functionally active Cry1B.868 and Cry1Da_7 protein from the consumption of MON 95379 or foods derived from MON 95379 is unlikely.

B.2(b)(iv) Specific serum screening where a new protein is derived from a source known to be allergenic or has sequence homology with a know allergen

Not relevant for this product.

B.2(b)(v) Information on whether the new protein(s) have a role in the elicitation of gluten-sensitive enteropathy, in cases where the introduced genetic material is obtained from wheat, rye, barley, oats, or related cereal grains

Not relevant for this product.

B.3 Other (non-protein) New Substances

Not applicable.

B.4 Novel Herbicide Metabolites in GM Herbicide-Tolerant Plants

Not applicable.

B.5 Compositional Assessment

For MON 95379, the introduced Cry1B.868 and Cry1Da_7 proteins confer protection from lepidopteran pests and lack catalytic activity that is intended or expected to affect the plant's metabolism. Given the nature of these introduced traits and the overall lack of meaningful unintended compositional characteristics observed for biotechnology-derived products characterized to date, compositional changes that would affect the levels of nutritional components in MON 95379 maize were not expected.

Food and Feed safety assessments of biotechnology-derived crops follow the comparative safety assessment process (Codex Alimentarius, 2009) in which the composition of grain and/or other raw agricultural commodities of the biotechnology-derived crop are compared to the appropriate conventional control that has a history of safe use. For maize, assessments are

performed using the general principles outlined in the OECD consensus document for maize composition (OECD, 2002a).

A review of compositional assessments conducted according to OECD guidelines, that encompassed a total of seven biotechnology-derived crop varieties, nine countries, and eleven growing seasons, concluded that incorporation of biotechnology-derived agronomic traits has had little impact on natural variation in crop composition. Most compositional variation is attributable to growing region, agronomic practices, and genetic background (Harrigan *et al.*, 2010; Zhou *et al.*, 2011). Numerous scientific publications have further documented the extensive variability in the concentrations of crop nutrients, anti-nutrients, and secondary metabolites that reflect the influence of environmental and genetic factors as well as extensive conventional breeding efforts to improve nutrition, agronomics, and yield (Ridley *et al.*, 2011; Taylor *et al.*, 2017; Venkatesh *et al.*, 2014; Zhou *et al.*, 2011).

Compositional equivalence between biotechnology-derived and conventional crops supports an "equal or increased assurance of the safety of foods derived from genetically modified plants" (OECD, 2002b). OECD consensus documents on compositional considerations for new crop varieties emphasize quantitative measurements of essential nutrients and known anti-nutrients or toxicants. These quantitative measurements effectively discern compositional changes that imply potential nutritional or safety (e.g., anti-nutritional) concerns. Levels of the components in grain and/or other raw agricultural commodities of the biotechnology-derived crop product are compared to: 1) corresponding levels in a conventional comparator, a genetically similar conventional line, grown concurrently under similar field conditions, and 2) natural ranges from data published in the scientific literature or in publicly available databases (e.g. ILSI[12] Crop Composition Database, (ILSI, 2019)). This second comparison places any potential differences between the assessed biotechnology-derived crop and its comparator in the context of the well-documented variation in the concentrations of crop nutrients, anti-nutrients and secondary metabolites.

This section provides analyses to measure the levels of nutrients, anti-nutrients and secondary metabolites in grain, as well as, nutrients in forage of MON 95379 compared to that of a conventional control maize (LH244 x HCL617) grown and harvested under representative environmental condition under which MON 95379 will be grown. The production of materials for compositional analyses used a sufficient variety of field trial sites, reflecting a range of environmental conditions under which MON 95379 is expected to be grown and robust experimental field designs (randomized complete block design with four replicates). Samples were subjected to sensitive analytical methods that allow quantitative and accurate measurements of components. The information provided in this section addresses relevant factors in Codex Plant Guidelines, Section 4, paragraphs 44 and 45 for compositional analyses (Codex Alimentarius, 2009).

[12] Effective May 1, 2020, the ILSI RF publishing the CCDB became an unaffiliated non-profit scientific organization, no longer part of the ILSI federation, and changed its name to Agriculture and Food Systems Institute (AFSI). There is no change to the current structure or function of the CCDB, only name change: AFSI CCDB. The CCDB working group and their website still the same https://www.cropcomposition.org/

B.5(a) Levels of key nutrients, toxicants and anti-nutrients in the food produced using gene technology compared with the levels in an appropriate comparator

Grain and forage samples were harvested from MON 95379 and a conventional control grown at a total of five sites (Boone County, Iowa (IAOG); Jefferson County, Iowa (IARL); Clinton County, Illinois (ILHY); York County, Nebraska (NEYO); and Miami County, Ohio (OHTR)) in the United States during 2018. The field sites were planted in a randomized complete block design with four replicates per site. MON 95379_and the conventional control were grown under agronomic field conditions typical for each of the different growing regions. The compositional analysis provided a comprehensive comparative assessment of the levels of nutrients, anti-nutrients and secondary metabolites in grain, as well as, nutrients in forage of MON 95379 and the conventional control.

The evaluation of MON 95379 followed considerations relevant to the compositional quality of maize as defined by the OECD consensus document on maize (OECD, 2002a). Harvested grain samples were assessed for moisture and levels of nutrients, including proximates (protein, total fat and ash), amino acids (18 components), fatty acids (22 components), carbohydrates by calculation, fiber (ADF, NDF, and TDF), minerals (calcium, copper, iron, magnesium, manganese, phosphorus, potassium, sodium and zinc) and vitamins (vitamin A, vitamin B_1, vitamin B_2, vitamin B_3, vitamin B_6, vitamin B_9 and vitamin E). Grain samples were assessed for levels of other components including anti-nutrients (phytic acid and raffinose) and secondary metabolites (ferulic acid, furfural and p-coumaric acid). Harvested forage samples were assessed for moisture and levels of nutrients including proximates (protein, total fat, and ash), carbohydrates by calculation, fiber (ADF and NDF) and minerals (calcium and phosphorus). In all, 78 different components were analyzed.

Of the 78 measured components, 15 components in grain (caprylic acid, capric acid, lauric acid, myristic acid, myristoleic acid, pentadecanoic acid, pentadecenoic acid, heptadecanoic acid, heptadecenoic acid, gamma linolenic acid, eicosadienoic acid, eicosatrienoic acid, arachidonic acid, sodium and furfural) had more than 50% of the observations below the assay limit of quantitation (LOQ), and were excluded from statistical analysis. Moisture values for grain and forage were measured for conversion of components from fresh to dry weight, but were not statistically analyzed. Therefore, 61 components were statistically analyzed for all samples (53 in grain and 8 in forage).

The statistical comparison of MON 95379 and the conventional control was performed on compositional data that was combined across all field sites. Statistically-significant differences were identified at the 5% level ($\alpha = 0.05$). A statistically-significant difference between MON 95379 and the conventional control does not necessarily imply biological relevance from a food and feed perspective. Therefore, statistically-significant differences observed between MON 95379 and the conventional control were evaluated further to determine whether the detected difference indicated a biologically relevant compositional change or supported a conclusion of compositional equivalence, as follows:

Step 1 – Determination of the Magnitude of Difference between MON 95379 and Conventional Control Means

The difference in mean values between MON 95379 and the conventional control was determined for use in subsequent steps. In addition, for protein and amino acids only, the relative magnitude of the difference (percent change relative to the control) between MON 95379 and the conventional control was determined to allow an assessment of any observed difference in amino acids in relation to the difference in protein.

Step 2 – Assessment of the Difference in the Context of Natural Variation within the Conventional Control across Multiple Sites

The relative impact of MON 95379 was evaluated in the context of variation within the conventional control germplasm grown across multiple sites (i.e., variation due to environmental influence). This assesses the mean difference between MON 95379 and the conventional control in the context of the range of replicate values for the conventional control (range value = maximum value minus the minimum value). When a mean difference is less than the variability seen due to natural environmental variation within the single, closely related germplasm, the difference is typically not a food or feed safety concern (Venkatesh *et al.*, 2014).

Step 3 – Assessment of the Difference in the Context of Natural Variation Due to Multiple Factors

The relative impact of MON 95379 on composition was evaluated in the context of sources of natural variation such as environmental and germplasm influences. This assessment determined whether the component mean value of MON 95379 was within the natural variability defined by the literature values or the ILSI Crop Composition Database (ILSI-CCDB, Table 34) values. This naturally occurring variability is important in assessing the biological relevance to food and feed safety of statistically-significant differences in composition between MON 95379 and the conventional control.

These evaluations of natural variation are important as crop composition is known to be greatly influenced by environment and variety (Harrigan *et al.*, 2010). Although used in the comparative assessment process, detection of statistically-significant differences between MON 95379 and the conventional control mean values does not imply a meaningful contribution by MON 95379 to compositional variability. Only if the impact of MON 95379 on levels of components was large relative to natural variation inherent to conventional maize would further assessments be required to establish whether the change in composition would have an impact from a food and feed safety and nutritional perspective. The steps reviewed in this assessment, therefore, describe the process for determining whether any statistically-significant differences observed between MON 95379 and the conventional control are meaningful from a food and feed perspective or whether they support a conclusion of compositional equivalence.

Results of compositional analysis of MON 95379 grain and forage compared to conventional maize

Compositional analysis was conducted on grain and forage of MON 95379 and a conventional control grown at five sites in the U.S. during 2018. In all, 78 different analytical components were measured. Of these, 15 components had more than 50% of the observations below the assay limit of quantitation (LOQ) and were excluded from statistical analysis. Moisture values for grain and forage were measured for conversion of components to dry weight but were not statistically analyzed. There were no statistically significant differences ($p<0.05$) for 43 of the 61 components analyzed (Table 28 to Table 33). There were 18 components in grain (protein, alanine, glutamic acid, isoleucine, leucine, methionine, phenylalanine, serine, threonine, valine, linolenic acid, carbohydrates by calculation, copper, iron, manganese, phosphorus, zinc and vitamin A) that showed a statistically significant difference ($p<0.05$) between MON 95379 and the conventional control. No statistical differences ($p<0.05$) were observed for forage analytes.

For protein, the difference was 0.43% dw (Table 27). As shown in Table 27, the magnitude of difference for protein between MON 95379 and the conventional control was less than the corresponding conventional control range value. This indicates that MON 95379 does not impact levels of this component more than the natural variation within the conventional control grown at multiple locations. The mean level of protein was within the natural variability of this component as published in the scientific literature on maize composition and/or the ILSI-CCDB (Table 34).

For nine amino acids (alanine, glutamic acid, isoleucine, leucine, methionine, phenylalanine, serine, threonine, and valine) the mean difference between MON 95379 and the control were between 0.011 and 0.096% dw (Table 27). As shown in Table 27, the magnitude of differences for alanine, glutamic acid, isoleucine, leucine, methionine, phenylalanine, serine, threonine, and valine between MON 95379 and the conventional control were less than the corresponding conventional control range values. This indicates that MON 95379 does not impact levels of these components more than the natural variation within the conventional control grown at multiple locations. In addition, the mean levels of these nine amino acids were all within the natural variability of these components as published in the scientific literature on maize composition and/or the ILSI-CCDB (Table 34).

For copper, iron, zinc, manganese, and phosphorus the mean differences between MON 95379 and the control were 0.18 mg/kg dw, 0.81 mg/kg dw, 1.46 mg/kg dw, 0.62 mg/kg dw and 0.010% dw, respectively (Table 30). As shown in Table 30, the magnitude of differences for copper, iron, zinc, manganese, and phosphorus between MON 95379 and the conventional control were slightly less than the corresponding conventional control range values. This indicates that MON 95379 does not impact levels of these components more than the natural variation within the conventional control grown at multiple locations. The mean levels of copper, iron, zinc, manganese, and phosphorus were within the natural variability of these components as published in the scientific literature on maize composition and/or the ILSI-CCDB (Table 34).

For linolenic acid, the difference was -0.023% Total Fatty Acid (Table 28). As shown in Table 28, the magnitude of the difference for linolenic acid between MON 95379 and the conventional control was less than the corresponding conventional control range value. This indicates that MON 95379 does not impact the level of this components more than the natural variation within the conventional control grown at multiple locations. The mean level of lenolenic acid was within the natural variability of this component as published in the scientific literature on maize composition and/or the ILSI-CCDB (Table 34).

For carbohydrates by calculation, the difference was -0.50% dw (Table 28). As shown in Table 28, the magnitude of the difference for carbohydrates by calculation between MON 95379 and the conventional control was less than the corresponding conventional control range value. This indicates that MON 95379 does not impact the level of this component more than the natural variation within the conventional control grown at multiple locations. The mean level of carbohydrates by calculation was within the natural variability of this component as published in the scientific literature on maize composition and/or the ILSI-CCDB (Table 34).

For vitamin A, the difference was 0.082 mg/kg dw (Table 31). As shown in Table 31, the magnitude of the difference for vitamin A between MON 95379 and the conventional control was less than the corresponding conventional control range value. This indicates that MON 95379 does not impact levels of this components more than the natural variation within the conventional control grown at multiple locations. The mean level of vitamin A was

within the natural variability of this component as published in the scientific literature on maize composition and/or the ILSI-CCDB (Table 34).

These data indicate that the statistically significant differences observed were not biologically meaningful from a food and feed safety perspective. These results support the conclusion that MON 95379 was not a major contributor to variation in component levels in maize grain or forage and confirmed the compositional equivalence of MON 95379 to the conventional control in levels nutrients, anti-nutrients, and secondary metabolites in grain, as well as, nutrients in forage.

For details, please refer to Appendix 14 ([redacted]2019 (MSL0030947)).

Table 27. Summary of Maize Grain Protein and Amino Acids for MON 95379 and the Conventional Control

Component (% dw)[1]	MON 95379 Mean (S.E.)[2] Range	Control Mean (S.E.) Range	Control Range Value[3]	Difference (MON 95379 minus Control) Mean (S.E.)	*p*-Value	% Relative[4]
Protein	9.61 (0.56) 7.97 - 12.47	9.18 (0.56) 7.54 - 11.58	4.04	0.43 (0.16)	0.012	4.70
Alanine	0.75 (0.051) 0.59 - 1.02	0.71 (0.051) 0.56 - 0.93	0.37	0.035 (0.015)	0.027	4.99
Arginine	0.48 (0.019) 0.40 - 0.56	0.46 (0.019) 0.40 - 0.53	0.13	0.016 (0.0082)	0.062	3.53
Aspartic acid	0.60 (0.030) 0.53 - 0.76	0.59 (0.030) 0.50 - 0.71	0.22	0.017 (0.0085)	0.057	2.94
Cystine	0.22 (0.010) 0.17 - 0.28	0.21 (0.010) 0.18 - 0.25	0.070	0.0060 (0.0048)	0.220	2.86
Glutamic acid	1.80 (0.13) 1.41 - 2.51	1.71 (0.13) 1.36 - 2.28	0.92	0.096 (0.035)	0.012	5.65

Table 27. Summary of Maize Grain Protein and Amino Acids for MON 95379 and the Conventional Control (Continued)

Component (% dw)[1]	MON 95379 Mean (S.E.)[2] Range	Control Mean (S.E.) Range	Control Range Value[3]	Difference (MON 95379 minus Control) Mean (S.E.)	*p*-Value	% Relative[4]
Glycine	0.37 (0.013) 0.32 - 0.43	0.36 (0.013) 0.31 - 0.41	0.095	0.0085 (0.0054)	0.130	2.39
Histidine	0.25 (0.013) 0.20 - 0.32	0.25 (0.013) 0.21 - 0.31	0.11	0.0063 (0.0048)	0.204	2.54
Isoleucine	0.34 (0.023) 0.28 - 0.45	0.33 (0.023) 0.27 - 0.43	0.16	0.015 (0.0059)	0.019	4.61
Leucine	1.24 (0.10) 0.93 - 1.74	1.17 (0.10) 0.91 - 1.62	0.71	0.070 (0.026)	0.012	5.99
Lysine	0.26 (0.0062) 0.21 - 0.30	0.26 (0.0062) 0.22 - 0.31	0.087	0.0011 (0.0067)	0.874	0.41
Methionine	0.22 (0.013) 0.18 - 0.29	0.21 (0.013) 0.17 - 0.27	0.098	0.012 (0.0042)	0.008	5.87

Table 27. Summary of Maize Grain Protein and Amino Acids for MON 95379 and the Conventional Control (Continued)

Component (% dw)[1]	MON 95379 Mean (S.E.)[2] Range	Control Mean (S.E.) Range	Control Range Value[3]	Difference (MON 95379 minus Control) Mean (S.E.)	*p*-Value	% Relative[4]
Phenylalanine	0.49 (0.035) 0.40 - 0.67	0.47 (0.035) 0.38 - 0.63	0.25	0.023 (0.0093)	0.025	4.87
Proline	0.88 (0.055) 0.71 - 1.15	0.86 (0.055) 0.69 - 1.07	0.38	0.028 (0.015)	0.138	3.22
Serine	0.48 (0.029) 0.40 - 0.65	0.45 (0.029) 0.37 - 0.56	0.19	0.024 (0.0085)	0.009	5.40
Threonine	0.34 (0.018) 0.30 - 0.44	0.33 (0.018) 0.28 - 0.41	0.12	0.011 (0.0052)	0.048	3.30
Tryptophan	0.077 (0.0036) 0.065 - 0.097	0.074 (0.0036) 0.066 - 0.090	0.025	0.0027 (0.0013)	0.106	3.69
Tyrosine	0.42 (0.027) 0.35 - 0.57	0.40 (0.027) 0.33 - 0.51	0.17	0.020 (0.0084)	0.073	5.05
Valine	0.45 (0.024) 0.39 - 0.57	0.43 (0.024) 0.36 - 0.53	0.17	0.016 (0.0076)	0.038	3.81

[1]dw=dry weight
[2] Mean (S.E.) = least-square mean (standard error) obtained from the linear mixed model analysis
[3]Maximum value minus minimum value for the control maize hybrid
[4]The relative magnitude of the difference in mean values between MON 95379 and the control, expressed as a percent of the control.

Table 28. Summary of Maize Grain Total Fat and Fatty Acids for MON 95379 and the Conventional Control

Component	MON 95379 Mean (S.E.)[1] Range	Control Mean (S.E.) Range	Control Range Value[2]	Difference (MON 95379 minus Control) Mean (S.E.)	*p*-Value
Total fat (% dw)[3]	3.86 (0.038) 3.69 - 4.08	3.80 (0.038) 3.59 - 4.06	0.47	0.059 (0.039)	0.204
Palmitic acid (% Total FA)[4]	12.69 (0.11) 12.31 - 13.06	12.79 (0.11) 12.15 - 13.58	1.43	-0.097 (0.080)	0.290
Palmitoleic acid (% Total FA)	0.13 (0.0020) 0.12 - 0.14	0.13 (0.0020) 0.12 - 0.14	0.026	-0.00093 (0.0017)	0.593
Stearic acid (% Total FA)	1.64 (0.027) 1.54 - 1.76	1.66 (0.027) 1.58 - 1.81	0.24	-0.023 (0.013)	0.092
Oleic acid (% Total FA)	28.31 (0.23) 27.17 - 29.45	28.41 (0.23) 27.77 - 29.50	1.74	-0.10 (0.13)	0.465
Linoleic acid (% Total FA)	55.24 (0.37) 53.67 - 56.93	54.99 (0.37) 52.94 - 56.19	3.26	0.25 (0.16)	0.126

Table 28. Summary of Maize Grain Total Fat and Fatty Acids for MON 95379 and the Conventional Control (Continued)

			Difference (MON 95379 minus Control)		
Component	MON 95379 Mean (S.E.)[1] Range	Control Mean (S.E.) Range	Control Range Value[2]	Mean (S.E.)	*p*-Value
Linolenic acid (% Total FA)	1.15 (0.016) 1.09 - 1.22	1.17 (0.016) 1.11 - 1.27	0.17	-0.023 (0.0091)	0.022
Arachidic acid (% Total FA)	0.41 (0.0084) 0.39 - 0.45	0.41 (0.0084) 0.39 - 0.45	0.061	-0.0046 (0.0037)	0.222
Eicosenoic acid (% Total FA)	0.26 (0.0023) 0.25 - 0.28	0.26 (0.0023) 0.25 - 0.28	0.033	-0.00042 (0.0024)	0.864
Behenic acid (% Total FA)	0.16 (0.0047) 0.15 - 0.19	0.17 (0.0047) 0.15 - 0.18	0.039	-0.0042 (0.0021)	0.052

[1]Mean (S.E.) = least-square mean (standard error) obtained from the linear mixed model analysis
[2]Maximum value minus minimum value for the control maize hybrid
[3]dw=dry weight
[4]FA=Fatty Acid
The following components with more than 50% of observations below the assay LOQ were excluded from statistical analysis: caprylic acid, capric acid, lauric acid, myristic acid, myristoleic acid, pentadecanoic acid, pentadecenoic acid, heptadecanoic acid, heptadecenoic acid, gamma linolenic acid, eicosadienoic acid, eicosatrienoic acid and arachidonic acid.

Table 29. Summary of Maize Grain Carbohydrates by Calculation and Fiber for MON 95379 and the Conventional Control

				Difference (MON 95379 minus Control)	
Component (% dw)[1]	MON 95379 Mean (S.E.)[2] Range	Control Mean (S.E.) Range	Control Range Value[3]	Mean (S.E.)	*p*-Value
Carbohydrates by calculation	85.23 (0.61) 82.24 - 87.10	85.73 (0.61) 83.22 - 87.53	4.31	-0.50 (0.16)	0.005
ADF	3.65 (0.098) 2.92 - 4.55	3.51 (0.098) 2.71 - 4.17	1.45	0.14 (0.12)	0.317
NDF	9.26 (0.15) 7.54 - 10.28	9.26 (0.15) 8.67 - 10.52	1.86	-0.0022 (0.22)	0.992
TDF	12.14 (0.22) 10.80 - 13.63	12.17 (0.22) 11.02 - 14.32	3.30	-0.024 (0.25)	0.928

[1]dw=dry weight
[2] Mean (S.E.) = least-square mean (standard error) obtained from the linear mixed model analysis
[3]Maximum value minus minimum value for the control maize hybrid

Table 30. Summary of Maize Grain Ash and Minerals for MON 95379 and the Conventional Control

				Difference (MON 95379 minus Control)	
Component	MON 95379 Mean (S.E.)[1] Range	Control Mean (S.E.) Range	Control Range Value[2]	Mean (S.E.)	*p*-Value
Ash (% dw)[3]	1.29 (0.024) 1.14 - 1.42	1.28 (0.024) 1.12 - 1.41	0.29	0.012 (0.022)	0.607
Calcium (% dw)	0.0033 (0.00013) 0.0026 - 0.0040	0.0033 (0.00013) 0.0027 - 0.0044	0.0017	0.00001 (0.00004)	0.885
Copper (mg/kg dw)	1.48 (0.095) 1.14 - 2.02	1.31 (0.095) 0.97 - 1.75	0.78	0.18 (0.058)	0.038
Iron (mg/kg dw)	17.16 (0.45) 14.38 - 19.63	16.35 (0.45) 14.48 - 18.72	4.24	0.81 (0.23)	0.001
Magnesium (% dw)	0.11 (0.0045) 0.090 - 0.13	0.10 (0.0045) 0.086 - 0.13	0.046	0.0027 (0.0016)	0.106
Manganese (mg/kg dw)	5.58 (0.43) 4.15 - 8.04	4.96 (0.43) 3.38 - 6.42	3.04	0.62 (0.17)	0.019
Phosphorus (% dw)	0.32 (0.0090) 0.27 - 0.34	0.31 (0.0090) 0.26 - 0.35	0.093	0.010 (0.0028)	0.001
Potassium (% dw)	0.37 (0.0072) 0.34 - 0.42	0.37 (0.0072) 0.34 - 0.42	0.078	0.0018 (0.0046)	0.704
Zinc (mg/kg dw)	19.40 (1.44) 14.95 - 23.92	17.93 (1.44) 13.85 - 22.42	8.57	1.46 (0.29)	<0.001

[1]Mean (S.E.) = least-square mean (standard error) obtained from the linear mixed model analysis
[2]Maximum value minus minimum value for the control maize hybrid
[3]dw=dry weight
The following components with more than 50% of observations below the assay LOQ were excluded from statistical analysis: sodium.

Table 31. Summary of Maize Grain Vitamins for MON 95379 and the Conventional Control

Component (mg/kg dw)[1]	MON 95379 Mean (S.E.)[2] Range	Control Mean (S.E.) Range	Control Range Value[3]	Difference (MON 95379 minus Control) Mean (S.E.)	*p*-Value
Vitamin A	1.11 (0.040) 0.97 - 1.42	1.03 (0.040) 0.85 - 1.15	0.30	0.082 (0.018)	<0.001
Vitamin B_1	4.05 (0.094) 3.58 - 4.53	3.99 (0.094) 3.55 - 4.35	0.80	0.060 (0.082)	0.506
Vitamin B_2	1.49 (0.059) 0.97 - 1.98	1.61 (0.059) 1.34 - 2.00	0.66	-0.11 (0.076)	0.210
Vitamin B_3	20.89 (1.45) 13.77 - 25.96	21.56 (1.45) 15.05 - 29.41	14.35	-0.67 (0.82)	0.461
Vitamin B_6	5.76 (0.085) 5.13 - 6.31	5.77 (0.085) 5.17 - 6.69	1.53	-0.013 (0.12)	0.913
Vitamin B_9	0.42 (0.031) 0.33 - 0.63	0.42 (0.031) 0.34 - 0.58	0.23	0.00034 (0.0087)	0.969
Vitamin E	13.67 (0.61) 11.14 - 16.10	13.31 (0.61) 10.37 - 14.81	4.44	0.36 (0.45)	0.467

[1]dw=dry weight;
Common names of vitamins: A=β-Carotene; B_1= Thiamine HCl; B_2=Riboflavin; B_3=Niacin; B_6= Pyridoxine HCl; B_9=Folic Acid; E=α-Tocopherol
[2]Mean (S.E.) = least-square mean (standard error) obtained from the linear mixed model analysis
[3]Maximum value minus minimum value for the control maize hybrid

Table 32. Summary of Maize Grain Anti-Nutrients and Secondary Metabolites for MON 95379 and the Conventional Control

				Difference (MON 95379 minus Control)	
Component	MON 95379 Mean (S.E.)[1] Range	Control Mean (S.E.) Range	Control Range Value[2]	Mean (S.E.)	*p*-Value
Phytic acid (% dw)[3]	0.74 (0.034) 0.46 - 0.91	0.70 (0.034) 0.49 - 0.92	0.43	0.045 (0.045)	0.351
Raffinose (% dw)	0.21 (0.014) 0.17 - 0.27	0.19 (0.014) 0.16 - 0.26	0.11	0.011 (0.0053)	0.105
Ferulic acid (µg/g dw)	1755.20 (35.29) 1515.50 - 1931.28	1806.81 (35.29) 1649.37 - 2007.04	357.68	-51.61 (38.62)	0.252
P-coumaric acid (µg/g dw)	117.16 (6.98) 98.12 - 164.18	121.01 (6.98) 90.40 - 190.53	100.13	-3.85 (4.28)	0.379

[1]Mean (S.E.) = least-square mean (standard error) obtained from the linear mixed model analysis
[2]Maximum value minus minimum value for the control maize hybrid
[3]dw=dry weight
The following components with more than 50% of observations below the assay LOQ were excluded from statistical analysis: furfural.

Table 33. Summary of Maize Forage Proximates, Carbohydrates by Calculation, Fiber and Minerals for MON 95379 and the Conventional Control

				Difference (MON 95379 minus Control)	
Component (% dw)[1]	MON 95379 Mean (S.E.)[2] Range	Control Mean (S.E.) Range	Control Range Value[3]	Mean (S.E.)	*p*-Value
Protein	6.95 (0.38) 5.52 - 8.69	6.64 (0.38) 4.68 - 9.01	4.32	0.32 (0.24)	0.203
Total fat	2.82 (0.12) 2.17 - 3.63	2.69 (0.12) 1.56 - 3.53	1.97	0.12 (0.15)	0.473
Carbohydrates by calculation	86.19 (0.58) 83.16 - 88.79	86.98 (0.58) 82.69 - 89.53	6.84	-0.79 (0.41)	0.064
ADF	22.04 (0.67) 18.18 - 28.00	21.26 (0.67) 16.83 - 25.04	8.22	0.78 (0.70)	0.282
NDF	34.07 (0.81) 27.29 - 43.83	33.99 (0.81) 27.87 - 40.38	12.51	0.080 (1.08)	0.941
Ash	4.02 (0.26) 2.71 - 6.27	3.72 (0.26) 2.46 - 4.87	2.41	0.29 (0.20)	0.155
Calcium	0.20 (0.019) 0.10 - 0.26	0.20 (0.019) 0.12 - 0.27	0.15	-0.0023 (0.0049)	0.646
Phosphorus	0.20 (0.0081) 0.16 - 0.24	0.19 (0.0081) 0.16 - 0.23	0.074	0.013 (0.0082)	0.182

[1]dw=dry weight
[2]Mean (S.E.) = least-square mean (standard error) obtained from the linear mixed model analysis
[3]Maximum value minus minimum value for the control maize hybrid

B.5(b) Information on the range of natural variation for each constituent measure to allow for assessment of biological significance

Table 34. Literature and ILSI Database Ranges for Components in Maize Grain and Forage

Tissue Components[1]	Literature Range[2]	ILSI Range[3]
Grain Nutrients		
Proximates		
protein (% dw)	8.27-13.33[a]; 9.17-12.19[b]	5.72-17.26
total fat (% dw)	2.95-4.40[a]; 3.18-4.23[b]	1.363-7.830
ash (% dw)	1.17-2.01[a]; 1.27-1.63[b]	0.616-6.282
Amino Acids		
alanine (% dw)	0.60-1.04[a]; 0.68-0.96[b]	0.40-1.48
arginine (% dw)	0.34-0.52[a]; 0.34-0.50[b]	0.12-0.71
aspartic acid (% dw)	0.52-0.78[a]; 0.59-0.76[b]	0.30-1.21
cystine (% dw)	0.19-0.26[a]; 0.20-0.26[b]	0.12-0.51
glutamic acid (% dw)	1.54-2.67[a]; 1.71-2.44[b]	0.83-3.54
glycine (% dw)	0.33-0.43[a]; 0.33-0.42[b]	0.184-0.685
histidine (% dw)	0.25-0.37[a]; 0.27-0.34[b]	0.14-0.46
isoleucine (% dw)	0.30-0.48[a]; 0.32-0.44[b]	0.18-0.69
leucine (% dw)	1.02-1.87[a]; 1.13-1.65[b]	0.60-2.49
lysine (% dw)	0.26-0.33[a]; 0.28-0.31[b]	0.129-0.668
methionine (% dw)	0.17-0.26[a]; 0.16-0.30[b]	0.11-0.47
phenylalanine (% dw)	0.43-0.72[a]; 0.45-0.63[b]	0.24-0.93
proline (% dw)	0.74-1.21[a]; 0.78-1.11[b]	0.46-1.75
serine (% dw)	0.39-0.67[a]; 0.43-0.6[b]	0.15-0.77
threonine (% dw)	0.29-0.45[a]; 0.31-0.39[b]	0.17-0.67
tryptophan (% dw)	0.047-0.085[a]; 0.042-0.07[b]	0.027-0.215
tyrosine (% dw)	0.13-0.43[a]; 0.12-0.41[b]	0.10-0.73
valine (% dw)	0.42-0.62[a]; 0.45-0.58[b]	0.27-0.86
Fatty Acids		
palmitic acid (% Total FA)	8.80-13.33[a]; 9.84-12.33[b]	6.81-26.55
palmitoleic acid (% Total FA)	0.059-0.23[a]	0.067-0.453
stearic acid (% Total FA)	1.36-2.14[a]; 1.3-2.1[b]	1.02-3.83
oleic acid (% Total FA)	19.50-33.71[a]; 19.59-29.13[b]	16.38-42.81
linoleic acid (% Total FA)	49.31-64.70[a]; 56.51-65.65[b]	34.27-67.68
linolenic acid (% Total FA)	0.89-1.56[a]; 1.03-1.38[b]	0.55-2.33
arachidic acid (% Total FA)	0.30-0.49[a]; 0.30-0.41[b]	0.267-0.993
eicosenoic acid (% Total FA)	0.17-0.29[a]; 0.17-0.27[b]	0.098-1.952
behenic acid (% Total FA)	0.069-0.28[a]; 0.059-0.18[b]	0.093-0.417
Carbohydrates By Calculation		
carbohydrates by calculation (% dw)	81.31-87.06[a]; 82.10-85.98[b]	77.4-89.7
Fiber		
ADF (% dw)	1.82-4.48[a]; 1.83-3.39[b]	1.41-11.34
NDF (% dw)	6.51-12.28[a]; 6.08-10.36[b]	4.28-24.30
TDF (% dw)	10.65-16.26[a]; 10.57-14.56[b]	5.78-35.31

Table 34. Literature and ILSI Database Ranges for Components in Maize Grain and Forage (Continued)

Tissue Components[1]	Literature Range[2]	ILSI Range[3]
Minerals		
calcium (% dw)	0.0036-0.0068[a]; 0.0035-0.007[b]	0.001-0.101
copper (mg/kg dw)	0.85-3.54[c]	0.55-21.20
iron (mg/kg dw)	14.17-23.40[a]; 15.90-24.66[b]	9.51-191.00
magnesium (% dw)	0.091-0.14[a]; 0.1-0.14[b]	0.06-0.19
manganese (mg/kg dw)	4.83-8.34[a]; 4.78-9.35[b]	1.69-14.30
phosphorus (% dw)	0.24-0.37[a]; 0.27-0.38[b]	0.13-0.55
potassium (% dw)	0.29-0.39[a]; 0.36-0.43[b]	0.18-0.60
zinc (mg/kg dw)	16.78-28.17[a]; 18.25-30.44[b]	6.5-42.6
Vitamins		
vitamin A (mg/kg dw)	0.14-11.27[d]	0.19-80.20
vitamin B_1 (mg/kg dw)	2.33-4.17[a]; 2.71-4.33[b]	1.26-40.00
vitamin B_2 (mg/kg dw)	0.94-2.42[a]; 1.64-2.81[b]	0.50-7.35
vitamin B_3 (mg/kg dw)	15.07-32.38[a]; 13.64-42.06[b]	7.42-46.94
vitamin B_6 (mg/kg dw)	4.93-7.53[a]; 4.97-8.27[b]	1.18-12.14
vitamin B_9 (mg/kg dw)	0.19-0.35[a]; 0.23-0.42[b]	0.09-3.50
vitamin E (mg/kg dw)	5.96-18.44[a]; 2.84-15.53[b]	0.84-68.67
Grain Other		
Anti-Nutrients		
phytic acid (% dw)	0.69-1.09[a]; 0.60-0.94[b]	0.111-1.940
raffinose (% dw)	0.079-0.22[a]; 0.061-0.15[b]	0.020-0.466
Secondary Metabolites		
ferulic acid (µg/g dw)	1205.75-2873.05[a]; 1011.40-2539.86[b]	291.93-4397.30
p-coumaric acid (µg/g dw)	94.77-327.39[a]; 66.48-259.68[b]	53.4-820.0
Forage Nutrients		
Proximates		
protein (% dw)	5.80-10.24[a]; 5.56-9.14[b]	2.37-16.32
total fat (% dw)	1.28-3.62[a]; 0.20-1.76[b]	0.296-6.755
ash (% dw)	2.67-8.01[a]; 4.59-6.9[b]	0.66-13.20
Carbohydrates By Calculation		
carbohydrates by calculation (% dw)	81.88-89.26[a]; 84.11-87.54[b]	73.3-92.9
Fiber		
ADF (% dw)	19.11-30.49[a]; 20.73-33.39[b]	5.13-47.39
NDF (% dw)	27.73-49.62[a]; 31.81-50.61[b]	18.30-67.80
Minerals		
calcium (% dw)	0.12-0.33[a]; 0.21-0.41[b]	0.04-0.58
phosphorus (% dw)	0.090-0.26[a]; 0.13-0.21[b]	0.07-0.44

[1]dw=dry weight; FA=Fatty Acid; mg/kg/ dw

[2]Literature range references: [a](Harrigan *et al.*, 2009) (see U.S. Field data);[b](Harrigan *et al.*, 2009) (see Chile field data);[c](Ridley *et al.*, 2011);[d](Egesel *et al.*, 2003)

[3]ILSI range is from ILSI Crop Composition Database, version 7, 2019 (Accessed January 25th, 2019).

C. INFORMATION RELATED TO THE NUTRITIONAL IMPACT OF THE FOOD PRODUCED USING GENE TECHNOLOGY

There are no nutritional impacts on the food and feed derived from MON 95379. This product is developed to confer insect protection. It is not a nutritionally altered product.

D. OTHER INFORMATION

The data and information presented in this submission demonstrate that the food and feed derived from MON 95379 are as safe and nutritious as those derived from commercially-available, conventional maize for which there is an established history of safe consumption. No additional studies have been supplied to add value to the safety of MON 95379.

PART 3 STATUTORY DECLARATION – AUSTRALIA

I, [redacted] declare the following points in this application:

1. The information provided in this application fully sets out the matters required.
2. The information provided in this application is true to the best of my knowledge and belief.
3. No information has been withheld that might prejudice this application, to the best of my knowledge and belief.

Signature: [redacted]

Declared before me ..... [redacted] ..... [redacted]

This ..... 25th ..... day of .....March..... 2021.

PART 4 REFERENCES

Anderson, J.E., J.-M. Michno, T.J.Y. Kono, A.O. Stec, B.W. Campbell, S.J. Curtin and R.M. Stupar. 2016. Genomic variation and DNA repair associated with soybean transgenesis: A comparison to cultivars and mutagenized plants. BMC Biotechnology 16:41.

Barker, R.F., K.B. Idler, D.V. Thompson and J.D. Kemp. 1983. Nucleotide sequence of the T-DNA region from the *Agrobacterium tumefaciens* octopine Ti plasmid pTi15955. Plant Molecular Biology 2:335-350.

Barry, G.F., G.M. Kishore, S.R. Padgette and W.C. Stallings. 2001. Glyphosate-tolerant 5-enolpyruvylshikimate-3-phosphate synthases. Patent 6,248,876, U.S. Patent Office, Washington, D.C.

Baum, J.A. 1998. Transgenic *Bacillus thuringiensis*. Phytoprotection 79:127-130.

Baum, J.A., T.B. Johnson and B.C. Carlton. 1999. *Bacillus thuringiensis*: Natural and recombinant bioinsecticide products. Pages 189-209 in Methods in Biotechnology: Biopesticides: Use and Delivery. Volume 5. F.R. Hall and J.J. Menn (eds.). Humana Press Inc., Totowa, New Jersey.

Betz, F.S., B.G. Hammond and R.L. Fuchs. 2000. Safety and advantages of *Bacillus thuringiensis*-protected plants to control insect pests. Regulatory Toxicology and Pharmacology 32:156-173.

Biron, D.G., C. Brun, T. Lefevre, C. Lebarbenchon, H.D. Loxdale, F. Chevenet, J.-P. Brizard and F. Thomas. 2006. The pitfalls of proteomics experiments without the correct use of bioinformatics tools. Proteomics 6:5577-5596.

Bradshaw, R.A., W.W. Brickey and K.W. Walker. 1998. N-terminal processing: The methionine aminopeptidase and N^{α}-acetyl transferase families. Trends in Biochemical Sciences 23:263-267.

Bravo, A., S.S. Gill and M. Soberón. 2007. Mode of action of *Bacillus thuringiensis* Cry and Cyt toxins and their potential for insect control. Toxicon 49:423-435.

Bravo, A., S. Likitvivatanavong, S.S. Gill and M. Soberón. 2011. *Bacillus thuringiensis*: A story of a successful bioinsecticide. Insect Biochemistry and Molecular Biology 41:423-431.

Burtet, L.M., O. Bernardi, A.A. Melo, M.P. Pes, T.T. Strahl and J.V. Guedes. 2017. Managing fall armyworm, *Spodoptera frugiperda* (Lepidoptera: Noctuidae), with Bt maize and insecticides in southern Brazil. Pest Management Science 73:2569-2577.

Cade, R., K. Burgin, K. Schilling, T.-J. Lee, P. Ngam, N. Devitt and D. Fajardo. 2018. Evaluation of whole genome sequencing and an insertion site characterization method for molecular characterization of GM maize. Journal of Regulatory Science 6:1-14.

Caetano-Anollés, G., M. Wang, D. Caetano-Anollés and J.E. Mittenthal. 2009. The origin, evolution and structure of the protein world. Biochemical Journal 417:621-637.

Capehart, T., O. Liefert and D. Olson. 2019. Feed outlook. FDS-19d. U.S. Department of Agriculture, Economic Research Service, Washington, D.C. https://usda.library.cornell.edu/concern/publications/44558d29f?locale=en [Accessed April 22, 2019].

Chen, J. 2018. Biopesticides: Global markets to 2022. BCC Research Report Overview. BCC Research, LLC., Wellesley, Massachusetts.

Codex Alimentarius. 2009. Foods derived from modern biotechnology. Second Edition. Codex Alimentarius Commission, Joint FAO/WHO Food Standards Programme, Food and Agriculture Organization of the United Nations, Rome, Italy.

Cornejo, M.-J., D. Luth, K.M. Blankenship, O.D. Anderson and A.E. Blechl. 1993. Activity of a maize ubiquitin promoter in transgenic rice. Plant Molecular Biology 23:567-581.

Damalas, C.A. and S.D. Koutroubas. 2018. Current status and recent developments in biopesticide use. Agriculture 8:13.

de Maagd, R.A., A. Bravo, C. Berry, N. Crickmore and H.E. Schnepf. 2003. Structure, diversity, and evolution of protein toxins from spore-forming entomopathogenic bacteria. Annual Review of Genetics 37:409-433.

de Maagd, R.A., A. Bravo and N. Crickmore. 2001. How *Bacillus thuringiensis* has evolved specific toxins to colonize the insect world. Trends in Genetics 17:193-199.

Deist, B.R., M.A. Rausch, M.T. Fernandez-Luna, M.J. Adang and B.C. Bonning. 2014. Bt toxin modification for enhanced efficacy. Toxins 6:3005-3027.

Depicker, A., S. Stachel, P. Dhaese, P. Zambryski and H.M. Goodman. 1982. Nopaline synthase: Transcript mapping and DNA sequence. Journal of Molecular and Applied Genetics 1:561-573.

Edgerton, M.D. 2009. Increasing crop productivity to meet global needs for feed, food, and fuel. Plant Physiology 149:7-13.

EFSA. 2012. Conclusion on the peer review of the pesticide risk assessment of the active substance *Bacillus thuringiensis* subsp. *kurstaki* (*strains ABTS 351, PB 54, SA 11, SA 12, EG 2348*). EFSA Journal 10:2540.

Egesel, C.O., J.C. Wong, R.J. Lambert and T.R. Rocheford. 2003. Gene dosage effects on carotenoid concentration in maize grain. Maydica 48:183-190.

Federici, B.A. and J.P. Siegel. 2008. Safety assessment of *Bacillus thuringiensis* and *Bt* crops used in insect control. Pages 45-102 in Food Safety of proteins in Agricultural Biotechnology. B.G. Hammond (ed.). CRC Press, Boca Raton, Florida.

Fisher, R. and L. Rosner. 1959. Toxicology of the microbial insecticide, Thuricide. Journal of Agricultural and Food Chemistry 7:686-688.

Fling, M.E., J. Kopf and C. Richards. 1985. Nucleotide sequence of the transposon Tn*7* gene encoding an aminoglycoside-modifying enzyme, 3"(9)-*O*-nucleotidyltransferase. Nucleic Acids Research 13:7095-7106.

Frederiksen, K., H. Rosenquist, K. Jørgensen and A. Wilcks. 2006. Occurrence of natural *Bacillus thuringiensis* contaminants and residues of *Bacillus thuringiensis*-based insecticides on fresh fruits and vegetables. Applied and Environmental Microbiology 72:3435-3440.

Gao, Y., K.J. Fencil, X. Xu, D.A. Schwedler, J.R. Gilbert and R.A. Herman. 2006. Purification and characterization of a chimeric Cry1F δ–endotoxin expressed in transgenic cotton plants. Journal of Agricultural and Food Chemistry 54:829-835.

Gilbertson, L. 2003. Cre-*lox* recombination: Cre-ative tools for plant biotechnology. Trends in Biotechnology 21:550-555.

Gill, S.S., E.A. Cowles and P.V. Pietrantonio. 1992. The mode of action for *Bacillus thuringiensis* endotoxins. Annual Review of Entomology 37:615-636.

Grimi, D.A., B. Parody, M.L. Ramos, M. Machado, F. Ocampo, A. Willse, S. Martinelli and G. Head. 2018. Field-evolved resistance to Bt maize in sugarcane borer (*Diatraea saccharalis*) in Argentina. Pest Management Science 74:905-913.

Hadley, W.M., S.W. Burchiel, T.D. McDowell, J.P. Thilsted, C.M. Hibbs, J.A. Whorton, P.W. Day, M.B. Friedman and R.E. Stoll. 1987. Five-month oral (diet) toxicity/infectivity study of *Bacillus thuringiensis* insecticides in sheep. Fundamental and Applied Toxicology 8:236-242.

Hammond, B. 2004. A review of the food/feed safety and benefits of *Bacillus thuringiensis* protein containing insect-protected crops. Pages 103-123 in Agricultural Biotechnology: Challenges and Prospects. M.K. Bhalgat, W.P. Ridley, A.S. Felsot, and J.N. Seiber (eds.). American Chemical Society, Washington, D.C.

Hammond, B.G. and J.M. Jez. 2011. Impact of food processing on the safety assessment for proteins introduced into biotechnology-derived soybean and corn crops. Food and Chemical Toxicology 49:711-721.

Hare, P.D. and N.-H. Chua. 2002. Excision of selectable marker genes from transgenic plants. Nature Biotechnology 20:575-580.

Harrigan, G.G., D. Lundry, S. Drury, K. Berman, S.G. Riordan, M.A. Nemeth, W.P. Ridley and K.C. Glenn. 2010. Natural variation in crop composition and the impact of transgenesis. Nature Biotechnology 28:402-404.

Harrigan, G.G., W.P. Ridley, K.D. Miller, R. Sorbet, S.G. Riordan, M.A. Nemeth, W. Reeves and T.A. Pester. 2009. The forage and grain of MON 87460, a drought-tolerant corn hybrid, are compositionally equivalent to that of conventional corn. Journal of Agricultural and Food Chemistry 57:9754-9763.

Hartung, M. and B. Kisters-Woike. 1998. Cre mutants with altered DNA binding properties. Journal of Biological Chemistry 273:22884-22891.

Hernandez-Garcia, C.M. and J.J. Finer. 2014. Identification and validation of promoters and cis-acting regulatory elements. Plant Science 217-218:109-119.

Herrmann, K.M. 1995. The shikimate pathway: Early steps in the biosynthesis of aromatic compounds. The Plant Cell 7:907-919.

Hileman, R.E., A. Silvanovich, R.E. Goodman, E.A. Rice, G. Holleschak, J.D. Astwood and S.L. Hefle. 2002. Bioinformatic methods for allergenicity assessment using a comprehensive allergen database. International Archives of Allergy and Immunology 128:280-291.

Hoess, R.H., A. Wierzbicki and K. Abremski. 1986. The role of the *lox*P spacer region in P1 site-specific recombination. Nucleic Acids Research 14:2287-2300.

Hunt, A.G. 1994. Messenger RNA 3' end formation in plants. Annual Review of Plant Physiology and Plant Molecular Biology 45:47-60.

Illergård, K., D.H. Ardell and A. Elofsson. 2009. Structure is three to ten times more conserved than sequence - A study of structural response in protein cores. Proteins 77:499-508.

ILSI. 2019. Crop composition database, Version 7.0. International Life Sciences Institute, Washington, D.C. https://www.cropcomposition.org/query/index.html.

Jeon, J.-S., S. Lee, K.-H. Jung, S.-H. Jun, C. Kim and G. An. 2000. Tissue-preferential expression of a rice *α*-tubulin gene, *OsTubA1*, mediated by the first intron. Plant Physiology 123:1005-1014.

Klee, H.J., Y.M. Muskopf and C.S. Gasser. 1987. Cloning of an *Arabidopsis thaliana* gene encoding 5-enolpyruvylshikimate-3-phosphate synthase: Sequence analysis and manipulation to obtain glyphosate-tolerant plants. Molecular and General Genetics 210:437-442.

Kovalic, D., C. Garnaat, L. Guo, Y. Yan, J. Groat, A. Silvanovich, L. Ralston, M. Huang, Q. Tian, A. Christian, N. Cheikh, J. Hjelle, S. Padgette and G. Bannon. 2012. The use of next generation sequencing and junction sequence analysis bioinformatics to achieve molecular characterization of crops improved through modern biotechnology. The Plant Genome 5:149-163.

Krause, E., H. Wenschuh and P.R. Jungblut. 1999. The dominance of arginine-containing peptides in MALDI-derived tryptic mass fingerprints of proteins. Analytical Chemistry 71:4160-4165.

Leath, M.N. and L.D. Hill. 1987. Economics of production, marketing, and utilization. Pages 210-219 in Corn: Chemistry and Technology. S.A. Watson and P.E. Ramstad (eds.). American Association of Cereal Chemists, St. Paul, Minnesota.

Lee, G. and I. Saito. 1998. Role of nucleotide sequences of *loxP* spacer region in Cre-mediated recombination. Gene 216:55-65.

Loy, D.D. and E.L. Lundy. 2019. Nutritional properties and feeding value of corn and its coproducts. Pages 633-659 in Corn: Chemistry and Technology. Third Edition. S.O. Serna-Saldivar (ed.). Woodhead Publishing and AACC International Press.

May, J.B. 1987. Wet milling: Process and products. Pages 377-397 in Corn: Chemistry and Technology. S.A. Watson and P.E. Ramstad (eds.). American Association of Cereal Chemists, St. Paul, Minnesota.

McClintock, J.T., C.R. Schaffer and R.D. Sjoblad. 1995. A comparative review of the mammalian toxicity of *Bacillus thuringiensis*-based pesticides. Pesticide Science 45:95-105.

Mendelsohn, M., J. Kough, Z. Vaituzis and K. Matthews. 2003. Are *Bt* crops safe? Nature Biotechology 21:1003-1009.

Metcalfe, D.D., J.D. Astwood, R. Townsend, H.A. Sampson, S.L. Taylor and R.L. Fuchs. 1996. Assessment of the allergenic potential of foods derived from genetically engineered crop plants. Critical Reviews in Food Science and Nutrition 36:S165-S186.

OECD. 2002a. Consensus document on compositional considerations for new varieties of maize (*Zea mays*): Key food and feed nutrients, anti-nutrients and secondary plant metabolites. ENV/JM/MONO(2002)25. Series on the Safety of Novel Foods and Feeds, No. 6. Organisation for Economic Co-operation and Development, Paris, France.

OECD. 2002b. Report of the OECD workshop on the toxicological and nutritional testing of novel foods. SG/ICGB(1998)1/FINAL. Organisation for Economic Co-operation and Development, Paris, France.

OECD. 2007. Consensus document on safety information on transgenic plants expressing *Bacillus thuringiensis*-derived insect control proteins. ENV/JM/FOOD(2007)14. Organisation for Economic Co-operation and Development, Paris, France.

Padgette, S.R., D.B. Re, G.F. Barry, D.E. Eichholtz, X. Delannay, R.L. Fuchs, G.M. Kishore and R.T. Fraley. 1996. New weed control opportunities: Development of soybeans with a Roundup Ready™ gene. Pages 53-84 in Herbicide-Resistant Crops: Agricultural, Environmental, Economic, Regulatory and Technical Aspects. S.O. Duke (ed.). CRC Press, Inc., Boca Raton, Florida.

Prado, J.R., G. Segers, T. Voelker, D. Carson, R. Dobert, J. Phillips, K. Cook, C. Cornejo, J. Monken, L. Grapes, T. Reynolds and S. Martino-Catt. 2014. Genetically engineered crops: From idea to product. Annual Review of Plant Biology 65:769-790.

Rademacher, T.W., R.B. Parekh and R.A. Dwek. 1988. Glycobiology. Annual Review of Biochemistry 57:785-838.

Rausch, K.D., D. Hummel, L.A. Johnson and J.B. May. 2019. Wet milling: The basis for corn biorefineries. Pages 501-535 in Corn: Chemistry and Technology. Third Edition. S.O. Serna-Saldivar (ed.). Woodhead Publishing, Duxford, United Kingdom.

Reay-Jones, F.P.F. 2019. Pest status and management of corn earworm (Lepidoptera: Noctuidae) in field corn in the United States. Journal of Integrated Pest Management 10:1-9.

Richins, R.D., H.B. Scholthof and R.J. Shepherd. 1987. Sequence of figwort mosaic virus DNA (caulimovirus group). Nucleic Acids Research 15:8451-8466.

Ridley, W.P., G.G. Harrigan, M.L. Breeze, M.A. Nemeth, R.S. Sidhu and K.C. Glenn. 2011. Evaluation of compositional equivalence for multitrait biotechnology crops. Journal of Agricultural and Food Chemistry 59:5865-5876.

Rogers, S.G. 2000. Promoter for transgenic plants. Patent 6,018,100, U.S. Patent Office, Washington, D.C.

Rooney, L.W. and S.O. Serna-Saldivar. 2003. Food uses of whole corn and dry-milled fractions. Pages 495-535 in Corn: Chemistry and Technology. Second Edition. P.J. White and L.A. Johnson (eds.). American Association of Cereal Chemists, St. Paul, Minnesota.

Rose, A.B. 2008. Intron-mediated regulation of gene expression. Current Topics in Microbiology and Immunology 326:277-290.

Russell, S.H., J.L. Hoopes and J.T. Odell. 1992. Directed excision of a transgene from the plant genome. Molecular and General Genetics 234:49-59.

Salomon, S. and H. Puchta. 1998. Capture of genomic and T-DNA sequences during double-strand break repair in somatic plant cells. EMBO Journal 17:6086-6095.

Schnepf, E., N. Crickmore, J. van Rie, D. Lereclus, J. Baum, J. Feitelson, D.R. Zeigler and D.H. Dean. 1998. *Bacillus thuringiensis* and its pesticidal crystal proteins. Microbiology and Molecular Biology Reviews 62:775-806.

Seiber, J.N., J. Coats, S.O. Duke and A.D. Gross. 2014. Biopesticides: State of the art and future opportunities. Journal of Agricultural and Food Chemistry 62:11613-11619.

Sidorov, V. and D. Duncan. 2009. *Agrobacterium*-mediated maize transformation: Immature embryos versus callus. Pages 47-58 in Methods in Molecular Biology: Transgenic Maize - Methods and Protocols. M.P. Scott (ed.). Humana Press, Inc, Totowa, New Jersey.

Siegel, J.P. 2001. The mammalian safety of *Bacillus thuringiensis*-based insecticides. Journal of Invertebrate Pathology 77:13-21.

Silvanovich, A., M.A. Nemeth, P. Song, R. Herman, L.Tagliani and G.A. Bannon. 2006. The value of short amino acid sequence matches for prediction of protein allergenicity. Toxicological Sciences 90:252-258.

Stalker, D.M., C.M. Thomas and D.R. Helinski. 1981. Nucleotide sequence of the region of the origin of replication of the broad host range plasmid RK2. Molecular and General Genetics 181:8-12.

Sutcliffe, J.G. 1979. Complete nucleotide sequence of the *Escherichia coli* plasmid pBR322. Cold Spring Harbor Symposia on Quantitative Biology 43:77-90.

Taylor, M., A. Bickel, R. Mannion, E. Bell and G.G. Harrigan. 2017. Dicamba-tolerant soybeans (*Glycine max* L.) MON 87708 and MON 87708 × MON 89788 are compositionally equivalent to conventional soybean. Journal of Agricultural and Food Chemistry 65:8037-8045.

Thomas, K., M. Aalbers, G.A. Bannon, M. Bartels, R.J. Dearman, D.J. Esdaile, T.J. Fu, C.M. Glatt, N. Hadfield, C. Hatzos, S.L. Hefle, J.R. Heylings, R.E. Goodman, B. Henry, C. Herouet, M. Holsapple, G.S. Ladics, T.D. Landry, S.C. MacIntosh, E.A. Rice, L.S. Privalle, H.Y. Steiner, R. Teshima, R. van Ree, M. Woolhiser and J. Zawodny. 2004. A multi-laboratory evaluation of a common in vitro pepsin digestion assay protocol used in assessing the safety of novel proteins. Regulatory Toxicology and Pharmacology 39:87-98.

Thomas, K., G. Bannon, S. Hefle, C. Herouet, M. Holsapple, G. Ladics, S. MacIntosh and L. Privalle. 2005. In silico methods for evaluating human allergenicity to novel proteins: International Bioinformatics Workshop Meeting Report, 23-24 February 2005. Toxicological Sciences 88:307-310.

U.S. EPA. 1986. *Bacillus thuringiensis* - Fact Sheet 9/86. U.S. Environmental Protection Agency, Washington, D.C.

U.S. EPA. 1996. Certain companies; Approval of pesticide product registrations. Federal Register 61:39960-39961.

U.S. EPA. 1998. Reregistration eligibility decision (RED): *Bacillus thuringiensis*. EPA738-R-98-004. U.S. Environmental Protection Agency, Washington, D.C.

U.S. EPA. 2001. Biopesticides registration action document - *Bacillus thuringiensis* plant-incorporated protectants. U.S. Environmental Protection Agency, Washington, D.C. http://www.epa.gov/pesticides/biopesticides/pips/bt_brad.htm [Accessed July 24, 2013].

USDA-FAS. 2020. Coarse grains. U.S. Department of Agriculture, Foreign Agricultural Service, Washington, D.C. https://apps.fas.usda.gov/psdonline/circulars/grain-corn-coarsegrains.pdf [Accessed August 14, 2020].

Vachon, V., R. Laprade and J.-L. Schwartz. 2012. Current models of the mode of action of *Bacillus thuringiensis* insecticidal crystal proteins: A critical review. Journal of Invertebrate Pathology 111:1-12.

Venkatesh, T.V., M.L. Breeze, K. Liu, G.G. Harrigan and A.H. Culler. 2014. Compositional analysis of grain and forage from MON 87427, an inducible male sterile and tissue selective glyphosate-tolerant maize product for hybrid seed production. Journal of Agricultural and Food Chemistry 62:1964-1973.

VKM. 2016. Risk assessment of the biological plant protection product Turex 50 WG, with the organism *Bacillus thuringiensis* ssp. *aizawai* CG-91. Opinion of the Panel on Plant Protection Product of the Norwegian Scientific Committee for Food Safety. VKM Report 2016:20.

Wang, C., K.C. Glenn, C. Kessenich, E. Bell, L.A. Burzio, M.S. Koch, B. Li and A. Silvanovich. 2016. Safety assessment of dicamba mono-oxygenases that confer dicamba tolerance to various crops. Regulatory Toxicology and Pharmacology 81:171-182.

Wang, C., W. Li, C.R. Kessenich, J.S. Petrick, T.J. Rydel, E.J. Sturman, T.C. Lee, K.C. Glenn and T.C. Edrington. 2018. Safety of the *Bacillus thuringiensis*-derived Cry1A.105 protein: Evidence that domain exchange preserves mode of action and safety. Regulatory Toxicology and Pharmacology 99:50-60.

Wang, Y., J. Wang, X. Fu, J.R. Nageotte, J. Silverman, E.C. Bretsnyder, D. Chen, T.J. Rydel, G.J. Bean, K.S. Li, E. Kraft, A. Gowda, A. Nance, R.G. Moore, M.J. Pleau, J.S. Milligan, H.M. Anderson, P. Asiimwe, A. Evans, W.J. Moar, S. Martinelli, G.P. Head, J.A. Haas, J.A. Baum, F. Yang, D.L. Kerns and A. Jerga. 2019. *Bacillus thuringiensis* Cry1Da_7 and Cry1B.868 protein interactions with novel receptors allow control of resistant fall armyworm, *Spodoptera frugiperda* (J.E. Smith). Applied and Environmental Microbiology 85:e00579-00519.

Watson, S.A. 1988. Corn marketing, processing, and utilization. Pages 881-940 in Corn and Corn Improvement. Third Edition. G.F. Sprague and J.W. Dudley (eds.). American Society of Agronomy, Inc., Crop Science Society of America, Inc., Soil Science Society of America, Inc., Madison, Wisconsin.

Yang, L., C. Wang, A. Holst-Jensen, D. Morisset, Y. Lin and D. Zhang. 2013. Characterization of GM events by insert knowledge adapted re-sequencing approaches. Scientific Reports 3:2839.

Zambryski, P., A. Depicker, K. Kruger and H.M. Goodman. 1982. Tumor induction by *Agrobacterium tumefaciens*: Analysis of the boundaries of T-DNA. Journal of Molecular and Applied Genetics 1:361-370.

Zastrow-Hayes, G.M., H. Lin, A.L. Sigmund, J.L. Hoffman, C.M. Alarcon, K.R. Hayes, T.A. Richmond, J.A. Jeddeloh, G.D. May and M.K. Beatty. 2015. Southern-by-sequencing: A robust screening approach for molecular characterization of genetically modified crops. The Plant Genome 8:1-15.

Zhang, W., S. Subbarao, P. Addae, A. Shen, C. Armstrong, V. Peschke and L. Gilbertson. 2003. Cre/*lox*-mediated marker gene excision in transgenic maize (*Zea mays* L.) plants. Theoretical and Applied Genetics 107:1157-1168.

Zhou, J., G.G. Harrigan, K.H. Berman, E.G. Webb, T.H. Klusmeyer and M.A. Nemeth. 2011. Stability in the composition equivalence of grain from insect-protected maize and seed from glyphosate-tolerant soybean to conventional counterparts over multiple seasons, locations, and breeding germplasms. Journal of Agricultural and Food Chemistry 59:8822-8828.